UNDERSTANDING SYNAPTIC AND CIRCUIT DISRUPTIONS OF EXCITATORY AND INHIBITORY FUNCTION IN FRAGILE X MENTAL RETARDATION

APPROVED BY SUPERVISORY COMMITTEE

Kimberly M. Huber, Ph.D., Mentor

Jay R. Gibson, Ph.D., Mentor

Julian Meeks, Ph.D., Chair

Jane Johnson, Ph.D.

Ege Kavalali, Ph.D.

DEDICATION

I would like to dedicate my accomplishments to my mentors, Jay and Kim, for their contribution to my graduate training. I am grateful for their patience, knowledge and guidance that have contributed to my professional and personal growth.

My success was only possible because of my incredible lab mates who not only provided professional support but also created a positive work environment to encourage my success.

I am also grateful to the love and support of my family and friends; my parents, for their steadfast support of my educational pursuits; my brother and sister-in-law, for their unbound love; and my friends, for providing me the social environment that harmonized my graduate experience.

NEOCORTICAL SYNAPTIC AND CIRCUIT DISRUPTIONS OF EXCITATORY AND INHIBITORY FUNCTION IN FRAGILE X MENTAL RETARDATION

by

ANKUR PATEL

DISSERTATION

Presented to the Faculty of the Graduate School of Biomedical Sciences

The University of Texas Southwestern Medical Center at Dallas

In Partial Fulfillment of the Requirements

For the Degree of

DOCTOR OF PHILOSOPHY

The University of Texas Southwestern Medical Center at Dallas

Dallas, Texas

May, 2013

NEOCORTICAL SYNAPTIC AND CIRCUIT DISRUPTIONS OF EXCITATORY AND INHIBITORY FUNCTION IN FRAGILE X MENTAL RETARDATION

ANKUR PATEL, Ph.D.

The University of Texas Southwestern Medical Center at Dallas,

2013

JAY R. GIBSON, Ph.D.

KIMBERLY M. HUBER, Ph.D.

TABLE OF CONTENTS

PRIOR PUBLICATIONS

"A target-cell specific role for presynaptic *Fmr1* in regulating glutamate release onto neocortical fast-spiking inhibitory neurons". (2013) **Ankur B. Patel**, Seth Hays, Ingrid Bureau, Kimberly M. Huber, Jay R. Gibson. (Journal of Neuroscience)

"Postsynaptic loss of *Fmr1* disrupts cell-to-cell pruning of neocortical circuits" (2013). **Ankur B. Patel**, Kimberly M. Huber, Jay R. Gibson. (submitted)

LIST OF FIGURES

LIST OF TABLES

LIST OF ABREVIATIONS

AAV – Adeno-associate virus
ACSF – Artificial cerebrospinal fluid
AMPA – α-amino-3-hydroxy-5-methylisoxzaole-4-propionic acid
ANOVA – Analysis of variance
APP – Amyloid Precursor Protein
ASD – Austism spectrum disorders
CA1 – *Cornu Ammonis* region 1 of the hippocampus
CA3 - *Cornu Ammonis* region 3 of the hippocampus
CdCl – Cadmium Chloride
CV – Coefficient of Variation
dFXR – *Drosophila* fragile X-related
DIC – Differential interference contrast
DNA – Deoxyribonucleic acid
uEPSC –unitary Excitatory postsynaptic current
FMR1 – Fragile X mental retardation 1 gene
FMRP – Fragile X mental retardation protein
FS – Fast-spiking
FXR1P – Fragile X-related protein 1
FXR2P – Fragile X-related protein 2
FXS – Fragile X syndrome
GABA – γ-aminobutyric acid
GFP – Green fluorescent protein
HITS-CLIP – High-throughput sequencing of mRNAs isolated by crosslinking immunoprecipitation
Hz – Hertz
ID – Intellectual disability
IR-DIC – Infrared illumination differential interference contrast
KAR – Kainate receptor
KO – knock-out
LTD – Long-term depression
LTP – Long-term potentiation
MAP1B – Microtubule-associated protein 1B
mEPSC – miniature excitatory postsynaptic current
mGluR – Metabotropic glutamate receptor
mM – millimole
MPFA – Multiple-probability Fluctuation Analysis
mRNA – Messenger ribonucleic acid

mV – Millivolt
NMDAR – N-methyl-D-aspartate-sensitive glutamate receptor
PPR – Paired-pulse ratio
RISC – RNA-induced silencing complex
RMS – Root mean square
RNA – Ribonucleic acid
STDP – Spike-timing-dependent plasticity
TTX - Tetrodotoxin
VGCC – Voltage-gated calcium channel
WT-Wildtype

CHAPTER ONE: BACKGROUND

Fragile X and Circuit Dysfunction

Fragile X Syndrome is the most prevalent inherited cause of intellectual disability and autism

Fragile X Syndrome, caused by the loss of a single gene, *FMR1* (Fragile X Mental Retardation 1) and its protein product, FMRP (Fragile X Mental Retardation Protein), is the most common inherited form of mental retardation. Loss of *FMR1*, an X-linked gene, is the single disrupted mutation that diagnoses 1 in 4,000 boys and 1 in 8,000 girls with the disease. The disease is characterized by repetitive behaviors, social withdrawal, hypersensitivity to sensory stimuli, epilepsy and cognitive decline (Berry-Kravis, 2002; Hagerman et al., 2009).

Loss of function mutations of the *FMR1* gene occur via enhanced DNA methylation of the promoter region that silences the transcription of the FMR1 gene. This enhanced methylation is triggered by the overt expansion of the CGG trinucleotide repeat in the promoter region of the gene. Female patients, who inherit only a single-copy of the mutated gene, in most cases will be mosaic for *FMR1* and due to one *FMR1* -expressing X-chromosome, will develop less severe impairments. Male patients on the other hand, will carry the *FMR1* mutation on

the single X chromosome they inherit, and therefore exhibit more severe impairments although due to variable silencing of the *FMR1* gene, mosaicism is often pertinent in male patients as well (Nolin et al., 1994; Pieretti et al., 1991).

With a high overlap of behavioral impairments between Fragile X and autism, the disease is the most common monogenic cause of autism. While only 4% of autistic patients are diagnosed with Fragile X, some 40% of Fragile X patients are diagnosed with autism (Belmonte and Bourgeron, 2006). Additionally, Fragile X is also a leading cause of intellectual disability (ID). Estimated life-long societal cost of ASD and ID patients is roughly $1,000,000 to $3,000,000 (CDC, 2004; Kogan et al., 2008) - a major impact to patients and caretakers. Such a devastating disease demands continued understanding of the disease from scientific research to develop therapies that will ease the societal suffrage.

Over the years, significant knowledge of Fragile X Syndrome has come from studies in the animal models of the disease. The *Fmr1* KO mouse, generated by the insertion of a neomycin cassette in exon 5 that prevents the transcription of *Fmr1*, was the first rodent model of Fragile X (Bakker, 1994). The *Fmr1* KO mouse well recapitulates many of the behavioral impairments seen in human patients, exemplifying learning deficits, hyperactivity, hypersensitivity,

vulnerability to seizures, increased exploratory behavior and macroorchidism (Bakker, 1994). Another more recent model of Fragile X is the mosaic model where female mice carry a wild-type X chromosome with a GFP-transgene insertion and an *Fmr1* KO X chromosome (Hadjantonakis et al., 2001; Hanson and Madison, 2007). While this *Fmr1* mosaic model has not been assessed for behavioral recapitulation of human behaviors, it has offered the opportunity to assess the cell-autonomous roles for endogenous FMRP within in vivo circuits (Hanson and Madison, 2007). FMRP is also present in the *Drosophila melanogaster* (Wan et al., 2000), and thus a *Drosophila melanogaster* model of Fragile X has also been widely used. Phenotypes observed in the Drosophila Fragile X line are more severe and different compared to the rodent models of Fragile X. This could be attributable to the presence of the two autosomal homologs of FMRP in mammals, Fragile X Related Proteins 1 and 2 (FXR1 and FXR2). These homologs share ~60% amino acid identity and have similar RNA binding motifs to FMRP but in the Drosophila lines the dFXR serves both the FMRP and FXRs functions.

Although FMRP shares redundant functional domains with the FXR1 and FXR2 proteins, which suggest compensatory potential when FMRP is deficient, evidence suggests that this is not the case. Rather, these homologs may have different functions. In the *Drosophila*, while FMRP alone rescues synaptic

connectivity deficits, the FXR paralogs do not (Coffee et al., 2010). Interestingly, non-neuronal deficits due to the loss of FMRP can be rescued in a compensatory manner by the FXR paralogs.

Fragile X Mental Retardation Protein as a regulator or protein translation

Significant advancements have brought to clarity the molecular and signaling mechanisms of FMRP. As an RNA-binding protein, FMRP exists in a complex with polyribosomes and other RNA binding proteins with some 800 mRNA targets. Its primary role has been identified as a protein translational suppressor in addition to the transportation of those target mRNAs between soma and dendrite (Bassell and Warren, 2008; Darnell et al., 2011). It is recognized that FMRP basally suppresses the translation of target mRNA's by existing in a phosphorylated state that complexes with polyribosomes and other RNA-binding proteins in the spine compartments of the postsynapse. Upon synaptic activity, predominantly mGluR-dependent, FMRP is dephosphorylated and as a result relieves its target mRNAs to undergo activity-dependent protein translation involved in processes such as LTD (Narayanan et al., 2007). Of course, FMRP's translational suppressive role could effectively cause indirect translational enhancements or suppression of some proteins or processes such as phosphorylation and so the overall effect of FMRP loss in Fragile X remains

complex. FMRP is expressed in all sub-localizations of neurons, including soma, dendrites, axons and the nucleus (Antar et al., 2006b; Sittler et al., 1996). Many cell-types have been studied in the context of FMRP and have shown its expression throughout the brain: parvalbumin-expressing interneurons, somatostatin-positive interneurons and pyramidal neurons are just a few examples. FMRP does not seem to be expressed in glia (Feng et al., 1997), even though glia from Fmr1 KO animals alter synaptic development (Jacobs et al., 2010).

While many of FMRP's target mRNAs have recently been identified (Darnell et al., 2011), most remain to be validated as disrupted in Fragile X. As functional and anatomical studies suggest impaired synaptic functions in Fragile X, interest toward the alterations of mRNA targets of FMRP that are synaptic proteins has been a progressive approach to understanding the mechanisms that cause disruptions of synaptic structure and function. Proteins such as Arc, GluR1 and GluR2, NMDARs, CamKII and APP are some synaptic proteins whose disruptions in Fragile X may have profound effects in synaptic function, plasticity and circuit physiology that mediates impaired behaviors (Guzowski et al., 2000; Hayashi et al., 2000; Kamenetz et al., 2003; Morishita et al., 2005).

Synaptic etiology of Fragile X Syndrome

As the evidence accumulates of alterations in synaptic genes and synaptic structures in ASDs and IDs, it has become clear that synaptic disruptions are often the hallmark phenotypes in these diseases and possibly the root causes of the behavioral impairments. The first implication of synaptic disruption in Fragile X came from anatomical evidence in human FXS patients that suggested that loss of *Fmr1* causes dendritic spine overabundance (Grossman et al., 2006). Substantiating evidence in recent years has come from its recapitulation in the *FMR1* KO mouse model of Fragile X. In the *FMR1* KO mouse, altered spine densities, structure, and dynamics have been evidenced in areas such as the visual cortex, somatosensory cortex, hippocampus, and cerebellum (Portera-Cailliau, 2012)

In postmortem tissues of Fragile X patients, anatomical staining of dendritic structures evidenced the overabundance of spines compared to normal age-matched controls (Irwin et al., 2001). While this structural evidence for spine overabundance has been recapitulated in many instances, this has not always been replicated (Portera-Cailliau, 2012). The first analyses of human postmortem tissue from Fragile X patients did not show elevated spine density but did note the increased presence of “long, tortuous spines with prominent terminal heads and

irregular dilations mixed in with normal short and stubby spines" (Hinton et al., 1991; Rudelli et al., 1985)

Much later after these initial findings subsequent examinations of spine anatomy in cortical pyramidal neurons from postmortem tissue of Fragile X patients showed increased spine density along with the previously recognized alterations in spine length (Galvez and Greenough, 2005; Irwin et al., 2001). Differences were attributed to technical limitations of previous enquiries. However, it is becoming clearer that variable accounts of spine phenotypes, in human patients as well the Fragile X mouse model, may be due to variable effects of Fmr1 loss in different brain regions, as well as differences due to the developmental ages that spine phenotype are probed for. In fact, recent work has identified no differences in spine density early in development of cortical barrel and prefrontal regions of the Fragile X mouse model (Cruz-Martin et al., 2010; Harlow et al., 2010; Meredith et al., 2007).

In contrast to the lack of spine density changes in early development, increased spine density seems to be a universal identification in adult *FMR1* KO mice (Comery et al., 1997; Dolen et al., 2007; McKinney et al., 2005). Thus, the overabundant spine phenotype of Fragile X may be specific to adult periods of

development in the Fragile X mutant model and the synaptic dysfunctions that alter circuit functionality may specifically occur at these mature periods.

Recent studies have added a different complexity to the altered spine structures in Fragile X where spine density remains unaltered early in development. While spine density remain unaltered, spine dynamics or spine turnover may be disrupted such that spines of layer 2/3 pyramidal neurons have a much greater turnover rate compared to wild-type littermates (Cruz-Martin et al., 2010). Rapid dynamics and altered shapes of spines from *FMR1* KOs may be the reason for some of the inconsistent findings previously reported if dendritic staining methods are limited in capturing these dynamic spines.

While significant knowledge is gained from these anatomical studies of spine development, spine density, and spine turnover, only speculative effects on the functional outcomes of cortical circuits can be made based on these findings. If FMRP has regulatory roles that are not ubiquitous but rather cell-type, projection-type, and as the anatomical findings suggest, developmental period-specific, then it will require the functional probing of very specific circuits to delineate the information flow in Fragile X cortex. Additionally, to delineate whether spine overabundance or "long, tortuous spines" of Fragile X simply represents non-functional structural spines, functional assays of inputs onto

dendrites where such overabundant spine phenotypes exist need to be performed. Along the same theme, only the functional characterization of the highly dynamic spines identified by Cruz-Martin et al. would clearly delineate what impact these inputs have on circuit performance.

It remains unclear what mechanisms lead to the altered spine morphology in Fragile X. Some evidence suggests the misregulation of cytoskeletal or scaffold proteins such as MAP1B, PSD-95, and Shank, whose mRNAs are targets of FMRP (Antar et al., 2006a; Darnell et al., 2011; Todd et al., 2003) . These proteins, among many others, are known to be important for synapse development and spine stability and thus their disruptions may alter the spine morphologies in Fragile X. Recent studies also suggest FMRP's role in microRNA-induced alterations in spine morphology (Edbauer et al., 2010). While FMRP itself it not necessary for RNAi-mediated cleavage of mRNAs, FMRP has been identified to interact with Argonaut and Dicer in the RISC complex and other miRNAs (Bolduc et al., 2008; Caudy et al., 2002; Cheever and Ceman, 2009a, b). Loss of FMRP prevents miRNA-induced pruning of spines, and causes a reduction in NMDA receptor expression and synaptic strength (Edbauer et al., 2010). Given the idiopathic phenotypes of Fragile X, it will be important to recognize how these targets are disrupted by the loss of FMRP, and what signaling mechanisms are altered to disrupt spine structure.

Fmr1 and functional disruptions

Initial anatomical findings of altered spine density, spine motility and structure in Fragile X have subsequently led to more recent functional studies in these circuits. While no direct functional implications can be made of the spine alterations identified in Fragile X, some evidence correlates spine structures to functionality in normal mice. For example, larger spines express morereceptors and have larger excitatory inputs (Kasai et al., 2010). Filopodial spines have been functionally characterized as having NMDA receptor expression but lacking AMPA receptor expression and are defined as "silent" because their NMDA function is minimal in the presence of extracellular magnesium at resting potential (Liao et al., 1999). Mushroom spines, as the name suggests morphologically mushroom-like, have large functional AMPA receptor expression (Matsuzaki et al., 2001).

More direct physiological evidence of disrupted functionality may explain some of the spine phenotypes of Fragile X that alter network function. In the *Drosophila melongaster* fly model of Fragile X, alterated circadian rhythms suggest network changes (Gatto and Broadie, 2009). In the somatosensory barrel

cortex of *Fmr1* KO mice, local excitatory connectivity between spiny-stellate neurons of layer 4 is reduced at young adolescent ages (Gibson et al., 2008). This could be due to the prevalence of unstable spines identified at these ages (Cruz-Martin et al., 2010) or immature filopodia-like spines (Nimchinsky et al., 2001). Local excitation onto fast-spiking inhibitory interneurons is also disrupted, and network synchrony in the gamma-range is reduced (Gibson et al., 2008) Complimentary to this work, long-range inputs from layer 4 spiny-stellate neurons onto layer 3 excitatory neurons shows reduced connectivity at 2 weeks age, with no effects on quantal strength or postsynaptic AMPA receptor expression (Bureau et al., 2008). Moreover, layer 5 to layer 3 projections are unaltered, suggesting some projection-specific effect. Interestingly, the layer 4 to layer 3 deficit is temporally restricted, such that at 3 weeks age the hypoconnectivity phenotype disappears. This finding compliments the developmental period when there is normalization of the thin, tortuous spine phenotype of layer 5 pyramidal spines (Galvez and Greenough, 2005; Nimchinsky et al., 2001). Studying the developmental interconnectivity of young and adolescent pyramidal neurons in the prefrontal cortex, *Fmr1* KO mice display hyperconnectivity at young ages, but again this phenotype is transient such that it normalizes by adult development (Testa-Silva et al., 2011). Because no structural analysis of spine density, turnover, or shape of prefrontal cortical neurons has

been done in these functional studies, it is difficult to relate the structure-function phenotypes for this particular brain region.

The underlying mechanisms that alter spine structure, function, and network circuitry are still not clear but evidence from fly and mouse models of Fragile X do suggest disruptions in calcium signaling. A recent study identified reduced postsynaptic calcium signaling in response to spike-timing dependent plasticity (STDP) in *Fmr1* KO mice (Meredith et al., 2007). Remarkably, environmental enrichment rescued the elevated threshold for inducing plasticity in these mice.

Loss of FMRP has also shown to disrupt homeostatic plasticity mediated by retinoic acid, a molecule that is synthesized in response to reduced network activity to upregulate AMPAR expression at the synapse (Soden and Chen, 2010). Loss of FMRP may alter network circuitry from the unregulated translation of FMRP's target mRNAs. Arc/Arg3.1, an FMRP target, an immediate-early gene, is another homeostatic gene translated in postsynaptic compartments in response to elevated synaptic activity (Peebles et al., 2010; Shepherd et al., 2006). Elevated basal expression of Arc protein in *Fmr1* KO mice has been evidenced (Niere et al., 2012). This elevated basal Arc in *Fmr1* KO mice may occlude activity-dependent homeostatic function of Arc as mGluR-activation increased Arc

protein in wild-type but did not increase Arc protein in *Fmr1* KOs (Niere et al., 2012).

Recent work has also suggested altered function of membrane potassium channels in *Fmr1* KO mice; Elevated Kv4.2 expression has been identified in *Fmr1* KO mice and shown to disrupt long-term potentiation through NMDA channels (Lee et al., 2011). Another report identified reduced protein expression of the sodium-activated potassium channel, Slack (Brown et al., 2010). Slack channels are suggested to maintain a temporal fidelity of firing induced by high-frequency inputs, thus reduced levels of Slack may render inefficient responses to complex stimuli and cause disrupted activity-dependent plasticity and network circuitry in Fragile X (Yang et al., 2007). Overall, it can be seen that loss of FMRP may indirectly and directly alter mechanisms that participate in network circuitry.

Evidence for FMRP's regulation of synaptic function has also come from the hippocampus and the fly model of Fragile X. Cell-autonomous postsynaptic loss of FMRP increases synaptic connectivity onto cultured CA1 pyramidal cells at equivalent adolescent ages (Pfieffer and Huber, 2008). Postsynaptic transfection of FMRP reduced synapse number per axon without affecting synaptic maturity. It has also been shown that presynaptic FMRP enhances synaptic connectivity between CA3 pyramidal neurons (Hanson and Madison,

2007). In *Drosophila* FMRP (dFXR) reduces synaptic bouton number at the NMJ (Zhang, et al.,2001).

FMRP is has also been shown to associate with forms of plasticity that are involved in learning in memory. Long-term depression (LTD), a process that is activity-dependent, engages the endocytosis of synaptic AMPA receptors which leads to spine size shrinkage from mushroom-like to filopodial-like structures (Huber and Bear, 1998; Huber et al., 2000). This process is disrupted in the Fragile X mouse whereby the induction of mGluR-dependent LTD is exacerbated, and is protein-synthesis independent (Huber et al., 2002). Given that FMRP is a negative regulator of protein translation, it is hypothesized that loss of FMRP in Fragile X may basally upregulate many target mRNAs and thus reduce the activity-dependent protein-synthesis to engage downstream mechanisms necessary for processes like LTD (Bassell and Warren, 2008). Interestingly, a 50% reduction in mGluR5 expression reduces the spine density in Fragile X mice (Dolen et al., 2007), although the functional rescue of spine maturity was not tested. It is worth recognizing however, that in the hippocampus, while mGluR5-dependent plasticity mechanisms are altered, spine alterations are not apparent in Fragile X mice (Pfeiffer and Huber, 2009). It has been shown that whisker-deprivation (induced by trimming of rodent whiskers) induces long-term depression of neocortical synaptic function that is specific to the deprived whisker. This process is particularly well evidenced in layer 4 projections onto

layer 3 excitatory neurons in barrel somatosensory cortex (Allen et al., 2003; Shepherd et al., 2003). The ~47% weakening of layer 4 input onto layer 3 after whisker-deprivation, is completely absent in the Fragile X mouse (Bureau et al., 2008) Because the connectivity onto layer 3 neurons is basally reduced, perhaps due to immature spine development (Nimchinsky et al., 2001), it is hypothesized that whisker-deprivation fails to induce synaptic depression because the projections are already depressed. This compliments the notion that lack of FMRP may lead to the basal upregulation of the protein products of target mRNAs that occludes sensory experience-induced processes such as LTD.

Long-term potentiation (LTP) phenotypes also exist in Fragile X circuits. While LTP in hippocampus is not altered, mGluR-dependent LTP is absent in the necortex of Fragile X mice (Wilson and Cox, 2007). These disruptions may explain the learning and memory deficits in Fragile X. It remains unclear as to why elevated basal acitivity of mGluR signaling occurs in some brain regions and not others. Differences in developmental mechanisms could be the reason. It is seen that mGluR-dependent LTD mechanisms developmentally switch, and thus these changes may alter the differences identified in neocortex (Nosyreva and Huber, 2005).

In an attempt to recognize how loss of FMRP impacts synaptic function and plasticity, studies have focused on the expression and signaling mechanisms of glutamatergic receptors at the synapse but delineation of these effects has not been straight-forward, particularly because the alterations on some glutamatergic receptors may be dependent on developmental period and brain region. Moreover, understanding differences in basal transmission will be critical to recognizing how complex plasticity-inducing inputs differentially affect structural and physiological changes in different brain regions.

Fragile X and Synapse Elimination

A hallmark of synaptic refinement is the elimination of priorly-formed redundant axonal connections – an important process that determines the eventual size and functional capacity of neuronal networks (Lichtman and Colman, 2000). Early postnatal development is characterized by abundant synaptogenesis where redundant synaptic connectivity occurs (Bourgeois et al., 2000; Zuo et al., 2005). This period is subsequently followed by a process of synaptic elimination, or pruning of previously formed redundant connectivity toward more refined networks (Zuo et al., 2005). In cerebellum, multiple climbing fiber inputs onto individual Purkinje cells are eliminated to single climbing fiber innervations onto individual purkinje cells – a process necessary to avoid ataxic behavior (Crepel et

al., 1976; Lohof et al., 1996); preganglionic inputs are eliminated from ganglion cells in the autonomic system (Lichtman, 1977), and in the visual system, thalamocortical projections onto layer IV are eliminated (Hubel et al., 1977). Synaptic elimination can be of 2 types: A reduction in synapse number, where the number of postsynaptic targets remain the same but the strength of connections onto the targets are reduced (weighted pruning), or a reduction in synapse number where the number of postsynaptic targets is reduced while the strength of connections onto remaining targets are maintained (circuit pruning) (See Fig. 1).

Synapse elimination may not only be necessary to establish refined circuits from redundant connections developed during early postnatal life but may also be critical for ongoing long-term memory throughout life. While the proliferation of spines is transient during learning in the hippocampus, it is shown that inputs onto neurons that were active during learning undergo spine elimination (Sanders et al., 2012). In the whisker barrel system of the mouse, associative learning induced by whisker-stimulation pairing with footshock led to a reduction in the number of neurons that responded to the trained whisker compared to an untrained whisker (Gdalyahu et al., 2012). This suggests that synaptic elimination plays an important role in efficient structural and functional allocation of experience-dependent memory and maintain a high number of modifiable parameters available for learning (Chklovskii et al., 2004). While little

evidence exists, it can be envisaged that FMRP participates in this learning-related synapse elimination.

Due to the overabundant spine phenotype in Fragile X, it has been hypothesized that the lack of FMRP leads to a deficit in synaptic pruning. Surprisingly, little evidence of developmental pruning in neocortex exists, and this has left the evidence of FMRP's role in the process consequentially unknown. Anecdotal evidence of circuit pruning among pyramidal neurons of layer 5A has been made (Frick et al., 2007) with some pruning evidenced by golgi-stained spine count in layer 5 pyramidal neurons (Galvez and Greenough, 2005). In the same study developmental pruning of Golgi-stained pyramidal neurons of layer 5 somatosensory cortex spines from p25 to p56 was absent in the *Fmr1* KO mouse (Galvez and Greenough, 2005) and spiny-stellate cells of layer 4 barrel fail to prune their dendrites from septal regions (Galvez and Greenough, 2005). Whether loss of FMRP disrupts learning-induced synaptic elimination is unknown but given the structural evidence it is possible that cognitive impairments in learning and memory in Fragile X may be due to the lack of this process.

While little evidence of FMRP's role in synaptic pruning in mammalian models exists, there has been some evidence of its role in the *Drosophila melongaster* model of Fragile X Syndrome. Recent work has identified

developmental pruning of axons within the Mushroom Bodies – the learning and memory center of the fly. Loss of dFMRP in these flies resulted in a lack of timely pruning. Interestingly, pruning in the FMRP mutant flies resulted in a delayed and "over-pruned" state (Tessier and Broadie, 2008). This is interesting because elimination of climbing fibers in the Fmr1 KO cerebellum is also enhanced (Koekkoek et al., 2005).

Evidence suggests that synaptic pruning may be an experience-dependent process in some circuits. For example, somatosensory deprivation of whisker-activity in young mice prevents the subsequent pruning of spines (Zuo et al., 2005). At sensory relay synapses in the VPM thalamus sensory-deprivation at p12, but not p16, prevents subsequent axonal elimination (Wang and Zhang, 2008). It is also suggested that NMDA receptor activity is necessary for the elimination of redundant connections at vibrissal relay synapses in the thalamus (Zhang et al., 2013), and that while single induction of mGluR-LTD causes weakening of synaptic strength, repeated mGluR-LTD causes synapse elimination (Shinoda et al., 2005). In the hippocampus, subsequent to synapse formation, synapse elimination occurs through activity-dependent competition with active axons (Yasuda et al., 2011). It has been identified that activity enhances the expression of FMRP (Todd and Mack, 2000; Weiler et al., 1997). Moreover, sensory deprivation induced depression of synaptic connectivity of L4 excitatory

projections onto layer 3 neurons, is absent in Fragile X mutant mice. This suggests that loss of FMRP may disrupt the "transmission of experience" required to initiate synaptic pruning. In the *Drosophila melongaster*, synaptic pruning within the mushroom bodies was identified as an activity-dependent process. Moreover, loss of FMRP delayed pruning that was not experience-dependent (Tessier and Broadie, 2008). Based on the evidence in the fly, it could be suggested that FMRP drives experience-dependent synaptic pruning and loss of FMRP disrupts timely pruning and engages in altered mechanisms of synaptic pruning in a delayed manner. Whether the findings in the fly can be mimicked in the mouse models of Fragile X remains to be studied. Interestingly, while sensory deprivation doesn't alter spine density in layer 2/3 pyramidal neurons, it does reduce spine and filopodia motility or turnover rates (Lendvai et al., 2000). This particular process may be critical to establishing sensory-experience driven "relevant" connectivity, such that subsequent pruning mechanisms may occur. If loss of FMRP alters spine turnover rates in Fragile X, as suggest by Cruz-Martin et al., 2010, then stable (relevant) synapses may never establish to subsequently initiate pruning mechanisms in *Fmr1* KO mice.

Molecular mechanisms for FMRP's regulation of synapse elimination are becoming more evident. Recent work suggests that synaptic elimination driven by the transcription factor, Mef2, requires FMRP (Pfeiffer et al., 2010). While it

remains unknown to what extent elimination in the neocortex is Mef2-dependent, it is likely that loss of FMRP could disrupt developmental as well as learning-induced Mef2-mediated synapse elimination. Synapse elimination by Mef2 is also activity-dependent, thus it could explain the experience-dependent elimination of synapses described earlier. As mentioned before, disrupted mGluR signaling and altered mGluR-mediated plasticity may also disrupt synapse elimination and recent work in our lab shows that Mef2-induced synapse elimination is mGluR receptor depedent (unpublished data from Julia Wilkerson). These studies suggest that activity-dependent mechanisms in the postsynaptic compartment may be regulated by FMRP to induce synapse elimination but mechanistically it remains poorly understood.

FMR1 and inhibitory dysfunction

While there exists significant evidence for enhanced excitatory function in Fragile X based on the numerous spine anomalies, behavioral impairments such as hypersensitivity to sensory stimuli and vulnerability to seizures, it is quite possible that part of the enhanced circuit excitability could be due to reduced inhibitory function. Driven by numerous cell-types, inhibitory neurons developmentally establish recurrent connections to excitatory neurons to engage in feedback inhibition so as to prevent prolonged and runaway excitation –

potential triggers for hyperexcitability and seizures. Recruitment of inhibition also contributes to the enhanced signal-to-noise ratio for excitatory signal flow and is critical for cognitive performance (Atallah et al., 2012; Fuchs et al., 2007; Sohal et al., 2009) and critical period plasticity (Hensch, 2005). Recent work has shown that genetic deletion of glutamate receptors on fast-spiking parvalbumin interneurons in the hippocampus severely disrupts working and episodic-like memory (Fuchs et al., 2007) Thus, disruptions in inhibitory circuitry, function, or recruitment of inhibition by excitatory inputs, could significantly contribute to the overall cognitive, hyperexcitability and hypersensitivity phenotypes of Fragile X Syndrome.

In the context of FMRP, studies have shown disruptions in GABA-mediated inhibition in the Fragile X mouse model. A significant decrease in the number of parvalbumin-positive fast-spiking interneurons has been identified, although this could be attributable to reduced levels of parvalbumin protein per cell (Selby et al., 2007). Altered expression levels of GABAergic receptor have also been shown. Protein levels of GABAA subunits, β and δ, have lower expression levels (Curia et al., 2008). mRNA transcripts of GABAA are also reduced, in both fly and mouse models of Fragile X (D'Hulst and Kooy, 2007). These findings suggest that inhibitory drive may be reduced in Fragile X circuits.

Functional evidence has suggested a reduction in tonic, but not phasic, GABA signaling onto subicular pyramidal neurons of Fragile X mice (Curia et al., 2008). In the amygdala of Fragile X mice, tonic GABA signaling, miniature frequency and amplitude, inhibitory synapse number and multivesicular release are reduced (Olmos-Serrano et al., 2010). In the somatosensory cortex, excitation of somatostatin-positive interneurons in layer 2/3 shows reduced DHPG-induced activation of group 1 mGluR receptors and synchronization of inhibition (Paluszkiewicz et al., 2011). In medium spiny neurons of the striatum, miniature inhibitory GABA currents are increased. While this might seem to counter excitability, because interstriatal projections are themselves inhibitory, increased inhibitory function would actually disinhibit striatal output, thus increasing excitability (Centonze et al., 2008). Another study identified a robust, 50% reduction in the excitation of fast-spiking parvalbumin-positive inhibitory interneurons in layer 4 barrel cortex (Gibson et al., 2008). This phenotype is particularly interesting because it recognizes a synaptic deficit that lacks the very structure whose disruption is linked to Fragile X synaptic etiology – spines. Excitatory input onto these fast-spiking interneurons is purely onto dendritic shafts and soma. The finding suggests the possibility that disruptions in synaptic function, caused by the loss of FMRP, are not purely dependent on postsynaptic spine abnormalities, and thus postsynaptic FMRP. The mechanistic nature of the

phenotype was not pursued in the work and will be the major mechanistic insight in my work.

While plasticity at excitatory inputs onto inhibitory neurons hasn't been studied, the process may be disrupted by this significant reduction in synaptic strength. Contrary to previous notions, inputs onto fast-spiking interneurons do undergo Hebbian long-term potentiation (Lamsa et al., 2005) and if such plasticity depends on basal strength of transmission, then Fragile X circuits may establish fewer excitatory connectivity onto fast-spiking interneurons. Such development would increase the excitation/inhibition ratio and prolong excitatory states in Fragile X circuits.

Homeostatic plasticity that responds to circuit excitability also requires adjustment in AMPA-mediated transmission of excitatory inputs onto parvalbumin fast-spiking interneurons of the hippocampus (Bartley et al., 2008; Chang et al., 2010). If recruitment of inhibition by these interneurons is reduced in Fragile X, the homeostatic response to sensory-stimuli-induced circuit excitation may not be proficient, leading to a prolonged excitatory state of the circuit. Such outcomes could be the reasoning behind the behavioral vulnerability to seizures in Fragile X.

It is apparent that GABAergic function in Fragile X Syndrome is disrupted but whether they are simply a consequence of altered excitatory glutamatergic circuitry remains unknown. Cell-autonomous studies that isolate presynaptic vs postsynaptic FMRP may shed a clearer light on the role for FMRP in inhibitory recruitment and function. Developmentally, disrupted inhibition in Fragile X could alter the critical period plasticity that depends on excitation onto fast-spiking interneurons (Balmer et al., 2009). Indeed, the developmental unsilencing of thalamic projections onto layer 4, a critical period process is delayed in the *Fmr1* KO mouse (Harlow et al., 2010). It is also necessary to recognize the collective outcome of signal flow in the context of potential inhibitory cell-type-specific alterations in Fragile X. Indeed, while findings from Gibson et al., 2008 identify disrupted recruitment of parvalbumin-positive fast-spiking interneurons recruitment of somatostatin-positive interneurons is unaltered. Interestingly, somatostatin-positive inhibitory synapses are onto spines, unlike the aspiny excitatory synapses onto parvalbumin-positive neurons. Whether spine overabundance, and thus increased synaptic strength, masks presynaptic deficits in transmission at excitatory synapses onto somatostatin interneurons remains unknown. Recent work has suggested that dendritic inputs from somatostatin-positive inhibitory interneurons enhance the excitatory glutamatergic signal while also inhibiting parvalbumin-positive fast-spiking interneurons that synapse somatically (Lovett-Barron et al., 2012). In the Fragile X mouse model, how

intact recruitment of somatostatin-induced inhibition, but disrupted recruitment of parvalbumin-induced inhibition collectively alters circuit and behavioral outcome will need to be understood (Gibson et al., 2008).

While most of the structural work has implicated that loss of FMRP disrupts pruning and as a result enhances excitatory function, recent work has suggested that visual experience-dependent plasticity is associated with pruning of inhibitory synapses as well, predominantly those that are onto spines – a process deemed necessary to strengthen visual inputs without alterations of excitatory circuits (van Versendaal et al., 2012). If pruning deficits in Fragile X are not specific to excitatory synapses, it is possible that disrupted pruning of inhibitory synapses prevents the strengthening of sensory inputs in response to experience.

Presynaptic FMRP

While most attention toward resolving the mechanistic alterations in Fragile X has focused on the postsynaptic compartment, more recent studies point to the significance of presynaptic FMRP. Evidence for this is substantiated by robust expression of FMRP in growth cones, axons, and terminals (Till et al., 2012). Immunoelectron microscopy work has shown FMRP in a subset of neurons

in the brain (Feng et al., 1997). FMRP has also been identified in the form of Fragile X Granules (FXGs) in presynaptic axons (Christie et al., 2009). Interestingly, the expression of these FXGs is apparent at projections that undergo long-term presynaptic plasticity: hippocampal mossy fibers and cerebellar parallel fibers, suggesting a role for presynaptic FMRP in presynaptic plasticity.

While significant work, even in the context of FMRP, has recognized the protein-synthesis-dependent mechanisms that establish long-term changes in synaptic function, it is accepted that protein synthesis mechanisms in the axon mediates axon guidance. For example, studying the axonal guidance in response to attractants like netrin-1 or repellants like Sema3A have shown that growth cone motility depends on protein synthesis (even when the cell body is isolated) (Li et al, 2004). Recent work has shown that FMRP in the growth cone regulates Sema3A induced growth cone collapse (Li et al., 2009). Interestingly, presynaptic loss of FMRP reduced the protein synthesis-dependent collapse in response to Sema3A, suggesting that FMRP promotes extracellular signaling-mediated protein synthesis-dependent axonal development. These findings suggest that lack of axonal FMRP may reduce the ability of the developing axon to respond to external signals and induce protein-synthesis mechanisms that will promote better motility and eventual synapse formation. Whether this mechanism is protein-synthesis dependent throughout the entire projectional development of an axon to

its final destination, the synapse, is yet to be understood and whether FMRP's role becomes less obligatory as far as mediating protein-synthesis dependent synapse maintenance is not known either. The relevance of presynaptic FMRP, not just for protein-synthesis mechanisms but also the eventual synaptic functional outcome is also not clear.

While evidence for presynaptic FMRP in growth cone motility is recognized, it remains unclear what effect presynaptic loss of FMRP has on developmental, experience-dependent synaptic formation in more at mature ages. Recent work by Bureau and colleagues (Bureau et al., 2008) identified defasciculated axons of layer 4 excitatory neurons projecting to layer 3 during a critical period of development in *Fmr1* KO mice. Using laser-scanning photostimulaton (LSPS) to uncage glutmate at presynaptic neurons, it was found that *Fmr1* KO mice displayed a 40% reduction in strength due to reduced connectivity. Whether this represents reduced connectivity caused by reduced number of presynaptic neurons or reduced bouton number per neuron was not identified. At the cell-autonomous level, mosaic Fmr1 expression in CA3 slice culture, identified that loss of presynaptic, and not postsynaptic FMRP, reduces functional excitatory connectivity between pyramidal neurons (Hanson and Madison, 2007) but because this effect isn't identified in *Fmr1* KO slices, it is unclear what role presynaptic FMRP has in vivo. While plasticity mechanisms

have been differentially affected in hippocampus versus the neocortex, what role presynaptic FMRP has in synaptic development in the neocortex remains unknown. In *Drosophila* neuromuscular junction, genetic manipulation in the fly model of Fragile X, the dfmr1 null fly, that re-introduced Fmr1 expression in the presynaptic neurons, rescued altered axonal branching, boutons number, and abundance of mini-satellite boutons (Gatto and Broadie, 2008). Surprisingly, no functional rescue was identified with this presynaptic re-introduction of FMRP. Another interesting set of studies have suggested a role for presynaptic FMRP in nociceptive pain sensitivity (Price et al., 2006; Price et al., 2007). Interestingly, the nociceptive processing is mGluR5- and protein-synthesis-dependent (Jimenez-Diaz et al., 2008), suggesting disrupted presynaptic mGluR-signaling in Fragile X. While several functional deficits have been identified in intact circuits of Fragile X mice that have complete loss of FMRP, there is little to no evidence that has determined the potential presynaptic roles for FMRP in intact cortical structures.

Recent work using high-throughput sequencing of mRNAs isolated by crosslinking immunoprecipitation (HITS-CLIP) identified several presynaptic mRNA targets of FMRP – targets that are vital to synaptic function (See Fig. 2) (Darnell et al., 2011). It is possible that the expression and thus function of many of these targets may be significantly disrupted with the loss of FMRP. While none

of the targets have been functionally linked to FMRP, it will be critical to identify which of these secondary effects, whether molecularly identified or physiologically implicated based on identifications of synaptic mechanisms, can be targeted for therapeutic purposes to rescue deficits caused by presynaptic, and not postsynaptic loss of FMRP.

Acute versus Developmental roles for FMRP at the synapse

Increasing evidence from anatomical analysis of dendritic spines and functional analysis through physiological techniques is determining the effects of FMRP as developmental or acute, but it remains unclear whether FMRP is critical during certain developmental periods or is functionally necessary in an ongoing manner throughout life. Identification of the temporal windows when FMRP is critical to establishing brain circuitry will be important to developing interventional therapies.

If FMRP-mediated regulation of synaptic structure and function is experience-dependent, the developmental nature of experience-dependent plasticity may itself define FMRP's function as developmental rather than acute.
It remains unclear whether spine elimination is an acute or developmental process. FMRP transfection into postsynaptic CA1 pyramidal neurons requires

only 3-7 days to alter synaptic structure and function (Pfeiffer and Huber, 2007). Thus an acute, ongoing role for FMRP may exist to maintain balanced connectivity when synapse proliferation rates and synapse elimination rates are equal in mature circuits. More evidence of this is needed in the neocortex however. Alternatively, whether FMRP functions acutely or developmentally to regulate pruning may depend on whether pruning itself is developmental or ongoing. In the neocortex, for example, critical period plasticity is present only during early postnatal periods, and if the engagement of synaptic pruning in those circuits is developmental period-dependent, then FMRP's regulation of pruning may be developmental and not acute. Indeed in the *Drosophila,* timely synaptic pruning, identified as dependent on FMRP, can only occur during a particular developmental period in an activity-dependent manner (Tessier and Broadie, 2008). Moreover, activity after this developmental period will no longer engage synaptic pruning, suggesting that FMRP may be necessary at certain developmental periods for pruning.

Since very little is known of the presynaptic functions of FMRP, the acute versus developmental roles of presynaptic FMRP remain to be identified such that therapies can best be developed and strategized for particular developmental periods when circuits are most vulnerable to the loss of FMRP (Meredith et al., 2012).

MOTIVATION FOR STUDIES

Loss of FMRP in Fragile X Syndrome significantly alters structure and function at the synapse. Based on the overwhelming evidence for hyperexcitability, hypersensitivity and impaired cognitive function in Fragile X, an imbalanced excitation/inhibition function is obvious but the variable effects from the loss of FMRP, likely due to cell-type specificity, projection-specificity, and developmental period-specificity, demands for deeper inquiry into the circuit developments in Fragile X.

Postsynaptic loss of *FMR1* disrupts developmental pruning of L5A excitatory networks

While structural evidence of immature spine development in young and prevalence of overabundant spines in adults suggests enhanced circuit excitability, the functional outcomes of these remain unknown. Moreover, inconsistency in the anatomical findings demands additional inquiry of overabundant spines that uses a different approach to assert a clearer understanding of Fragile X circuitry. In

addition, the contexts in which these alterations in spine structure and function occur is not clear: It remains unclear whether the overabundance of spines, caused by the loss of FMRP, actually impacts circuits that developmentally, through experience-dependent mechanisms, undergo pruning. If so, then what impact loss of FMRP has in circuits that don't undergo experience-dependent developmental pruning needs clarification. While there is evidence that elimination is an ongoing process, and it is only the balanced rate of formation and elimination that maintains a set number of synapses after adolescence, whether FMRP regulates this "ongoing elimination" process or only experience-dependent elimination, remains unclear. Toward understanding these demarcations for FMRP's role in synaptic elimination, functional evidence for FMRP in driving experience-dependent pruning is required. In my work here, using multi-patch recordings between layer 5A pyramidal neurons, I show developmental pruning of layer 5A interconnectivities, and additionally show that loss of complete or postsynaptic *Fmr1* disrupts this developmental pruning that is purely circuit pruning and not weight pruning (Fig 1).

Loss of Presynaptic *FMR1* reduces Glutamate Release Probability onto FS Inhibitory Interneurons

Because spine dysgenesis has been the foundational effect in Fragile X Syndrome, little attention has inquired FMRP's mechanisms at synapses onto aspiny dendrites and soma. These synapses, because they lack the spine anomalies identified previously, may shed a different light on the synaptic disruptions at these synapses. Given that the spine anomalies are absent postsynaptically, are these synapses affected by presynaptic loss of FMRP? And what impact do these changes have on circuit function and the excitation/inhibition imbalance? A major aspiny input is that of the excitatory recruitment of fast-spiking inhibition that in the *FMR1* KO mouse has shown a robust deficit (Gibson et al., 2008). Whether this physiological phenotype represents relevance for presynaptic or postsynaptic FMRP remains unclear. In my current efforts, I mechanistically identify a role for presynaptic, and not postsynaptic, FMRP in driving optimal vesicular release onto fast-spiking interneurons. Moreover, I show that this role for FMRP may be global across different layers of the neocortex. Additionally, I show that acute ongoing FMRP is required to maintain this optimal transmission.

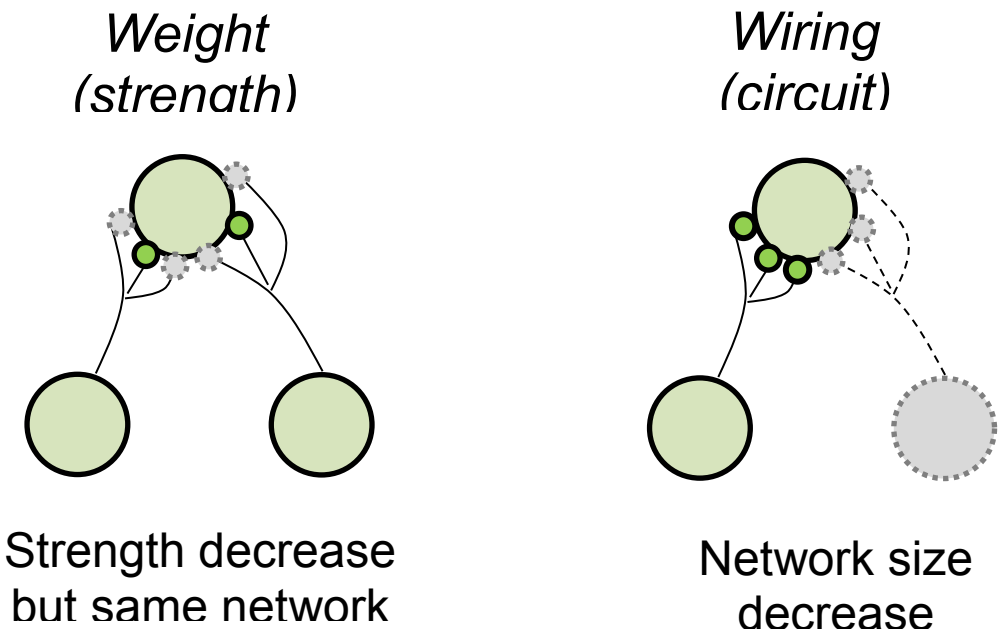

Figure 1. A schematic representation of the two forms of synaptic pruning

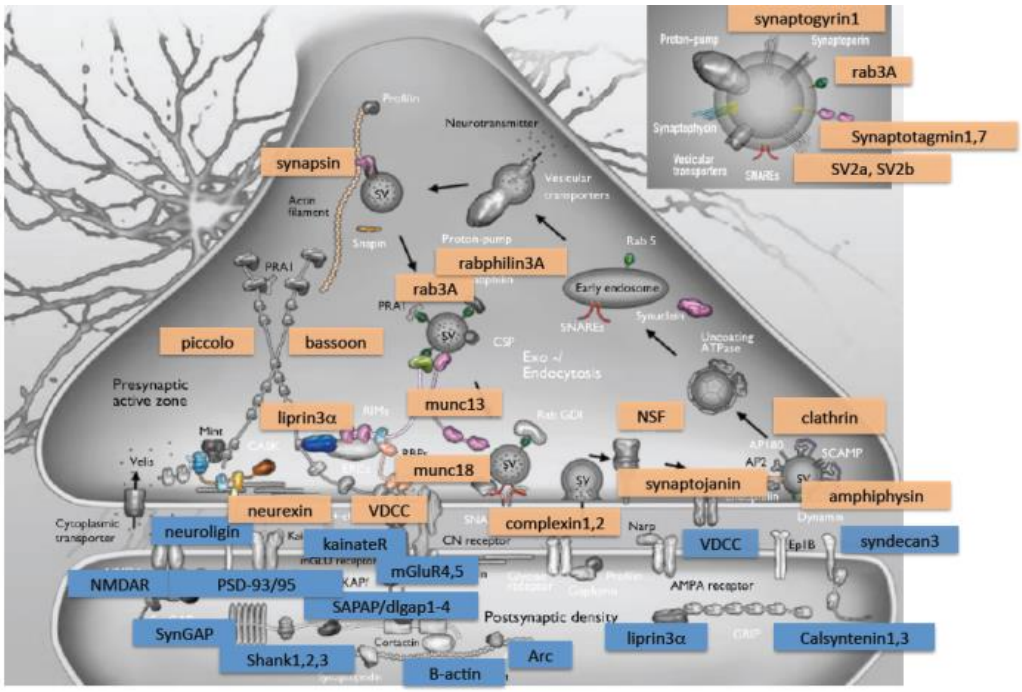

Courtesy of Jennifer Darnell

Figure 2. Presynaptic mRNA targets of FMRP

Based on the HITS-CLIP assay by Darnell et al., 2011, orange boxes represent FMRP targets that function presynaptically for optimal transmission.

CHAPTER TWO: METHODS

Methods

Mice

Congenic *FMR1* KO mice on the C57BL6 background were originally obtained from Dr. Stephen Warren (Emory University) (Bakker, 1994). X-linked GFP mice were originally composed of a mixed genetic background (Jackson Lab) (Hadjantonakis et al., 2001), but we have backcrossed them onto the C57Bl6 background for at least 4 generations. GFP/ *Fmr1* mosaic females did not express FMRP in about half of all neurons due to X-inactivation and were made by breeding X-linked GFP males with *Fmr1* KO females. To control for genetic and litter variability, only within litter comparisons were used for comparing *Fmr1* KO versus WT data. For all *Fmr1* KO experiments, we used males since this makes littermate comparisons of KO versus WT more feasible.

Immunocytochemistry

Mice (P14-20) were anesthetized with Euthasol and transcardially perfused following protocols approved by UT Southwestern. Perfusion rate was 1.7 mls/minute and began with ice cold saline for 1 minute followed by 15 minutes of 4% paraformaldehyde. The brain was then removed and postfixed in 4% paraformaldehyde for 30 minutes. The brain was removed and resectioned into 80μm slices. Antigen retrieval was performed by placing the slices into warm 200

mM sodium citrate and microwaving for 1 min at low power. The slices were blocked for 1 h at room temperature in PBS with 3% normal goat serum and 0.5% Triton-X. Primary antibodies were dissolved in blocking solution and applied overnight at 4°C. Secondary antibodies were dissolved in blocking solution and applied for 1 h at room temperature. Primary antibodies used were mouse anti-FMRP (2F5, 1:200, gift from Dr. Jennifer Darnell, Rockefeller University, New York, NY) and rabbit anti-GABA (A2052, 1:1000, Sigma). The specificity of 2F5 has been demonstrated previously (Gabel et al., 2004) and by our comparison of labeling inFmr1 KO versus WT tissue. Antibodies were for GFP (1:1500, chick, Aves lab, #GFP-1020; secondary: Alexa488, Invitrogen) and FMRP (1:200, mouse, 2F5, gift from Jennifer Darnell, Rockefeller University, New York, NY; secondary: Alexa555, Invitrogen). Images were collected on an inverted Zeiss LSM confocal microscope.

Electrophysiology

Mice (P13-P16) were anesthetized with Euthasol and the brain removed following protocols approved by UT Southwestern. Thalamocortical slices, 350 μm thick, were cut at ~4° C in dissection buffer, placed in normal ACSF at 35° C for 30 minutes, and slowly cooled to 21° C over the next 30 minutes. This slice preparation preserves thalamic input to the barrel cortex, interlayer projections within neocortex, as well as the local connectivity in all layers, and therefore, it is

a good preparation to examine circuit changes in mutant mice (Agmon and Connors, 1991). In the barrel field of somatosensory cortex, whole-cell recordings were performed in either layer 4 (inside a barrel) or layer 5 using IR-DIC visualization and an Olympus FV300 confocal microscope. The use of a confocal microscope enabled more reliable identification of GFP-negative neurons since background GFP fluorescence was high (~50% of cells express GFP). Recordings were performed at 21° C (Figs. 1-5) and at 32° C (Figs. 6-8). Data were collected with a 10 kHz sampling rate and a 3 KHz Bessel filter.

Layer 4 fast-spiking (FS) cells were identified by their large size and non-adapting, high firing rates (Connors and Gutnick, 1990; Gibson et al., 1999). The rare occurrence of FS neurons necessitated a high number of both *Fmr1* WT and KO neurons found in GFP/ *Fmr1* mosaic females since we needed to find FS-excitatory pairs in the 4 possible *Fmr1* expression configurations that were close in distance where the probability of connection is highest. Layer 5 FS neurons in the *Fmr1* KO line were identified by GFP fluorescence by cross breeding with the G42 mouse line.

For Layer 5A pyramidal neuron interconnectivity studies, 24 to 48 paired connections were tested per animal. On average, 3 slices were used from each animal. For NMDA experiments, different slices were used for every experiment to avoid ineffective washout of DNQX. Patched neurons were 0 – 30 um apart.

Electrophysiology Solutions

ACSF contained (mM): 126 NaCl, 3 KCl, 1.25 NaH_2PO_4, 2 $MgSO_4$, 26 $NaHCO_3$, 25 dextrose, and 2 $CaCl_2$. All slices were prepared in a sucrose dissection buffer as follows (mM): 75 sucrose, 87 NaCl, 3 KCl, 1.25 NaH_2PO_4, 7 $MgSO_4$, 26 $NaHCO_3$, 20 dextrose, and 0.5 $CaCl_2$. All solutions were pH 7.4. ACSF was saturated with 95% O_2 / 5% CO_2. The pipette solution consisted of (mM): 130 K-Gluconate, 6 KCl, 3 NaCl, 10 HEPES, 0.2 EGTA, 4 ATP-Mg, 0.3 GTP-Tris, 14 phosphocreatine-Tris, 10 sucrose. This was adjusted to pH 7.25 and 290 mOsm. The junction potential was ~10 mV and was not corrected. For NMDA interconnectivities in L5A, ACSF contained 4mM $CaCl_2$ and with no MgCl.

Drug Applications

For quantal and wild-type mimic experiments we reduced release probability using cadmium chloride ($CdCl_2$, Sigma). Quantal experiments also contained the $GABA_A$ receptor antagonist, picrotoxin (50 µM, Sigma), and the NMDA receptor antagonist, AP5 **[**D-2-Amino-5-phosphonovaleric acid**]** (50 µM, Sigma). For multivesicular release experiments we used Kynurenic acid (Sigma), gamma-D-glutamylglycine (γ-DGG, Tocris) and NBQX (Sigma). For miniature EPSC experiments, action potentials were blocked with tetrodotoxin (TTX, 1 µM,

Sigma) and $GABA_A$ receptors were blocked with picrotoxin.

For Layer 5 interconnectivity studies, To block AMPA currents and visualize NMDA currents, we washed on the AMPA receptor antagonist, DNQX (6,7-dinitroquinoxaline-2,3-dione;20 µM, Tocris) and the NMDA receptor co-agonist, Glycine (20 µM, Sigma). Cells were held at -50mV. To validate NMDA currents, we additionally washed on the NMDA receptor antagonist, CPP (3-[(R)-2-carboxypiperazin-4-yl]-prop-2-enyl-1-phosphonic acid; 15 µM, Tocris). Unitary NMDA EPSCs were generally smaller but we optimized the detection by providing enough time for complete magnesium washout, using glycine and holding the cells at -50mV. To avoid false positives, we averaged 50 stimulus responses and only accepted responses that were 3 times the average noise responses calculated in CPP (0.545 pA; n=7). Using this threshold, only 3/35 AMPA-mediated responses failed to show a corresponding NMDA response > 1.635pA (given that AMPAR expression is unlikely without NMDAR expression), suggesting that our NMDA uEPSC detection method was 86% accurate. Additionally, the distribution of responses < detection threshold was not biased to WT neurons (WT=2/9; KO=4/21). For L5A studies, miniature spontaneous recordings were made after blocking Sodium channels using 1µM TTX and blocking GABA currents using 25µM Picrotoxin.

MK-801 experiments

This protocol is based on previous studies (Castro-Alamancos and Connors, 1997; Rosenmund et al., 1993). All train intervals were 10 seconds, and the following compounds were part of a modified ACSF to isolate and promote NMDA-R mediated currents: 20 μM DNQX (Sigma), 3 mM Ca^{2+}, 0 mM Mg^{2+}, and 5 μM glycine (Sigma). The postsynaptic FS neuron was held at -50 mV. An initial train of 8 uEPSCs were acquired to obtain an average baseline uEPSC amplitude. Then MK-801 (40 μM) was applied. After a 10 minute wait to allow the compound to completely permeate the slice, a train of 75 uEPSCs were acquired. uEPSC amplitudes mediated by NMDA-Rs averaged around 15 pA. All uEPSC amplitudes during MK-801 were normalized to the average baseline amplitude. We then performed 2 sets of analyses. First, we fit a single exponential decay to the data obtained from each experiment (see Fig. 5G), and then compared the time constant for these decays between WT and KO. Fitting was performed in Sigmaplot 12 using the Levenberg-Marquardt method. Second, we binned and averaged the responses in each experiment based on the following intervals (ms): 1-5, 6-16, and every interval of 10 up to 75 (see Fig. 5H). Then we averaged this data across experiments and performed a 2-way ANOVA (presynaptic genotype x time interval), with the time interval dimension being repeated-measures. We examine the differences between WT and KO at each interval to confirm the changes in time constant derived for each experiment individually.

Cd^{2+} experiments measuring quantal amplitude

Experiments were performed in 5 µM $CdCl_2$. As in a previous study (Gibson et al., 2009), long action potential trains were applied, and the number (10-30) of action potentials were modified at a frequency of 20Hz to reduce the percent of action potentials evoking a uEPSC to < 20%. These uEPSCs are referred to as "successes" and were only analyzed if they occurred within ±0.3 ms of the average latency. The successes are considered to be "putative" quantal events. Systematic error in average quantal amplitude measurements was calculated in a previous study, where the overestimate in quantal amplitude (q) was dependent on the number of release sites, ranging from 0% for 1 release site to 18% for 10 release sites and the error in the relative difference in q between WT/WT and KO/WT pairs would be < 5% (Gibson et al., 2009). This analysis was performed on traces further filtered by a 3 point running average.

Multiple-probability fluctuation analysis (MPFA)

This method is based on a previous publication (Silver, 2003). The mean and the variance of the uEPSC were obtained at different release probabilities (P_V) and then were fitted to the parabolic equation, $Variance_A = q*A-(A^2/N_V)$, where A is the average uEPSC amplitude. The sample number for each point on the curve was 15-20. Fitting was performed in Sigmaplot 12 using the Levenberg-Marquardt method. The same stimulus train (3 action potentials at 33 Hz or 20

Hz) was employed at 2 different external Ca^{2+} concentrations (2 and 5 mM) to create different release probabilities (Bagnall et al., 2011; Huang et al., 2010; Silver, 2003) (also see Fig. 6A). Once the data were fitted with the parabolic function, the derived q and N_V were used to calculate P_V for the first uEPSC in the train (uEPSC1) in 2 mM Ca^{2+} using the equation (A/q)/ N_V. The AMPAR competitive antagonist, kynurenate (250 μm), was included in the ACSF to reduce postsynaptic saturation of responses. In figure 5, we show that kynurenate differentially blocks uEPSC1 in cases of presynaptic WT and KO neurons (33% and 48% blockade, respectively). Therefore, uEPSC1 and the accompanying variance were scaled down an additional 23% and 8% (for WT and KO, respectively) to match the blockade for uEPSCs occurring after uEPSC1 (55%). Some experiments were not included for analysis for the following reasons: 1) the average response amplitude changed by more than 25% during the experiment, 2) P_V range could not be extended to high enough values such that only a monotonic, increasing function was attained (not parabolic) (Huang et al., 2010; Lu and Trussell, 2000), or 3) the fitted curve crossed the y-axis at >20% maximum variance which indicates postsynaptic receptor saturation (Huang et al., 2010).

N_V and q were corrected for variance within single release sites and among all release sites by modification using CV_q (for details, see) (Hull et al., 2009; Meyer et al., 2001; Silver, 2003). CV_q was the coefficient of variation of q obtained from the Cd^{2+} experiments which directly measured q (CV_q = 0.25±0.02

and 0.29±0.02 for WT and KO, respectively. See Fig. 4). Again, these values were corrected for the use of kynurenate in the MPVA experiments.

Control experiments showed that AMPAR desensitization was not occurring during the trains applied above. We measured uEPSCs during 6 pulse trains (33 and 20 Hz) before and after wash-in of cyclothiazide (Sigma, 50 μM) – a blocker of AMPAR desensitization. Short-term plasticity was unaltered with the wash-in (uEPSC2/uEPSC1; 0.43±0.09 vs. 0.48±0.05; baseline, wash-in; n=7), while the fast component of the response decay increased (1.35±0.14 vs. 2.44±0.30 ms; $p<0.05$). Overlap of uEPSCs in a train with the longer decay were still minimal as seen by uEPSC2 amplitude only increasing <3% if we took the decay into account.

Adeno-associated virus

AAV was acquired from The University of Pennselvenia Vector Core Laboratory. Two AAV sereotypes were utilized: AAV2.1 Cre GFP and AAV2.9 Cre GFP. AAV2.1 GFP did not show Cre-GFP expression in spiny-stellate neurons of layer 4 in barrel cortex at age p21 suggesting this sereotype does not infect these cell-types well. Expression with the sereotype was apparent in all other layers. AAV2.9 Cre GFP showed Cre-GFP expression in all layers of the barrel cortex. Immunostaining of AAV-Cre-GFP mediated knockdown of FMRP was done primarily using AAV2.1 Cre GFP (Fig. 14).

Statistical Analysis

All statistics were performed using Sigmaplot (Systat Software, Inc.), and statistical significance was $p<0.05$. Unless otherwise stated, we used the nonparametric unpaired t-test (Mann-Whitney) when comparing 2 groups. For greater than 2 groups, Kruskal-Wallis one-way ANOVA on ranks was performed followed by a post hoc comparisons test (Dunn's method). Sample number (n) is cell or synaptically connected pair number. Data are represented by the mean ± SEM. Connectivity frequency changes are detected using the χ-square test, and a Fishers Exact P-value was used to determine significance.

CHAPTER THREE: EXCITATION OF FS INTERNEURONS

Loss of Presynaptic *FMR1* reduces Glutamate Release Probability onto FS Inhibitory Interneurons

Summary

In the mouse model of Fragile X Syndrome, the *Fmr1* knockout, local excitation of layer 4 fast-spiking (FS) inhibitory neurons is robustly decreased by 50%, but the mechanisms mediating this change are unknown. Here, I performed recordings in acutely prepared slices obtained from *Fmr1* "mosaic" mice where *Fmr1* is deleted in about half of all neurons, and I find that loss of presynaptic, but not postsynaptic, *Fmr1* fully recapitulates the deficit. The change in connection strength is primarily due to a decrease in multivesicular release and release probability indicating that FMRP normally positively regulates these processes. This change in presynaptic neurotransmitter release is observed both in the mosaic mice and in the constitutive *Fmr1* knockout mice. Manipulations in release probability enabled both the mimic and rescue of the impaired function in this synaptic pathway. Loss of presynaptic *Fmr1* has no effect on excitatory synapses onto excitatory neurons, indicating a target-cell specific function for presynaptic FMRP. Finally, I demonstrate that the excitation decrement onto FS

neurons also exists in layer 5 of the *Fmr1* KO suggesting a widespread role for presynaptic *Fmr1* in the excitation of inhibitory neurons. In summary, I identify a novel function for presynaptic FMRP in promoting presynaptic neurotransmitter release, and I show that loss of this function accounts for impaired excitation of neocortical FS inhibitory neurons. These changes may contribute to the cognitive dysfunction and circuit hyperexcitability associated with Fragile X Syndrome – including patients with complete deletion of FMRP and those with mosaic expression of FMRP.

Introduction

While a lot of evidence has suggested a significant role for FMRP at the post-synaptic site, only recent interest has revealed potential roles for FMRP at the presynapse (Akins et al., 2009) . FMRP does localize in axons and growth cones (Antar et al., 2006b). FMRP has been shown to regulate MAP1B (microtubule-associated protein 1B), a microtubule assembling protein important in axonal guidance. Recent work has also shown that FMRP, in a protein-synthesis-dependent manner, regulates growth cone motility in response to Semaphorin 3A, a guidance factor that regulates axonal projections during development (Li et al., 2009). Additionally, FMRP's role in axon guidance may incur misguided synapse formation toward modified functionality. Recent work

by Bureau et al. showed that cortical projections of the somatosensory cortex from layer 4 to layer 3 were defasciculated suggesting that FMRP promotes axon guidance and synapse formation toward functional synaptic strength (Bureau et al., 2008). Because this work was does in the global Fmr1 KO mouse it does not isolate the cell-autonomous roles of FMRP at the presynapse and postsynapse however. One cannot eliminate the possibility that the effects on synaptic function are a result of postsynaptic dysfunctions that drive presynaptic axons to defasciculate from their targets. Therefore, to better address the role of FMRP at the presynapse, axonal and synaptic physiology must be measured across presynaptic and postsynaptic Fmr1 genotypes. This would isolate a presynaptic vs. postsynaptic contribution of FMRP. Moreover, a lot of attention has gone into recognizing postsynaptic FMRP's role in functional deficits at synapses onto dendritic spines while little attention has been given to recognize what synaptic compartment FMRP regulates synaptic function onto aspiny terminals.

Recent work from our lab assessed the microcircuitry in layer 4 of the somatosensory cortex in the fragile X mouse model (Gibson et al., 2008). This work was motivated toward understanding synaptic physiology and neuron interconnectivity that could explain some of the behavioral deficits of FXS such as epilepsy and cognitive dysfunction – behaviors that are hypothesized to be mediated by altered neocortical function. The study identified a 50 % deficit in

the excitation of fast-spiking (FS) parvalbumin-positive inhibitory neurons by spiny-stellate excitatory neurons at adolescence and adult ages. This excitatory synapse terminates onto aspiny proximal dendrites and soma.

Using the mosaic Fmr1 mouse model, I show that loss of presynaptic, and not presynaptic FMRP determines the excitatory deficit onto fast-spiking inhibitory interneurons. Moreover, I recognize that the deficit is due to a reduction in multivesicular release without a significant change in the number of boutons. I also show the ability to rescue the phenotype with increased external calcium – a finding that suggests that the vesicular capacity to mediate optimal release is intact in presynaptic FMRP KO terminals. I also show that this role for presynaptic FMRP is target-cell specific such that excitation or neighboring excitatory neurons is not altered by the loss of presynaptic FMRP.

Excitation of fast-spiking neurons decrease with presynaptic Fmr1 deletion

I used GFP/*Fmr1* mosaic females where cells either co-express GFP and FMRP or express neither which I refer to as *Fmr1* WT and *Fmr1* KO neurons, respectively. FMRP is expressed in layer 4 barrel cortex at this age (Harlow et al., 2010). However, I wanted to validate that GFP expression in GFP/*Fmr1* mosaic mice faithfully reports FMRP expression. Immunohistochemistry

indicated that GFP reliably reported FMRP expression in the neocortex at the ages examined in this study (Fig. 3) – 159/159 GFP-positive (GFP+) neurons were also FMRP-positive (FMRP+), and conversely 159/168 FMRP+ neurons were GFP+. I next determined if FMRP is expressed in parvalbumin-positive inhibitory neurons since these are the biochemical identity of the FS neurons I examine in this study (Cauli et al., 1997; Gibson et al., 1999) . Using the G42 mouse line which selectively expresses GFP in parvalbumin-positive neurons, I found that 54/55 GFP+ neurons in the neocortex also express FMRP (in layer 4, this was 17/17) (Fig. 3).

I performed simultaneous whole-cell recordings of presynaptic excitatory and postsynaptic FS inhibitory neurons where I knew the genotype of all neurons (GFP indicating *Fmr1* WT, Fig. 3). Up to 4 neurons could be recorded simultaneously. I examined unitary excitatory postsynaptic currents (uEPSCs) in FS neurons in response to action potentials evoked in a single presynaptic excitatory neuron (Fig. 4). I compared the amplitude of the first uEPSC in a train (uEPSC1, 4 at 20 Hz) between all 4 groups of pre- and postsynaptic genotypic combinations, and found that *Fmr1* deletion in the presynaptic excitatory neuron greatly decreased uEPSC1 amplitude (Figs. 5A). The 2 presynaptic KO groups were both significantly different from the WT/WT (pre/post) group ($p<0.05$, $p<0.05$; 71.8±10.1, 34.4±5.1, 43.1±7.2 pA; WT/WT, KO/KO, KO/WT;

n=44,35,49), and the average amplitude of both presynaptic KO groups merged was only 54% of the WT/WT group. On the other hand, no difference was detected with postsynaptic *Fmr1* deletion (71.8±10.1, 79.2±15.5; WT/WT versus WT/KO; n=46,39). The difference between presynaptic *Fmr1* KO and WT groups represented a uniform shift in the distribution as indicated by the cumulative probability distribution (Fig. 5B). If I restrict our analysis to experiments in which I recorded presynaptic KO and WT neurons simultaneously and both had connections to the same WT postsynaptic FS neuron, I observe the same decrement with presynaptic *Fmr1* deletion ($p<0.05$; 117.5±26.2, 50.8±9.2 pA; WT/WT, KO/WT; n=10,10; paired t-test), indicating that our results are not due to heterogeneity of FS neurons or our biases in targeting FS neurons.

Both the probability of the occurrence of functional connections and short-term depression during the stimulus train were not detectably different among the four groups (Figs. 5D,E). No changes in the following uEPSC1 properties were observed: rise-time (0.66±0.1, 0.60±0.1, 0.68±0.1, 0.66±0.2 ms; WT/WT, KO/KO, WT/KO, KO/WT; n=24,17,16,25), decay time-constant (6.8±0.6, 6.0±0.6, 5.9±0.4, 6.5±0.4 ms; n=24,17,16,25), or onset latency (0.97±0.04, 1.08±0.05, 0.96±0.06, 0.93±0.03 ms; n=29,30,25,23). If we quantify connection probability in all WT/WT and KO/WT pairs in this study, the higher sample number allows us to detect an 18% decrease with presynaptic *Fmr1* deletion ($p<0.05$, 66% versus 54%; 85/129, 86/160; does not include MK-801

experiments). I did not perform control experiments testing the effect of GFP alone in GFP mosaic mice since a previous study, using the same GFP/*Fmr1* mosaic strategy to study synaptic transmission, performed this control and observed no effect on synaptic transmission between hippocampal pyramidal neurons (Hanson and Madison, 2007).

To determine if presynaptic deletion of *Fmr1* selectively affected excitation of FS neurons, I also examined the local excitation onto postsynaptic excitatory neurons in the GFP/*Fmr1* mosaic mice (Fig. 6). In this instance, I did not detect any effect on uEPSC1 amplitude or connection probability under any combination of *Fmr1* deletion (Figs. 6). Therefore, while the decrease in excitation is due to *Fmr1* deletion in presynaptic excitatory neurons, this decrease is postsynaptic-specific and only occurs at FS inhibitory neurons. These results implicate a target-cell specific function for presynaptic *Fmr1*.

I next examined the role of selective pre- and postsynaptic deletion of *Fmr1* on local inhibitory synaptic function of FS neurons. Similar to what I observed in the complete *Fmr1* KO (Gibson et al., 2008), I did not detect any changes in unitary inhibitory postsynaptic currents (uIPSCs) originating from FS neurons as a function of pre- or postsynaptic deletion of *Fmr1* (amplitude: 14.2±2.4, 16.1±3.1, 16.4±3.5, 13.0±1.4 pA; n=16,17,25,15; connection probability: 34,33,31,26%; n=47,51,80,57; WT/WT, KO/KO, WT/KO, KO/WT

for Excitatory/FS neurons). These results suggest that the cell autonomous role of presynaptic *Fmr1* is specific for excitatory synaptic transmission.

The results concerning both uEPSCs and uIPSCs very closely follow that found in the constitutive *Fmr1* KO mouse where the identical synaptic connections have been examined (Gibson et al., 2008). On the other hand, the increased membrane excitability found in L4 excitatory neurons in the *Fmr1* KO (Gibson et al., 2008) was not observed in KO neurons in the mosaic. No changes in input resistance (594±42, 592±31 MΩ; WT,KO), resting potential (-63±1, -64±1 mV), the number of action potentials evoked with 15 pA and 30 pA steps (data not shown), or threshold current to evoke an action potential (30±4, 32±3 pA) were observed in excitatory neurons (n=46,47). Similarly, no changes were observed in FS neurons (n=63,68; data not shown). Therefore, while I cannot rule out a role for sex since the *Fmr1* KO data were collected from males, changes in intrinsic membrane properties in the constitutive *Fmr1* KO appear to not be cell autonomous.

Quantal content is decreased with presynaptic Fmr1 deletion

To determine the mechanism underlying the decrease in uEPSC size, I used a simple classical model of neurotransmission that defines a unitary response: uEPSC = m*q, where m is quantal content (the total number of quanta released over all synapses) and q is average quantal size over all synapses (Johnston and

Wu, 1995). Therefore, a decrease in uEPSC amplitude may be due to a decrease in either m or q. I first examined quantal content (m). According to the model above, if quantal content is decreased with presynaptic deletion of *Fmr1*, the coefficient of variation (CV, see methods) of the uEPSC1 amplitude must increase. Indeed, the CV was significantly increased with presynaptic *Fmr1* deletion (Figs. 7A,B; $p<0.05$ and $p<0.05$ for WT/WT versus KO/KO and WT/WT versus KO/WT; 0.24±0.01, 0.40±0.03, 0.42±0.02; WT/WT, KO/KO, KO/WT, n=28,22,29), but no difference was detected with postsynaptic deletion (0.24±0.01, 0.25±0.02; WT/WT versus WT/KO; n=28,23).

I also examined the failure rate of uEPSC1s – the proportion of trials in which a presynaptic action potential evoked no uEPSC1 (Fig. 7C). As expected with decreased quantal content, failure rate was increased with presynaptic deletion (Fig. 7D; $p<0.01$; 0.02±0.01 vs. 0.11±0.02; WT/WT vs. KO/WT, n=44,49). Finally, the relationship of CV to uEPSC1 amplitude was unchanged with presynaptic deletion (Fig. 7E, F) indicating that the CV change can be best explained by the shift in uEPSC1 amplitude.

While the decrease in uEPSC amplitude with presynaptic deletion of *Fmr1* involves a decrease in quantal content, average quantal amplitude (q) may also play a role. To investigate this possibility, in a subset of recordings involving only WT/WT and KO/WT genotypic combinations, I washed in the general Ca^{2+}-channel blocker, Cd^{2+} (5 μM $CdCl_2$), to reduce release probability to a point

where a train of presynaptic action potentials (10-30 at 20Hz, see Methods) successfully evoked a uEPSC only 20% of the time or less (Figs. 8 C,D). Under these conditions, I consider "successes" to be putative quantal events (i.e. the release of a single vesicle) (Gibson et al., 2009; Gil et al., 1999). I found no genotypic differences in success amplitude with application of Cd^{2+} (Fig. 8E; 9.9±1.2 vs. 10.5±1.5 pA; WT/WT vs. KO/WT; n=18,14) even though average uEPSC amplitude before application was decreased with presynaptic *Fmr1* deletion (Fig. 8A,B,F). In conclusion, most of the decrease in uEPSC amplitude is most likely due to a decrease in quantal content and not quantal amplitude (q).

Multivesicular release is decreased with presynaptic Fmr1 deletion

Multivesicular release is the ability for a single action potential to induce the fusion of multiple vesicles at a single locus with the resulting release of neurotransmitter binding to a common pool of postsynaptic receptors (Foster et al., 2002; Oertner et al., 2002; Wadiche and Jahr, 2001). From now on, I refer to this single release locus and postsynaptic receptor pool as a single synapse. Multivesicular release occurs at excitatory synapses targeting FS neurons in somatosensory cortex (Bagnall et al., 2011; Watanabe et al., 2005), and therefore, the average quantal content released at single synapse (m_{syn}) can be greater than 1. In our simple model of neurotransmission, quantal content (m) can be described

as a function of the number of synapses (N_{Syn}) and m_{syn}: $m = N_{Syn} * m_{Syn}$ (modified from (Johnston and Wu, 1995)). Measuring a change in N_{Syn} in the context of paired recordings would be difficult, but measuring a change in m_{Syn} might be relatively straightforward. In the above model, m_{Syn} is directly proportional to release probability at the synapse (P_{Syn}). The lack of change in short-term plasticity might suggest no change in P_{Syn}, but these two processes are not always simply linked (Brody and Yue, 2000; Kraushaar and Jonas, 2000; Regehr and Stevens, 2001). I used measurements of multivesicular release (m_{Syn} >1) at this synaptic connection to probe for changes in P_{Syn} as a possible mechanism underlying the decrease in uEPSC amplitude. Consistent with our logic, it has been shown that P_{Syn} controls the extent of multivesicular release this synaptic connection (Watanabe et al., 2005).

Multivesicular release is usually inferred by varying release probability and observing changes in both the transient glutamate concentration and the degree of postsynaptic receptor saturation (Foster et al., 2002; Wadiche and Jahr, 2001). Changes in transient glutamate concentration and receptor saturation at individual synapses are assayed by the amount of blockade of the EPSC by a low-affinity competitive AMPA receptor (AMPAR) antagonist, such as kynurenate (Wadiche and Jahr, 2001). To determine if the decrement in excitation of FS neurons was due to changes in multivesicular release, I washed in kynurenate (250 μM) and varied release probability by applying 2 presynaptic action

potentials per trial (50 ms interval) (Rudolph et al., 2011). For each uEPSC, I measured the amount of blockade by kynurenate ($uEPSC_{Before}$-$uEPSC_{Antag}$)/$uEPSC_{Before}$). Because of short-term depression and vesicle depletion, multivesicular release, when it exists, is more prominent during uEPSC1 than uEPSC2, and therefore, blockade would be less than uEPSC2 due to more glutamate being in the cleft. Recordings with WT/WT pairs shoId greater blockade with the second uEPSC (uEPSC2) compared to the first (uEPSC1) (Figs. 9A,B ; $p<0.02$; 0.32±0.03 vs. 0.51±0.04; uEPSC1 vs uEPSC2; n=14) which indicated a higher transient glutamate concentration in the synaptic cleft, and hence multivesicular release, during uEPSC1. The same was true for KO/WT pairs since the blockade of uEPSC2 was greater (Fig. 9B; $p<0.01$; 0.47±0.02 vs. 0.58±0.02; uEPSC1 vs uEPSC2; n=13). This effect was specific for the competitive nature of kynurenate since a non-competitive antagonist, NBQX (75 nM), decreased uEPSC1 and uESPC2 equally (Figs. 9C). When comparing the block of uEPSC1 between WT/WT and KO/WT pairs, the blockade was greater in KO/WT pairs (Fig. 9D; $p<0.01$) indicating that less glutamate was released and less multivesicular release occurred with presynaptic *Fmr1* deletion. No genotypic difference was observed with NBQX blockade of uEPSC1 (Fig. 9E).

In addition to multivesicular release, changes in spillover from neighboring synapses and the efficacy of single quanta (q) could account for the differences in cleft glutamate concentration. I observed no change in q (see Fig.

6E). Inadequate pore-fusion during normal synaptic transmission could also change q but this is probably not occurring since both risetime and decay time-constants were not detectably altered (risetimes: 0.40±0.03, 0.43±0.02 ms; decay times: 4.6±0.6, 4.8±0.5 ms; WT/WT, KO/WT; n=11,9) (Christie and Jahr, 2006). Spillover has not yet been observed in cortical structures at the low frequency stimulation that I applied nor under any circumstance during AMPAR-mediated glutamate transmission (Arnth-Jensen et al., 2002; Christie and Jahr, 2006; Sun and Beierlein, 2011). A role for spillover is also unlikely since kynurenate did not affect the decay times of the uEPSCs in WT/WT pairs (4.6±0.6,4.5±0.7 ms; before versus during kynurenate; n=14) (DiGregorio et al., 2002). Therefore, I attribute the effects of presynaptic *Fmr1* deletion on kynurenate sensitivity to a decrease in multivesicular release (or in other words, a decrease in m_{Syn}).

As explained above, a decrease in multivesicular release most likely reflects a decrease in P_{Syn} since fewer vesicles are released per action potential. As in figure 1H, I did not observe a change in short-term plasticity (Fig. 9F). Receptor saturation was not masking a change since short-term depression was not different between presynaptic WT and KO conditions during kynurenate application (normalized EPSC2: 0.40±0.02, 0.42±0.02; pre-WT,pre-KO).

AMPAR desensitization likely did not confound our results for 3 reasons: 1) I observed no desensitization using cyclothiazide in control experiments (see Methods, MPFA) which is consistent with previous studies using train stimulation

frequencies (Galarreta and Hestrin, 1998; Rozov et al., 2001) (but see (Watanabe et al., 2005)), 2) the NBQX results reveal the specificity of the kynurenate results for competitive blockade, and 3) our conclusions based on uEPSC1 would not be affected by desensitization.

Release Probability Is decreased with presynaptic Fmr1 deletion

To confirm our interpretation that a decrease in P_{Syn} is occurring with presynaptic *Fmr1* deletion, I made a second, independent measure of release probability by isolating NMDA-R mediated uEPSCs and determining how quickly the irreversible, open-channel NMDA-R antagonist, MK-801 (40 μM), could block responses during a 75 pulse stimulus train (Castro-Alamancos and Connors, 1997; Rosenmund et al., 1993) (see Methods, Fig. 10G). If P_{Syn} decreases with presynaptic *Fmr1* deletion, then the rate to full blockade by MK-801 should be slower. Single exponential decay functions were fit to the data for each experiment (Fig. 10G). Two forms of analysis of this data indicated that the rate was indeed slower with presynaptic *Fmr1* deletion. First, the binned and averaged data from each experiment were averaged across all experiments (see Methods, Fig. 10H), and 4 of the points were higher with presynaptic *Fmr1* deletion indicating that the rate to full blockade was slower. Second, the average time constant, derived from each individual experiment, was higher with

presynaptic deletion (Fig. 10I). It is unlikely that the difference in MK-801 blockade was due to different NMDA-R subtypes being expressed since the decay time constant of the uEPSC was unchanged (29.4 ± 5.5 vs. 26.8 ± 4.5 ms; n=8,6; WT,KO).

Presynaptic $GABA_B$-R activation is known to decrease release probability at glutamatergic synapses (Chalifoux and Carter, 2010; Isaacson et al., 1993) and GABAergic synaptic transmission is known to be altered in some brain structures of the *Fmr1* KO (D'Hulst and Kooy, 2007; Olmos-Serrano et al., 2010). Therefore, it is possible that increased $GABA_B$-R activation at presynaptic terminals mediated the effect, but I found this to not be the case since a comparison of uEPSC amplitude before and after wash-in of a $GABA_B$-R antagonist (CGP55845, 2 µM) had no effect at either presynaptic WT or KO connections (WT: 67.5 ± 13 vs. 66.9 ± 12; n=10. KO: 51.7 ± 13 vs. 49.9 ± 11; n=10: before vs. after). The lack of an effect was not due to ineffective CGP55845 since I demonstrated that it could bring uEPSC amplitude back to normal after suppression with the $GABA_B$-R agonist, Baclofen (500 nM) (n=2, data not shown).

The presynaptic Fmr1 KO phenotype is mimicked with a decrease in release probability

If presynaptic *Fmr1* deletion simply causes a decrease in release probability, I should be able to simultaneously mimic the uEPSC amplitude decrease and greater kynurenate block by simply decreasing release probability in a WT/WT pair. I did this by applying the Ca^{2+}-channel blocker, Cd^{2+} ($CdCl_2$). First, I experimentally determined the relationship between Cd^{2+} concentration and the fractional block of uEPSC1 (Fig. 11A, 2 pulses, 50 ms interval). I fit a sigmoid curve (see Methods) to the raw data points and found that approximately 2.6 μM Cd^{2+} reduced the WT/WT uEPSC1 by a fraction equal to that between the average uEPSC1 derived from WT/WT and KO/WT pairs (0.40, dashed lines in Fig. 11A; based on data from Figs. 5,8). Importantly, the average quantal content at this concentration (m_{Cd}) is assumed to equal that of the KO/WT pairs in normal ACSF (m_{KO}) since I have demonstrated that quantal size (q) is unchanged (see Fig. 8).

Next, I performed experiments in 2.6 μM Cd^{2+} and examined multivesicular release during uEPSC1 by again washing in kynurenate (250 μM) (Fig. 11B). There are 3 possible results when comparing blockade of uEPSC1 (B_{Cd}) with that of KO/WT data (B_{KO}), and I interpret these results based on the equation, $m= N*m_{Syn}$ (as defined above with $N= N_{Syn}$ for brevity), and on the assumption that Cd^{2+} does not alter N ($N_{Cd}=N_{WT}$): 1) $B_{Cd}>B_{KO}$ indicates $m_{Syn\_Cd}<m_{Syn\_KO}$ and $N_{WT}>N_{KO}$, 2) $B_{Cd}=B_{KO}$ indicates $m_{Syn\_Cd}=m_{Syn\_KO}$ and $N_{WT}=N_{KO}$, 3) $B_{Cd}<B_{KO}$ indicates $m_{Syn\_Cd}>m_{Syn\_KO}$ and $N_{WT}<N_{KO}$. Therefore, this

experiment potentially reveals the relative roles of release probability and functional synapse number to the change in uEPSC amplitude.

Our results most closely matched scenario 2 where blockade closely mimicked that of the KO/WT uEPSC1s (Fig. 11C; $p<0.01$ for WT/WT vs. WT/WT+ Cd^{2+}; 0.32±0.03, 0.44±0.02, 0.45±0.02; WT/WT, KO/WT, WT/WT+Cd^{2+}; n=14,15,11). These data support 3 conclusions: 1) that the difference in multivesicular release is a direct result of changes in P_{Syn}, 2) that a simple decrease P_{Syn} primarily accounts for the decrease in uEPSC1 amplitude with *Fmr1* deletion in the presynaptic neuron, and 3) that the a decrease in the number of functional synapses (N_{Syn}) plays a less significant, undectable role. Interestingly, I observed no change in short-term plasticity in 2.6 μM Cd^{2+} (Fig. 11D) further indicating that release probability and short-term plasticity are not strongly linked at this synapse – at least under these specific conditions. Risetime and decay time-constant were not different from WT or KO reported above (risetime = 0.47±0.03 ms; decay time = 4.8±0.05 ms; n=11).

The presynaptic Fmr1 KO phenotype is rescued with an increase in release probability

I next attempted the complimentary test by determining if the KO/WT uEPSC amplitude and kynurenate blockade can be simultaneously rescued to WT

characteristics. In this instance, I increased release probability in KO/WT pairs by applying higher Ca^{2+} concentrations. First, I experimentally determined the relationship between Ca^{2+} concentration and the fractional increase in uEPSC1 (Fig. 12A, 2 pulses, 50 ms interval), and I found that 6 mM increased uEPSC1 to a similar degree as the average fractional increase from KO/WT to WT/WT groups (0.62 increase; based on data from Figs. 5,9). I assume this increases the quantal content to the WT level ($m_{Ca}=m_{WT}$). This manipulation has a possible confound since AMPARs at glutamatergic synapses targeting FS neurons are Ca^{2+}-permeable, but I found this possibility to have minimal impact since mEPSC amplitude in FS cells was not detectably altered with 6 mM Ca^{2+} wash-in (17.8±0.26 vs. 17.3±0.24 pA; before vs. washin; n=5).

I proceeded to perform experiments in 6 mM Ca^{2+} and examined multivesicular release by again washing in kynurenate (250 μM) (Fig. 12B). As stated in the mimic experiment above, there are 3 possible results when comparing blockade of uEPSC1 with that of WT/WT data, each with an interpretation based on $m=N*m_{Syn}$ (again, $N= N_{Syn}$) and assuming $N_{Ca}=N_{KO}$. The kynurenate block very closely matched that found in WT/WT pairs indicating that a rescue to normal multivesicular release underlies the rescue to normal uEPSC1 amplitude. (Fig. 12C; $p<0.02$ for KO/WT vs. KO/WT+ Ca^{2+}; 0.32±0.03,0.44±0.02, 0.33±0.04; WT/WT, KO/WT, KO/WT+Ca^{2+}; n=14,15,7). Risetime and decay time-constant were not different from WT or KO reported

above (risetime = 0.36±0.06 ms; decay time = 4.9±1 ms; n=7). With this manipulation, I did observe a change in short-term plasticity where depression was slightly more pronounced (Fig. 12D), and therefore, the rescue could not mimic this aspect of synaptic transmission. In summary, both the mimic and rescue experiments further support a model where FMRP plays a prominent role in regulating glutamate release (P_{Syn}) and that its absence in the presynaptic neuron underlies decreased glutamatergic transmitter release, and consequently, decreased uEPSC amplitude. Both experiments suggest that changes in functional synapse number (N_{Syn}) play a less prominent role.

Multivesicular release is decreased in the constitutive Fmr1 KO

The similar decrement in uEPSC amplitude in the mosaic and constitutive KO suggests that both mouse models may share a common mechanism of impairment. If this is true, then I would predict that the excitatory connection onto FS neurons in the *Fmr1* male KO should also have decreased P_{Syn}. Because of experimental ease, I again used the multivesicular release assay as a measure of P_{Syn}. I performed the same experiment as in the mosaic (2 pulses, 50 ms interval) except that I used a more specific compound for competitively blocking AMPA receptors, γ-DGG (500 μM) (Fig. 13A). I observed that the glutamate cleft concentration during uEPSC1 was greater in WT connections since the amount of

block was less for uEPSC1 compared to uEPSC2 (Figs. 13A,B; $p<0.05$; 0.28±0.04 vs. 0.41±0.04; WT; n=11). As in the mosaic, γ-DGG blocked uEPSC1 in the *Fmr1* KO to a greater extent (Fig. 13C; $p<0.05$; 0.28±0.04 vs. 0.41±0.05; WT vs. KO; n=11,11) indicating that cleft glutamate concentration, multivesicular release, and P_{Syn} were indeed decreased in the *Fmr1* KO. I observed no change in short-term plasticity in the *Fmr1* KO slices (Fig. 13D) which is consistent with the data above and our previous study (Gibson et al., 2008).

Acute loss of presynaptic Fmr1 reduces excitation onto FS interneurons

In an effort to recognize whether early developmental or ongoing, acute loss of presynaptic Fmr1 determines the reduced unitary strength onto FS interneurons, I used AAV-Cre-GFP to acutely knockdown presynaptic or postsynaptic Fmr1 postnatally in floxed-Fmr1 mice. Using a previously applied method of stereotaxic injection of AAV-Cre-GFP into the ventricles of p1 pups, I recorded unitary strengths from presynaptic or postsynaptic infected and non-infected spiny-stellate neurons of layer 4 at p19-p21 (Lu et al., 2009). Based on the immunostaining for FMRP, complete loss of FMRP was predicted to have occurred at ~p13 using an AAV9 sereotype (Fig. 14). I found that acute, 6 to 8 days, loss of Fmr1 in the presynaptic, and not postsynaptic, compartment recapitulated the phenotype identified in the mosaic Fmr1 animal (Fig 14).

Control experiments nullifying Cre's effect on synaptic strength were not performed and will be required to confirm that it is purely Fmr1 deletion that acutely reduces the synaptic strength.

Impaired excitation of FS neurons in layer 5 in the Fmr1 KO mouse

To begin to determine if the impairment in the excitation of FS neurons exists outside of layer 4, I examined the same connection in layer 5. If it occurs there as well, this would increase the relevance of our findings above by opening the possibility that it occurs throughout the neocortex. I evoked action potentials in layer 5 pyramidal neurons (4 with a 50 ms interval) and measured uEPSCs in neighboring FS neurons (identified by GFP, see Methods) and compared uEPSC amplitude and connectivity between constitutive KO (*Fmr1* KO) and WT male mice. As I found previously for the same connection in layer 4 (Gibson et al., 2008), uEPSC1 amplitude was decreased in the *Fmr1* KO ($p<0.05$; 27.5±3.2, 19.2±2.9 pA; WT, KO; n=23,20). I observed no alteration in connection probability (41%, 41%; WT, KO n=23/56, 20/48) or short-term plasticity (Average(uEPSC3,uEPSC4)/uEPSC1; 0.26±0.02, 0.25±0.03; WT, KO; n=20,18).

For the uIPSC originating from the FS neuron and measured in the excitatory neuron, no change in uIPSC amplitude was observed (11.0±3 vs 9.4±1;

WT, KO; n=6, n=15), but there was increased connectivity in the *Fmr1* KO (p=0.02; 11% vs. 31%; 6/56,15/48). Together with the lack of any uIPSC change at this connection in layer 4, these data indicate that GABAergic synaptic input originating from nearby neocortical FS neurons is either normal or slightly enhanced in the *Fmr1* KO.

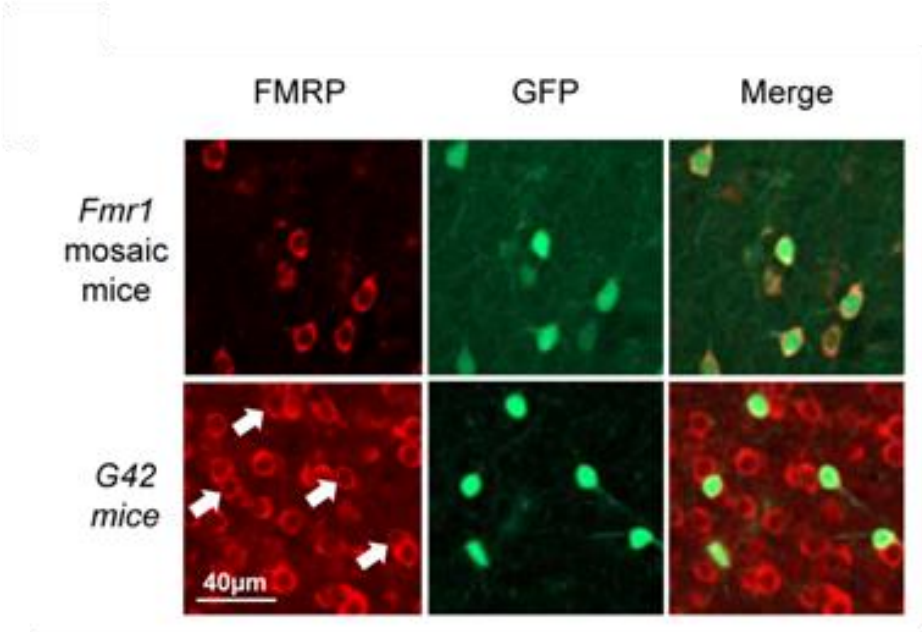

Figure 3. Immunohistochemistry for GFP and FMRP in somatosensory neocortex of mosaic Fmr1 female mice Immunohistochemistry for GFP and FMRP in somatosensory neocortex at P14. Top: In GFP/*Fmr1* mosaic mice, GFP marks neurons that express FMRP, while lack of GFP indicates no FMRP. Bottom: In WT mice expressing GFP in parvalbumin-positive FS neurons, FMRP colocalizes with GFP indicating that FS neurons express FMRP. (From Patel et al., 2013)

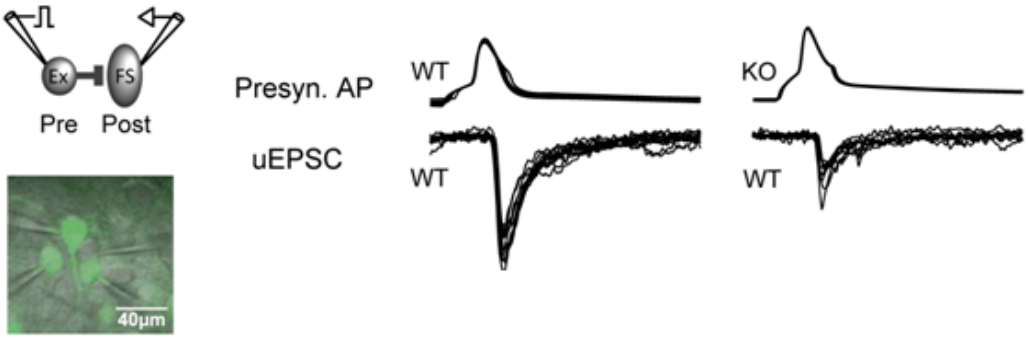

Figure 4. Traces of evoked single-axon unitary EPSCs

Diagram (left) of glutamatergic connection examined. Bottom: In live mosaic slices, GFP-positive and GFP–negative neurons were clearly identified. (Right) unitary EPSC responses to presynaptic action potentials. (From Patel et al., 2013)

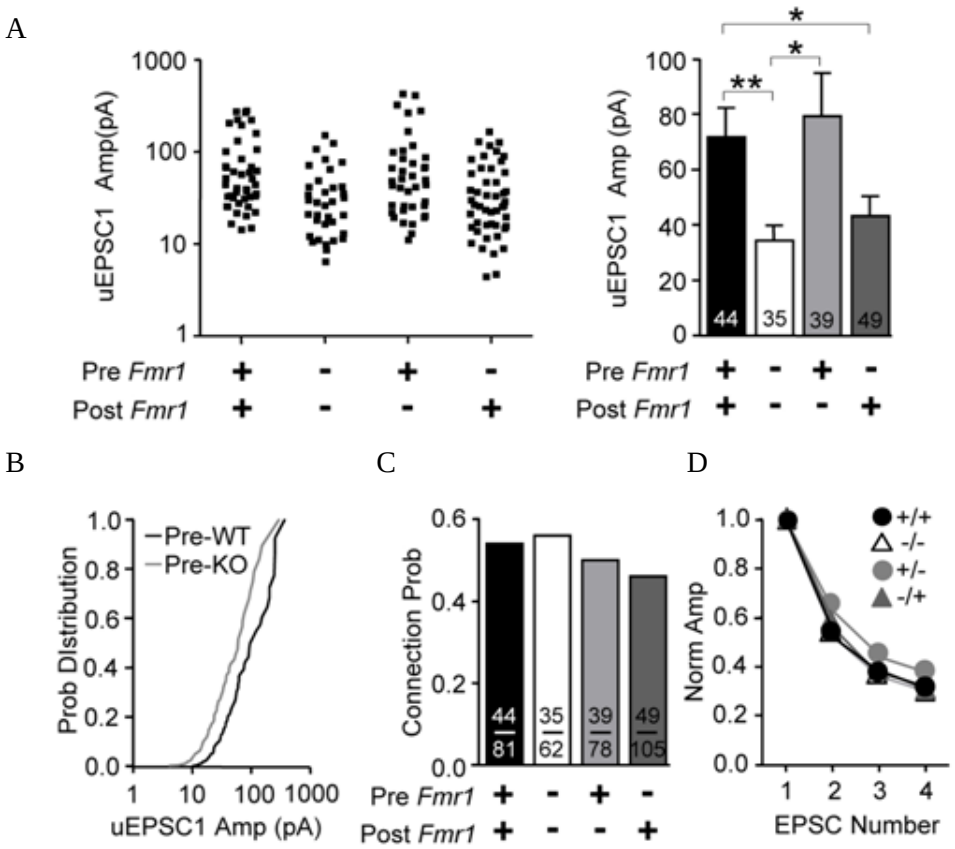

Figure 5. Unitary EPSC strength is reduced with presynaptic loss of Fmr1 A) Scatterplot (left) and bargraph (right) showing that average uEPSC1 amplitude was smaller whenever *Fmr1* was deleted from the presynaptic excitatory neuron. (B) Cumulative distribution of uEPSC1 amplitude for merged presynaptic KO and merged presynaptic WT groups. (C) No detectable change in connection probability was observed. (D) Average normalized uEPSC amplitude during the train of 4 presynaptic action potentials was unchanged. * $p < 0.05$, ** $p < 0.01$. (From Patel et al., 2013)

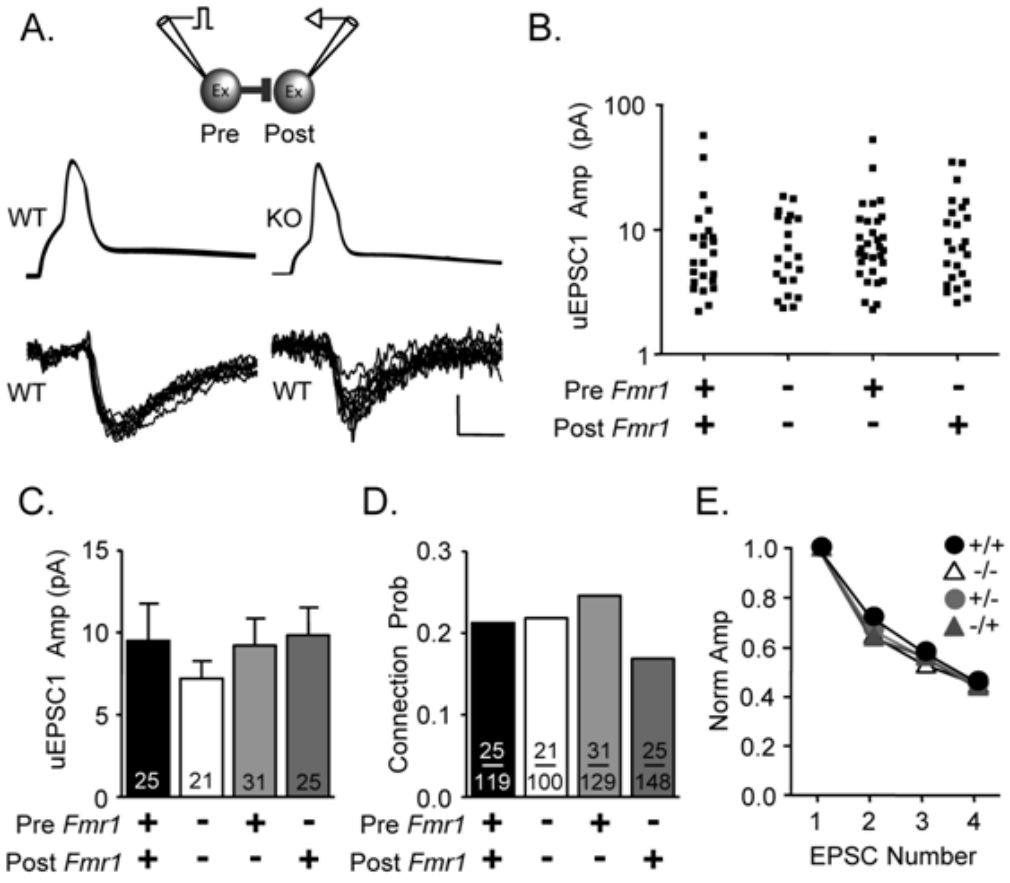

Figure 6. Unitary excitation of postsynaptic excitatory neurons was not affected by *Fmr1* deletion in mosaic mice . (A) Top: Diagram of the connection examined. Bottom: Example traces of simultaneous recordings of excitatory neurons. Scale bars: vertical = 50 mV, 10 pA; horizontal = 5 ms. (B,C) Scatterplot and bargraph showing that average uEPSC1 amplitude was not affected by *Fmr1* deletion. (F) Connection probability was unchanged. (E)

Average normalized uEPSC amplitude during the train of 4 presynaptic action potentials was unchanged. (From Patel et al., 2013)

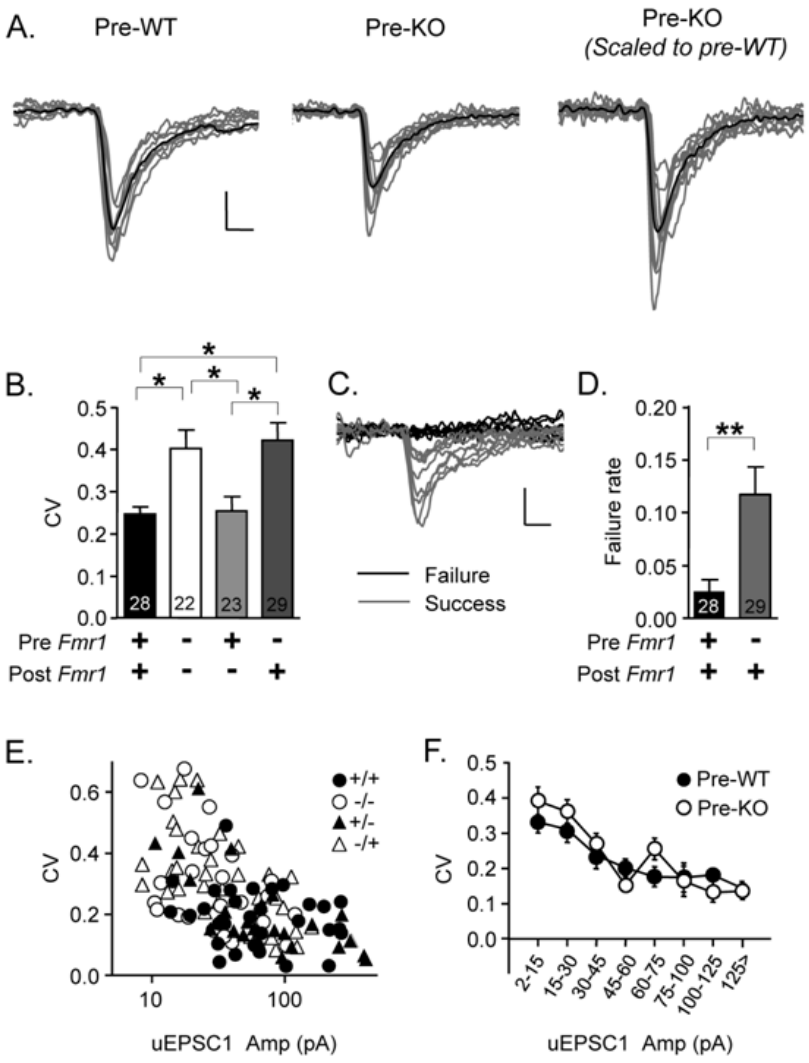

Figure 7. Increases in the coefficient of variation (CV) and unitary failures with presynaptic *Fmr1* deletion indicate quantal content is decreased. (A) Left and middle: Example uEPSC1s from WT/WT and KO/WT pairs. Right:

Same KO/WT traces scaled to match average WT/WT uEPSC1 and to highlight variability. Black traces are average. (B) Plot of CV versus genotypic combination of pre- and postsynaptic neurons. CV is higher with presynaptic deletion of *Fmr1*. (C) Examples of unitary "failures" from a KO/WT pair. (D) The proportion of unitary failures was higher in KO/WT pairs compared to WT/WT pairs. (E) Scatter plot of CV versus uEPSC1 amplitude. (F) Data from E merged into presynaptic KO versus presynaptic WT groups and binned. * $p < 0.05$,** $p < 0.01$. Individual uEPSC traces in A and C are a running average of 3 samples. Scale bars in A and C: 20 pA, 2 ms. (From Patel et al., 2013)

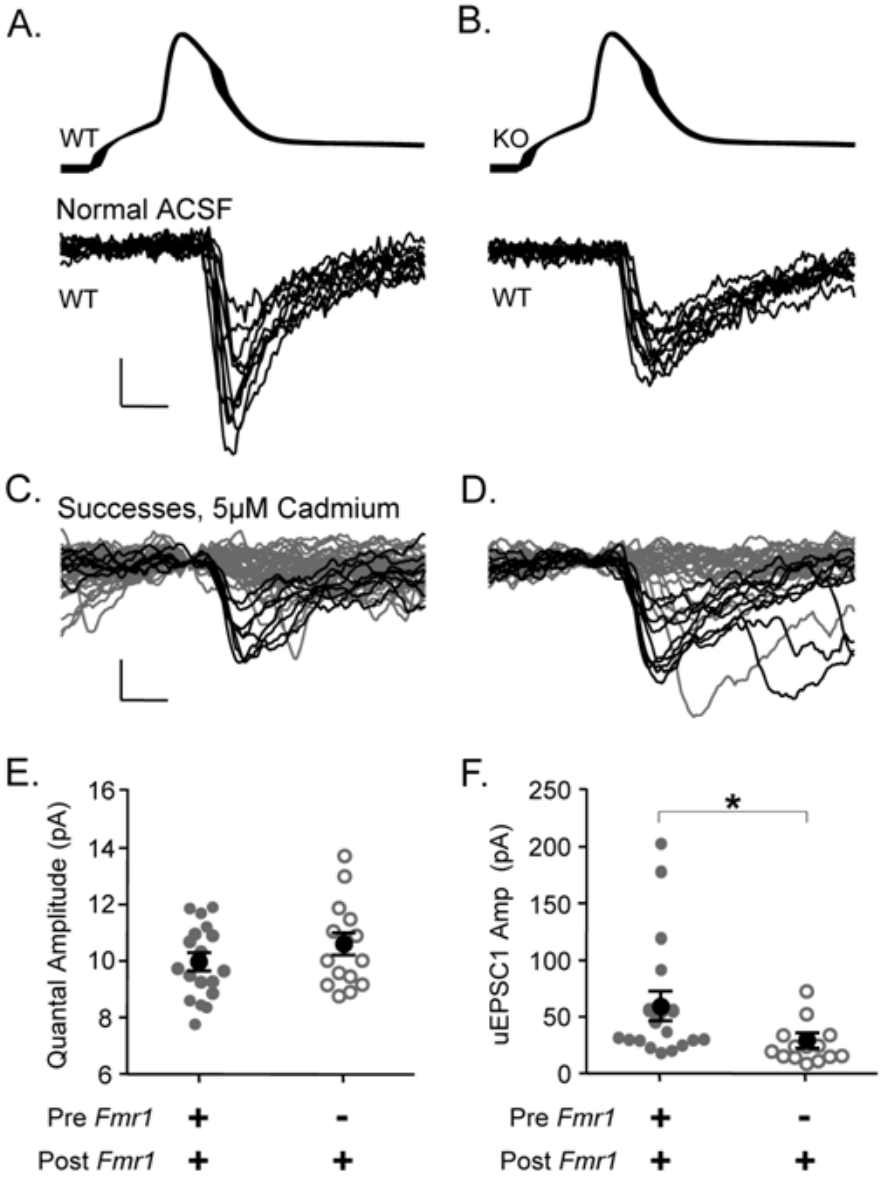

Figure 8. Quantal amplitude (q) does not depend on presynaptic *Fmr1* expression. Examples of uEPSCs before (A,B) and after (C,D) wash-in of $CdCl_2$ to lower the probability of release to the point where it is assumed isolated single quanta are observed. Note the decreased uEPSC amplitude and increased failures

after wash-in. Black and gray lines indicate successes and failures, respectively. Scale bars for A,B: vertical = 50 mV, 20 pA; horizontal = 2 ms. Scale bars for C,D: 10 pA, 2 ms. (E) uEPSCs were averaged during $CdCl_2$ application (excluding failures) to obtain an estimate of the average quantal amplitude. This was unchanged. (F) uEPSC amplitude before wash-in was smaller in the KO/WT pairs in these experiments. * $p < 0.05$. uEPSC traces are a running average of 3 samples. (From Patel et al., 2013)

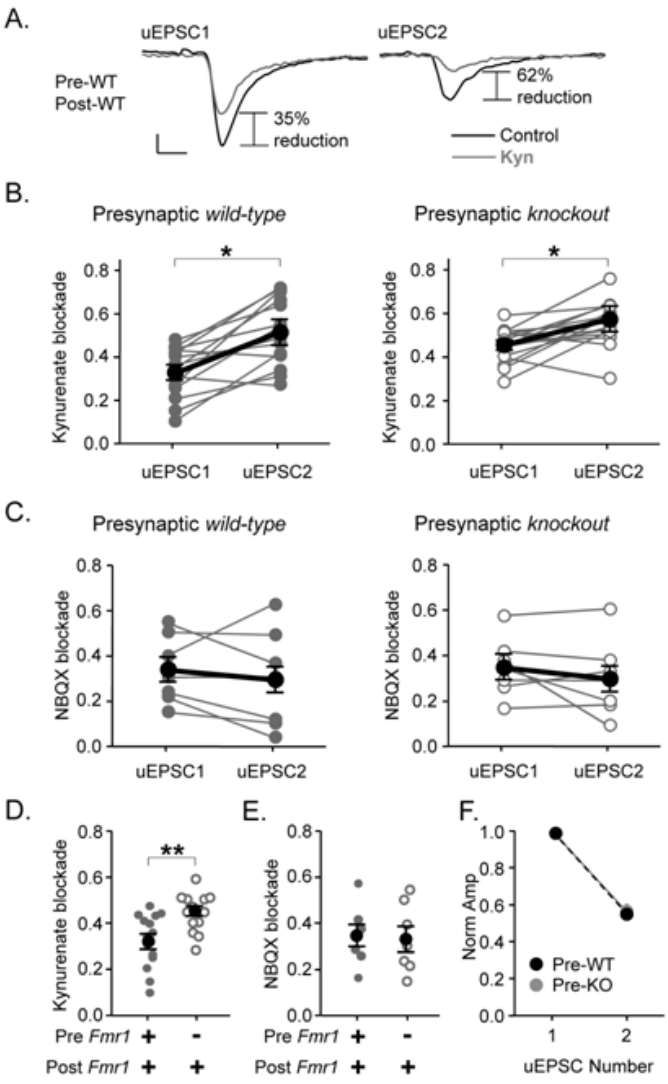

Figure 9. Presynaptic *Fmr1* deletion causes reduced multivesicular release and release probability. (A) Example average traces obtained from a WT/WT pair demonstrating the effect of the AMPAR competitive antagonist, kynurenate (Kyn, 250 µM). Note the greater blockade of uEPSC2 compared to blockade of

uEPSC1, indicating multivesicular release. Scale bars: 20 pA, 2 ms. (B) Paired line plots showing Kyn blockade for uEPSC1 and uEPSC2 with presynaptic WT (left) and presynaptic KO expression (right). Dark lines indicate average data. (C) Paired line plots showing blockade by the noncompetitive AMPAR antagonist, NBQX (75 nM). NBQX had uniform affects across uEPSC number. (D) Blockade by Kyn of uEPSC1 was greater with presynaptic KO, indicating less multivesicular release. (E) Blockade by NBQX of uEPSC1 was not different with presynaptic KO. (F) No change in short-term plasticity as observed by the average normalized uEPSC amplitude during the paired pulse train. (G) Individual examples of use-dependent NMDA-R blockade by MK-801. Curves are best fits of the data to single exponential decay functions. *Inset traces*: average NMDA-R mediated uEPSCs acquired during baseline measurement. Scale bars: 10 pA, 40 ms. (H) Binned and averaged responses from each individual experiment were then averaged across all experiments (see Methods). 4 intervals are higher in the KO data (2 way ANOVA followed by multiple comparisons; n=8,6; WT,KO). (I) The average time constant derived from each individual experiment is longer with presynaptic *Fmr1* deletion. * $p < 0.05$,** $p < 0.01$. (From Patel et al., 2013)

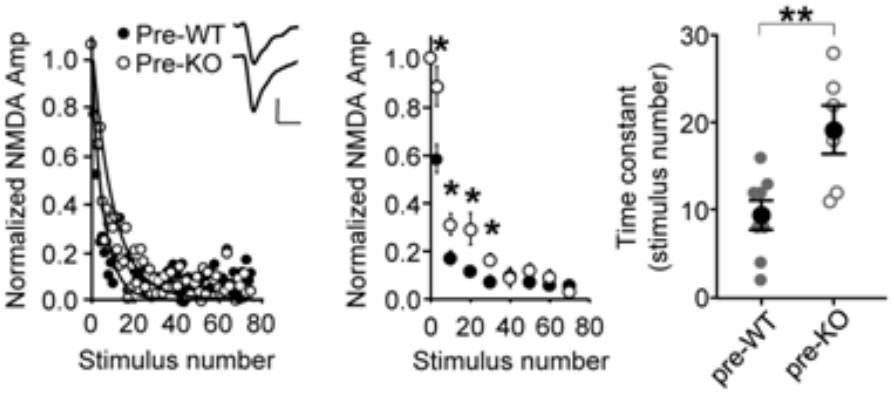

Figure 10. Presynaptic *Fmr1* deletion causes reduced release probability at single release sites. (A) An example of a single experiment employing the MPFA technique. We evoked trains of stimuli at 2 different Ca^{2+} concentrations to achieve different P_V states (black=average, gray=individual trace). Then the variance is plotted against the mean for every P_V state and a parabolic function is fitted to the data (right). Scale bars: 20 pA, 10 ms. (B-D) From a function fitted for every experiment, values for P_V, N_V, and q were derived and plotted. * $p < 0.05$. (From Patel et al., 2013)

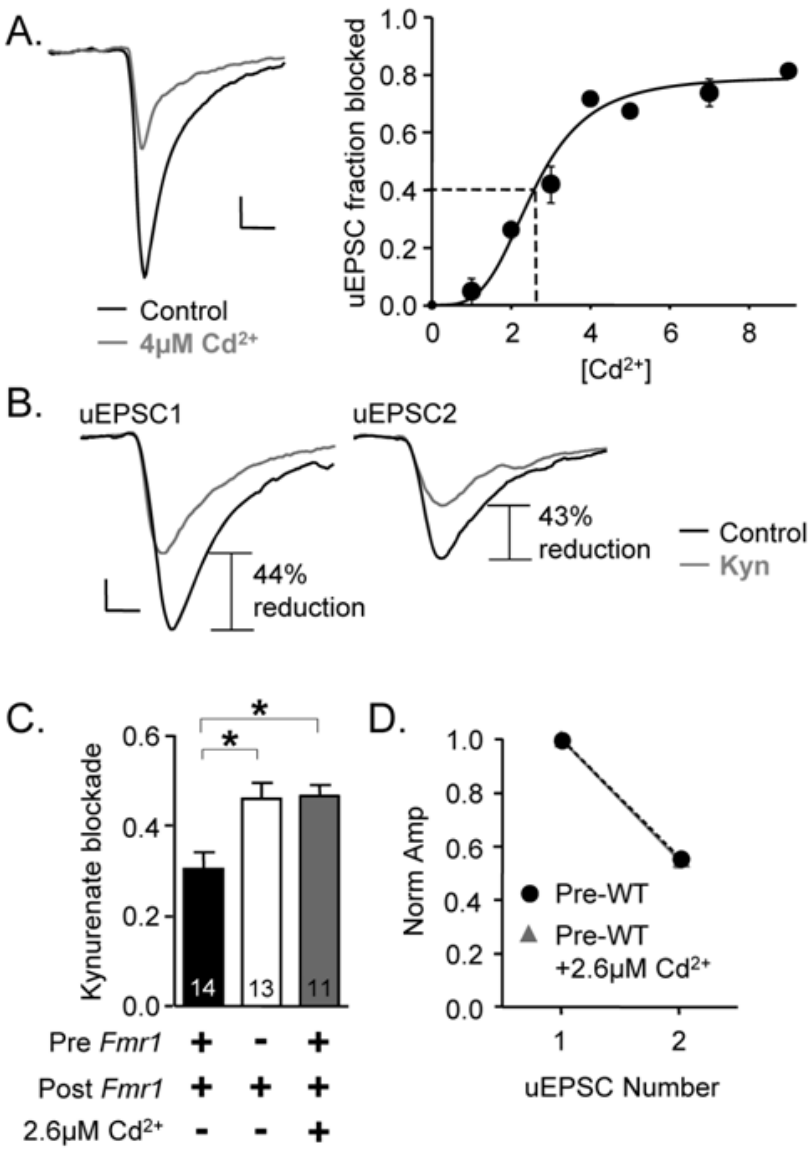

Figure 11. The presynaptic *Fmr1* deletion phenotype can be mimicked with a decrease in release probability in presynaptic WT pairs. (A) Left: Example average traces before and after 4 μM $CdCl_2$. Right: We obtained the relationship between $CdCl_2$ (Cd^{+2}) concentration and blockade of uEPSC1. Data were fitted

to a sigmoid curve. Dashed lines mark the [Cd^{+2}] (2.6 µM) that corresponds to the average fractional decrease of uEPSC1 amplitude found for presynaptic *Fmr1* deletion (0.40). (B) Example average traces obtained from a WT/WT pair in the presence of 2.6 µM $CdCl_2$ before and after kynurenate (Kyn, 250 µM) application. (C) Average blockade by kynurenate with 2.6 µM $CdCl_2$ closely matched the blockade for presynaptic KO pairs. (D) No change in short-term plasticity with Cd^{2+} application. WT/WT and KO/WT data in C and D are replotted from fig. 5. * $p < 0.05$. Scale bars in A and B: 20 pA, 2 ms. (From Patel et al., 2013)

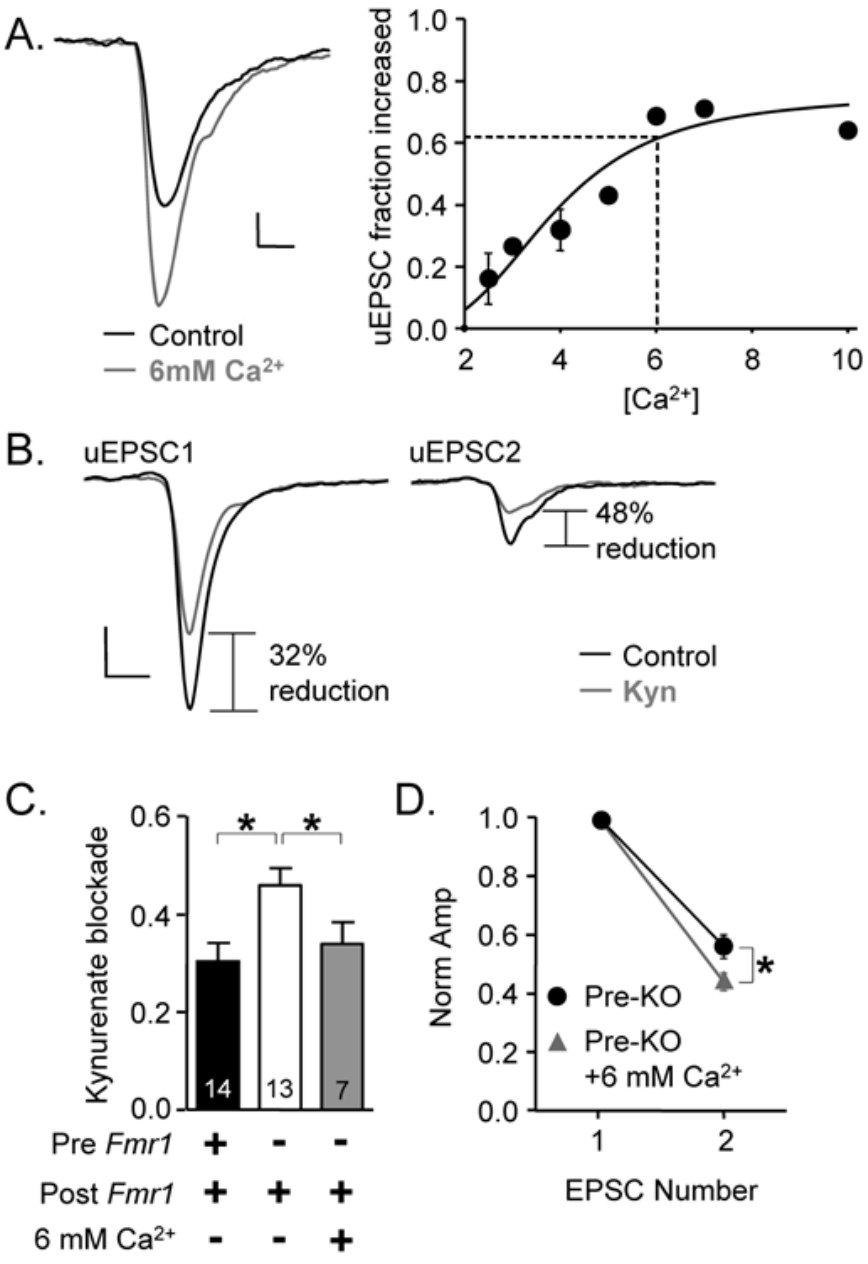

Figure 12. The presynaptic *Fmr1* deletion phenotype can be rescued with an increase in release probability in presynaptic KO pairs. (A) Left: Example

average traces before and after 6 mM $CaCl_2$. Right: We obtained the relationship between $CaCl_2$ (Ca^{+2}) concentration and increase of uEPSC1 amplitude. Data were fitted to a sigmoid curve. Dashed lines mark the [Ca^{+2}] (6 mM) that corresponds to the average fractional increase of uEPSC1 amplitude found for WT/WT pairs over KO/WT pairs (0.62). (B) Example average traces obtained from a KO/WT pair in the presence of 6 mM $CaCl_2$ before and after kynurenate (250 μM) application. (C) Average blockade by kynurenate with 6mM $CaCl_2$ closely matched the blockade for presynaptic WT pairs. (D) More short-term depression in high Ca^{2+}. KO/WT and WT/WT data in C and D are replotted from fig. 5. * $p < 0.05$. Scale bars in A and B: 20 pA, 2 ms. (From Patel et al., 2013)

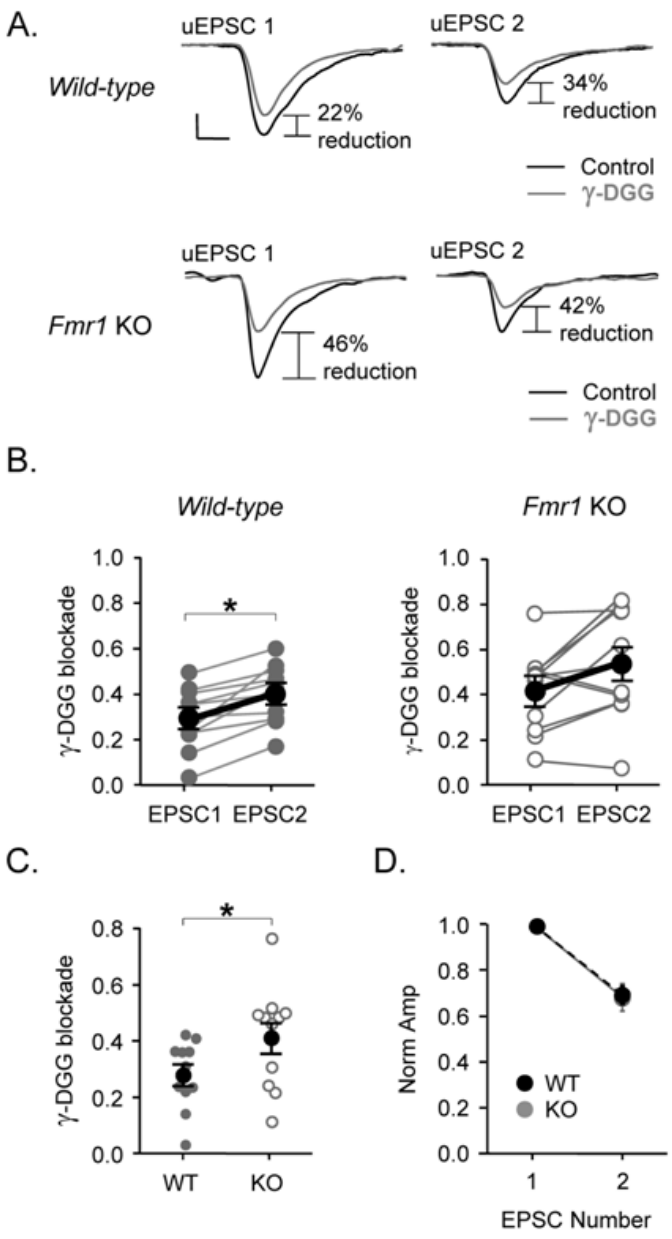

Figure 13. Decreased multivesicular release exists in the constitutive *Fmr1* KO. (A) Example average traces from *Fmr1* WT and KO slices demonstrating the

blockade caused by the AMPAR competitive antagonist, γ-DGG (500 μM). Note the greater blockade at uEPSC2 when compared to blockade at uEPSC1, indicating multivesicular release. Scale bars: 20 pA, 2 ms. (B) Paired line plots showing blockade for uEPSC1 and uEPSC2 in *Fmr1* WT (left) and KO slices (right). Dark lines indicate average data. (C) Average blockade for uEPSC1 was greater in KO slices indicating reduced multivesicular release. (D) No difference observed in short-term plasticity. * $p < 0.05$. (From Patel et al., 2013)

A)

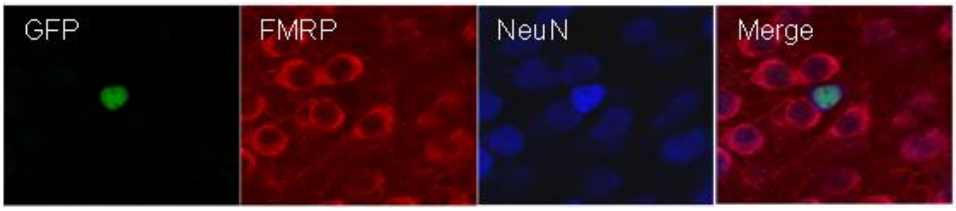
GFP
FMRP
NeuN
Merge

B)

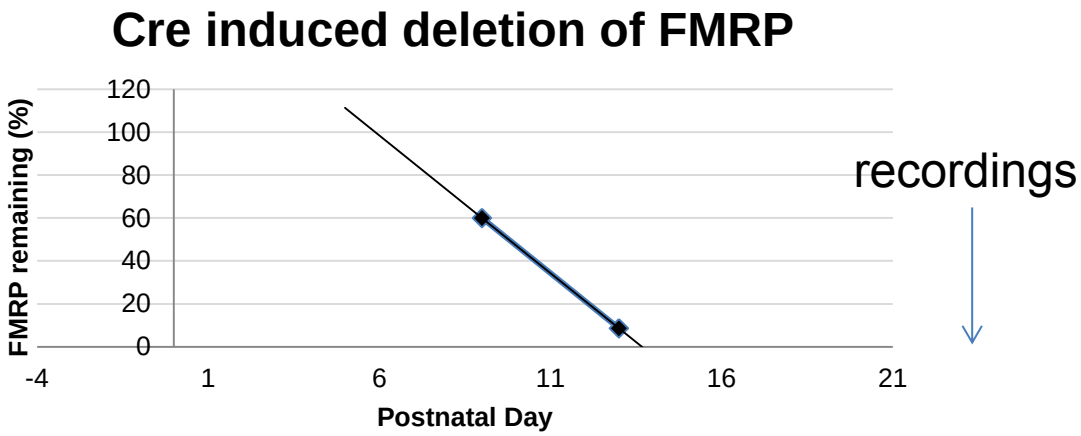
Cre induced deletion of FMRP
FMRP remaining (%)
120
100
80
60
40
20
0
-4
1
6
11
16
21
Postnatal Day
recordings

C)

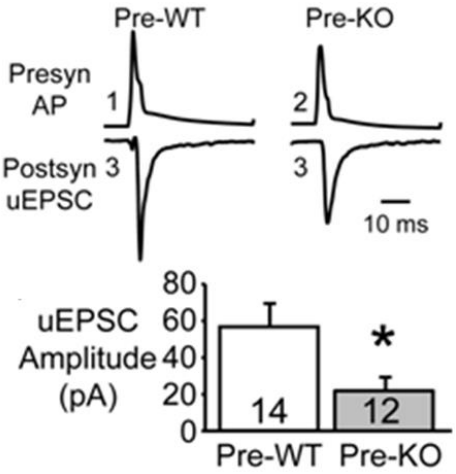
Pre-WT
Pre-KO
Presyn AP
1
2
Postsyn uEPSC
3
3
10 ms
uEPSC Amplitude (pA)
80
60
40
20
0
14
12
*
Pre-WT
Pre-KO

Fig. 14. Acute deletion of presynaptic Fmr1 reduces unitary excitatory strength onto FS interneurons. A) Immunostaining for GFP, FMRP and NeuN at p13 in floxed-Fmr1 males showing complete loss of FMRP expression in the GFP-expressing neuron. B) Age versus FMRP-remaining plot based on immunostaining data from p9 and p13. Whole-cell patch clamp recordings were performed at p21 (±2 days). C) Unitary strength grouped for presynaptic and postsynaptic genotype. (From Patel et al., 2013)

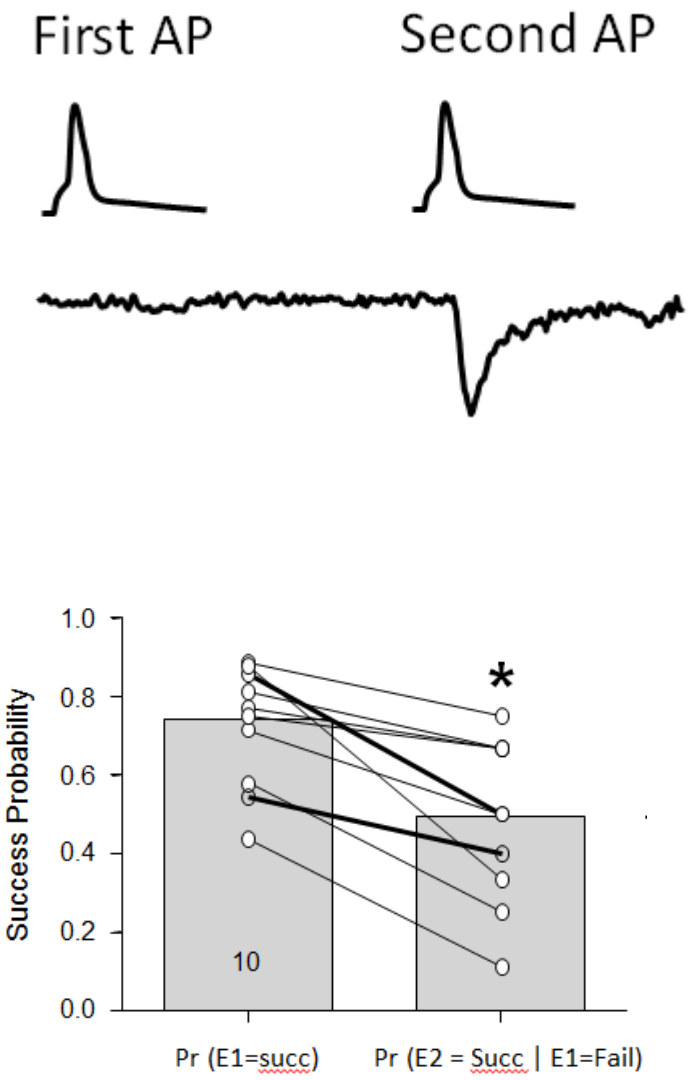

Fig. 15. Release-independent synapses fail to link paired-pulse ratio (PPR) to release probability. The observed connection probabilities of a success at uEPSC1 is the sum of the probability of a success at stimulus 1 but not 2 (Pr(0,1)) and the probability of a success at stimulus 1 and 2 (Pr(1,1)) combined as

Pr(E1=succ). This is compared to the probability of success at stimulus 2 when stimulus 1 fails (Pr (0,1)) shown as Pr(E2= Succ | E1=Fail). Because Pr(0,1) is significantly lower than Pr((1,0)+Pr(1,1)), it is suggested the STP at this synapse is release-independent. (Dobrunz et al., 1997; Thompson & Bannister, 1999; Huguenaard et al., 2002) (From Patel et al., 2013)

CHAPTER FOUR: FXS AND PRUNING OF EXCITATORY CIRCUITS

Postsynaptic loss of *FMR1* disrupts developmental pruning of L5A excitatory networks

Summary

In the mouse model of Fragile X Syndrome, the *Fmr1* knockout, the hallmark phenotype of dendritic spine dysgenesis suggests alterations in neocortical circuits, but the functional network architectures that develop as a result of these spine alterations has remained largely unexplored. Here, I examined the development of synaptic interconnectivities among local pyramidal neurons of layer 5A somatosensory cortex of the Fragile X mouse model. I found that during the third and fourth week of postnatal development, local projections undergo pruning whereby AMPAR-mediated interconnectivities between pyramidal neurons are reduced by 50%. In the Fmr1 KO mouse, synaptic refinement during these developmental periods is completely absent. Moreover, I find that a delayed maturity of AMPAR-mediated interconnectivities from silent synapses prevents Fmr1 KO cells from attaining maximal network connectivity early in development. Using the Fmr1 mosaic mouse model, I show that cell-autonomous loss of postsynaptic, and not presynaptic Fmr1, determines the delayed maturity

and lack of synaptic refinement phenotypes. Additionally, I show that delayed pruning in Fmr1 KO cells does not occur under the contingency of achieving delayed maximal network connectivity. This data suggests that hyperconnected pyramidal networks of the major output layer of the neocortex may be permanent in Fragile X syndrome and may contribute to circuit hypersensitivity and hyperexcitability impairments associated with the disease.

Introduction

A Critical process to establishing and maintaining developmental or learning-induced neural circuits is the elimination of synapses (Lichtman and Colman, 2000). In the cerebellum, multiple climbing fiber inputs onto individual Perkinje cells are eliminated to single climbing fiber innervations onto individual perkinje cells – a process necessary to avoid ataxic behavior (Crepel et al., 1976; Lohof et al., 1996); preganglionic inputs are eliminated from ganglion cells in the autonomic system (Lichtman, 1977); in the visual system, thalamocortical projections onto layer IV are eliminated (Hubel et al., 1977) and in the somatosensory cortex, Layer V spine density undergoes developmental decline (Galvez and Greenough, 2005). Synaptic elimination can be of 2 types: A reduction in synapse number, where the number of postsynaptic targets remain the same but the strength of connections onto the targets are reduced (synaptic

pruning), or a reduction in synapse number where the number of postsynaptic targets is reduced while the strength of connections onto the targets are maintained (connectivity pruning).

A key phenotype in Fragile X syndrome is increased spinogenesis in Fragile X patients as well as the Fragile X mouse model (Galvez et al., 2003; Galvez and Greenough, 2005). However, increased spine density has been an inconsistent phenotype (Cruz-Martin et al., 2010), which has left the understanding of functional outcomes of Fragile X circuits unclear. Mechanistically, studies suggest FMRP may regulate pruning toward efficient, functional networks. Postsynaptic FMRP decreases AMPA and NMDA synapses from single axons onto cultured CA1 pyramidal cells (Pfieffer and Huber, 2008); Drosophila FMRP (dFXR) reduces synaptic bouton number at the NMJ (Zhang et al., 2001). While these findings recognize FMRP's role in the negative regulation of synapse number, little evidence has identified Fmr1's effect on circuit formation through its regulation of developmental pruning. Structural evidence has suggested Fmr1 regulates developmental pruning, but this work does not resolve what eventual network sizes and synaptic drives develop as a result of Fmr1 loss. Without precise interconnectivity studies, it remains unclear whether Fmr1 regulates either or both of the disparate forms of developmental pruning and what impact this regulation has on circuit development. Circuit studies that specifically assess connectivity pruning and synapse pruning would better

recognize the information flow of sensory inputs in highly organized structures of the neocortex and will better link circuit functions to behavioral impairments in Fragile X Syndrome.

Here, I show that local connectivity among pyramidal neurons of layer 5A somatosensory cortex undergoes developmental connectivity pruning, without synaptic pruning; the process is completely absent in Fmr1 KO mice and is dependent on cell-autonomous expression of postsynaptic, and not presynapptic Fmr1. I make these observations with simultaneous recordings of pre- and postsynaptic neurons which provide precise measurements of cell-to-cell synaptic function and connectivity in circuits that have undergone in vivo development.

Pruning of L5A pyramidal interconnectivity during development is a circuit, not weighted change in synapse number

An earlier study anecdotally reported that connectivity among L5A pyramidal neurons decreases between 2 and 4 weeks of age in rat (Frick et al., 2007). This seemed like a promising system to study the role of FMRP in synaptic pruning with functional measurements, and therefore, I examined the development of this circuit more closely.

I performed simultaneous whole-cell recordings of neighboring L5A pyramidal neurons (up to 4 neurons, <35 µm intersomal distance) in the barrel field of somatosensory cortex in acutely prepared slices. Up to 12 potential E->E connections existed with this design. I measured unitary EPSCs (uEPSCs) evoked by single presynaptic neurons when a functional connection existed (Fig. 16A). Most potential E->E connections had no detectable uEPSC and were therefore deemed not connected. Layer 5A consists mainly of intracortical and striatal projecting neurons, and therefore our recording represent a mix of these populations. It is very unlikely that large, thick tufted neurons were included in our analysis since they represent a small number in L5A and since I excluded neurons that evoked high frequency bursts of action potentials in response to intracellular current injection (Figs. 16B and 21).

In wild-type (WT) mice, I measured the connectivity frequency and uEPSC amplitudes among neighboring L5A pyramidal neurons at 3 postnatal (P) ages – P15, P22, and P30 (all ±2 days). This represents a developmental time window where cortical circuits undergo significant maturation in synaptic function and connectivity(Feldmeyer and Radnikow, 2009). I found a monotonic decrease in connectivity frequency which decreased by 50% between P15 and P30 (Fig.'s 16 C,E). Over the same interval, I did not detect a change in uEPSC amplitude (Figs 16 D,E). Paired pulse ratio (PPR, uEPSC2/uEPSC1) increased (See Table 1) suggesting that release probability (Pr) may have slightly decreased

as previously reported (Frick et al., 2007). These data indicate a pruning of unitary, or cell-to-cell, connections during maturation of this L5A circuit.

Impaired circuit pruning in the Fmr1 KO mouse

In contrast to the Fmr1 wild-type mice, Fmr1 KO mice displayed a developmental increase, rather than a decrease, in connectivity - a finding that compliments a previous effect of Fmr1 loss at layer 4 projections onto layer 3(Bureau et al., 2008) (Figs 16F, 16E; $p<0.016$; KO p15, 13/202; KO p30, 36/212). Within-age comparisons between Fmr1 KO and Fmr1 wild-type animals showed that connectivity in Fmr1 KOs was reduced at p15 and significantly increased at p30 (Fig 16H; $p<0.016$; 32/179, 13/202; p15 WT, p15 KO; $p<0.016$; 19/212, 36/212; p30 WT, p30 KO). These findings indicate that loss of Fmr1 disrupts timely circuit pruning and delays the formation of functional AMPA-mediated connectivity. Like the wild-type animal, I identified no developmental, or within-age differences to wild-type animals, of synaptic strength in the Fmr1 KO animal (Fig. 16G; $p=0.17$; KO p15 vs KO p30). Differences in synaptic or membrane properties did not correlate with the connectivity differences (Table 1).

Cell-autonomous, postsynaptic Fmr1 drives circuit pruning

In an effort to delineate the cell-autonomous presynaptic or postsynaptic role of Fmr1 in circuit pruning, I used GFP/*Fmr1* mosaic females where cells either co-express GFP and Fmr1 or express neither (Hanson and Madison, 2007). I found that *Fmr1* in the postsynaptic, and not presynaptic, neuron recapitulated the developmental decrease in connectivity seen in the Fmr1 wild-type animal (Fig. 17A; $p<0.016$; p15 post-WT, 55/442; p30 post-WT, 13/229). Additionally, loss of postsynaptic, and not presynaptic, Fmr1 recapitulated the delayed formation of functional connectivity and lack of connectivity pruning seen in the Fmr1 KO mice (Fig. 17B; post-KO, 37/483; p30 post-KO, 27/221). Miniature frequency recordings trended the connectivity difference between Fmr1 wild-type and KO neurons but the lack of robustness may reflect a lack of pruning at all inputs onto L5A pyramidal neurons during this period (Fig 19). These findings indicate that cell-autonomous, postsynaptic mechanisms of Fmr1 permit the timely functional formation and elimination of circuit connectivity. Lack of a difference in synaptic strength was also recapitulated in the mosaics for presynaptic or postsynaptic genotypes (Fig. 17A; $p=0.80$, p15 post-WT vs p30 post-WT; $p=0.07$, p15 post-KO vs p30 post-KO).

For both postsynaptic WT and *Fmr1* KO neurons in mosaic slices, PPR increased and mEPSC amplitude increase 20% in the P15-30 interval (Table 1).

This suggested that release probability (Pr) may have slightly decreased as previously reported (Frick et al., 2007) . Quantal quantal size (q) isslightly increased in both postsynaptic WT and KO neurons from p15-p22. To interpret these data, I use the classical model of synaptic transmission, $A=N_U*Pr*q$, where A and N_U are uEPSC amplitude and total release sites mediating the unitary connection, respectively. I may reasonably speculate that the above changes in Pr and q with age are approximately offsetting. If A is unchanged, this suggests that N_U is very little changed for both neuron genotypes. Under these conditions, if pruning in the WT were distributed randomly over all synapses, one would expect a much smaller decrement in connection frequency and a ~50% decrease in uEPSC amplitude. But this is not the case. Instead, it appears the pruning occurs mainly by the removal of a subset of unitary connections. Conversely, in the *Fmr1* KO neurons, the impaired pruning is at the cell-to-cell connection level. In summary, in these data indicate that FMRP promotes connection pruning among neighboring L5A pyramidal neurons, and its loss results in local hyperconnectivity.

Prevalence of "silent", NMDA-only, synapses at p15 suggest delayed maturity of synapses onto Fmr1 KO neurons

Recent work has identified the developmentally delayed maturity of synaptic connections in Fmr1 KO mice from NMDAR-only silent connectivity to AMPAR-expressing mature connectivity after, rather than during the first week of postnatal development (Harlow et al., 2010). Given that I saw a delayed formation of functional AMPAR-mediated connections in both the Fmr1 KO animal and Fmr1 mosaic animal, I sought to identify whether our findings mechanistically convey delayed synaptic maturity. AMPAR and NMDAR-mediated unitary responses were collected as a function of presynaptic and postsynaptic genotype in p15 Fmr1 mosaic mice (Fig 18A). While AMPAR-mediated connectivity was lower, silent connectivity was higher in postsynaptic Fmr1 KO neurons compared to Fmr1 wild-type neurons (Fig 18 B; $p<0.025$, post-WT AMPA vs post-KO AMPA; $p<0.025$, post-WT Silent vs post-KO Silent). No differences in AMPA/NMDA ratios or total connectivity were detected (Fig 18C and D). This finding suggests that structural development of connectivity is not disrupted by the loss of Fmr1; rather, a delayed unsilencing of connectivity onto Fmr1 KO neurons explains the delayed maturation to AMPA-mediated connectivity.

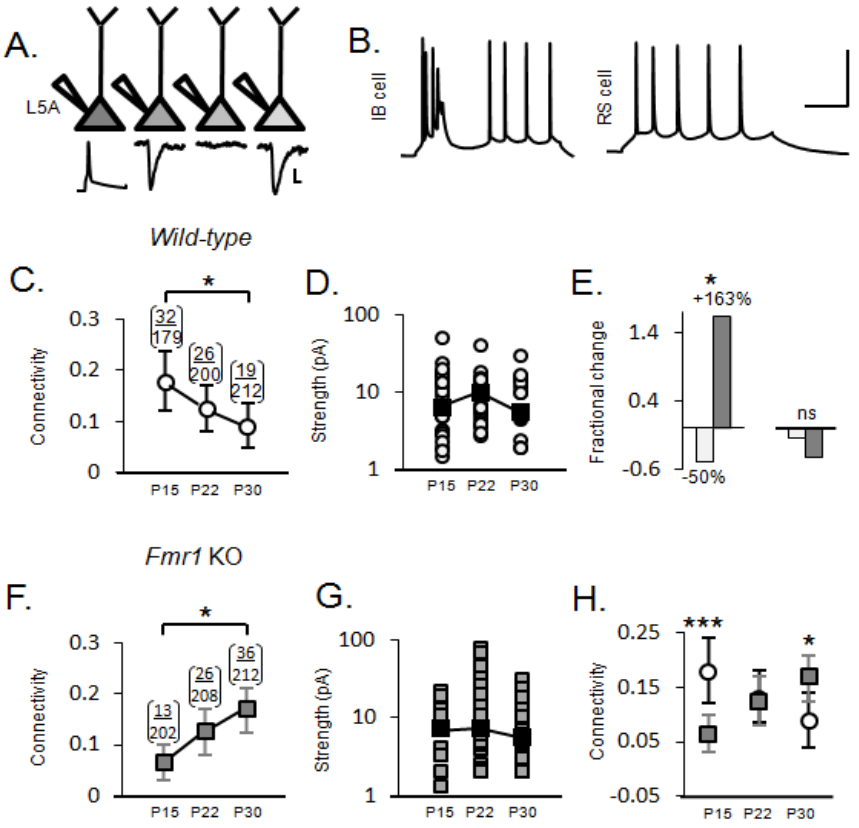

Fig 16. Loss of *Fmr1* disrupts connectivity pruning. Fmr1 KO mice display delayed connectivity and absent connectivity pruning (A) Cartoon depiction of multi-patched pyramidals (bottom) Traces of three connections out of a possible four connections from a stimulated neuron (B) Left, characteristic firing of a burst-spiking neuron. Right, characteristic firing of a regular-spiking neuron. Scale bars: vertical = 50 mV; horizontal =200 ms. (C) Wild-type connectivity with age (D) Wild-type strength with age (E) Fractional change in connectivity p15 to p30 (left) and strength (right);

white = wild-type; gray = Fmr1 KO (F) Fmr1 KO connectivity with age (G) Fmr1 KO strength with age. (H) Re-plot of wild-type and Fmr1 KO connectivity with age * $p < 0.05$, ** $p < 0.01$.

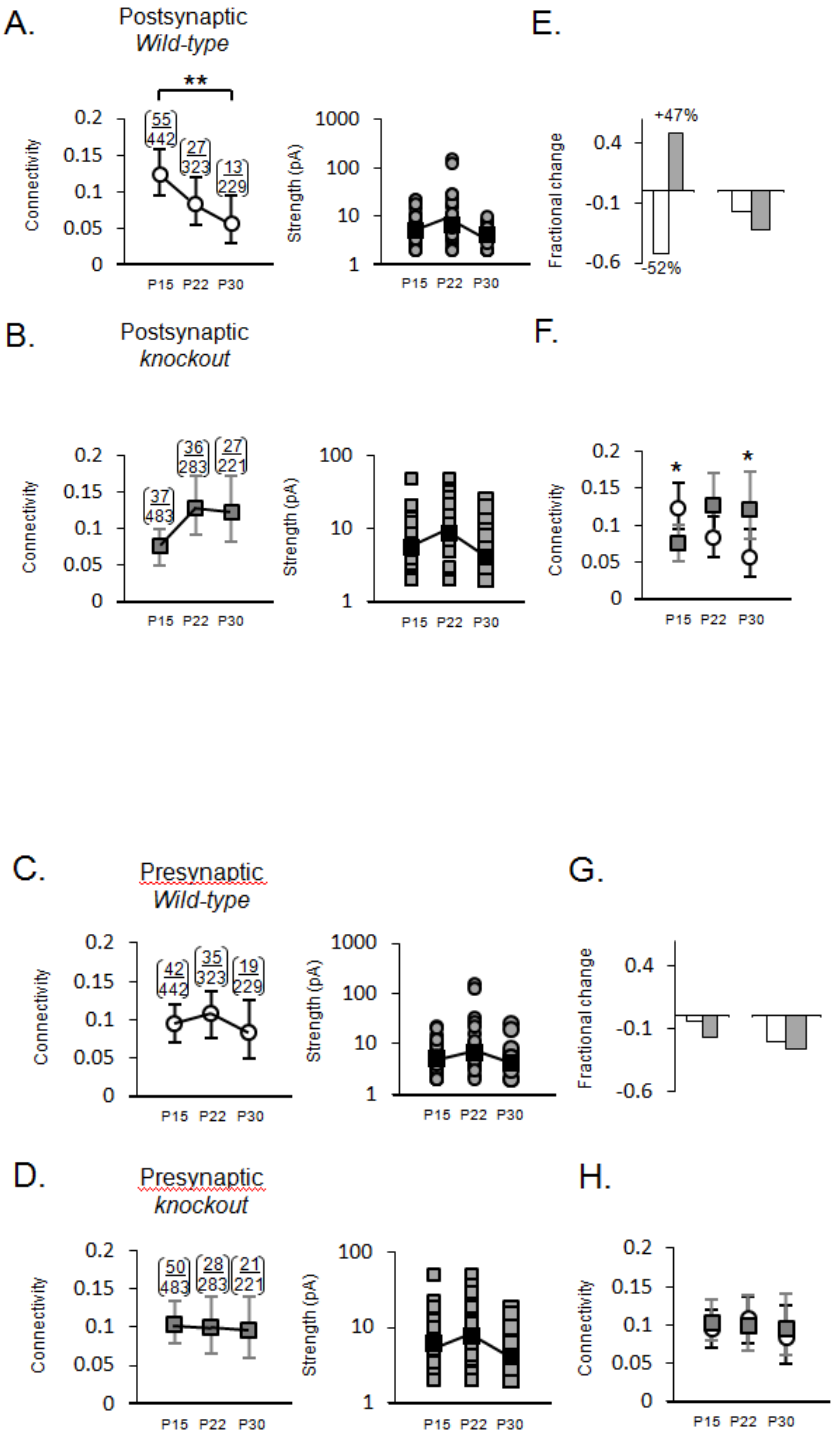
A.
Postsynaptic
Wild-type
**
Connectivity
Strength (pA)
55
442
27
323
13
229
P15 P22 P30
B.
Postsynaptic
knockout
37
483
36
283
27
221
C.
Presynaptic
Wild-type
42
442
35
323
19
229
D.
Presynaptic
knockout
50
483
28
283
21
221
E.
+47%
-52%
Fractional change
F.
*
*
G.
H.

Fig 17. Postsynaptic loss of Fmr1 causes delayed connectivity and lack of connectivity pruning (A) (Left) Connectivity rates and synaptic strengths with age for postsynaptic wild-type connections. (B) Connectivity rates and synaptic strengths with age for postsynaptic KO connections (C) Connectivity rates and synaptic strengths with age for presynaptic wild-type connections. (D) Connectivity rates and synaptic strengths with age for presynaptic KO connections. (E) Fractional change in postsynaptic genotypic group connectivity (left) and strength (right) p15 to p30; white = wild-type; gray = Fmr1 KO (F) Re-plot of postsynaptic wild-type postsynaptic KO connectivity with age (G) Fractional change in presynaptic genotypic group connectivity (left) and strength (right) p15 to p30 (H) Re-plot of preynaptic wild-type presynaptic KO connectivity with age.

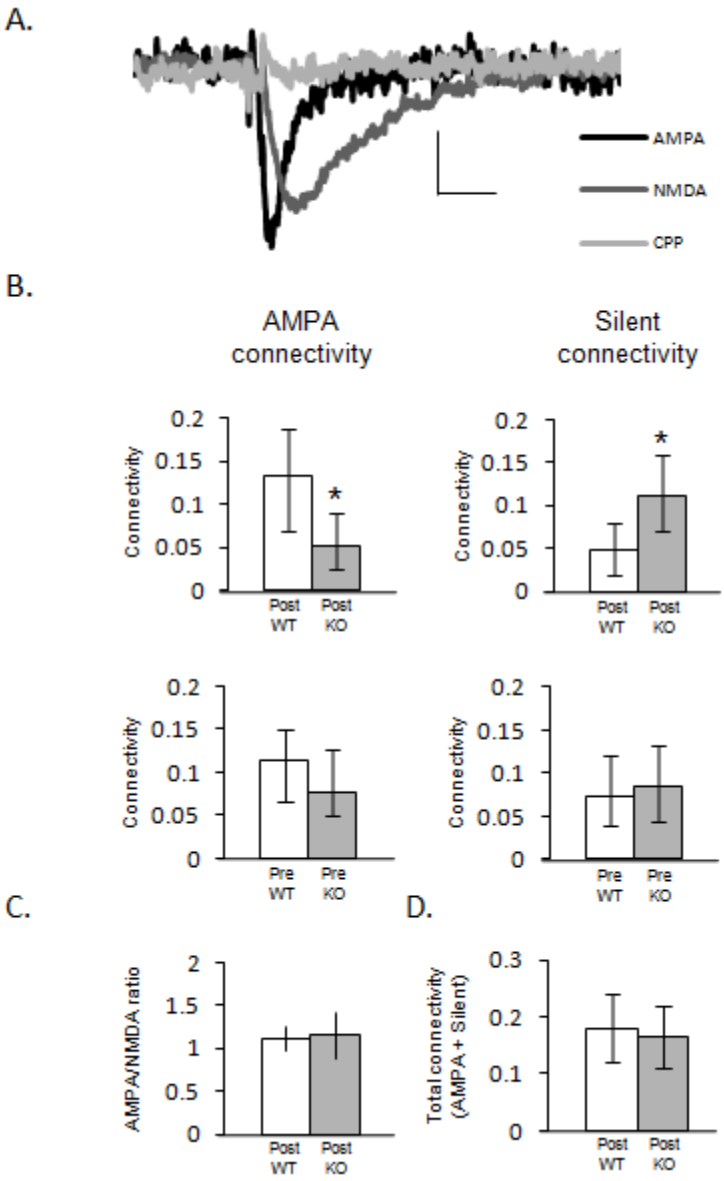

Fig 18. Prevalence of silent synapses suggests delayed synaptic maturity of *Fmr1* KO neurons during development. (A) Example trace of an AMPA current and CPP-sensitive NMDA current. (B) Postsynaptic (top) and presynaptic

(bottom) wild-type and KO AMPA connectivity and corresponding NMDA connectivity within the same circuits (B, (top, postsynaptic grouping) AMPA: WT=25/189, KO=10/189; NMDA-only Silent: WT=7/189, KO=17/189; (bottom, presynaptic grouping) AMPA: WT=20/189, KO=15/189; NMDA-only Silent: WT=11/189, KO=13/189 (C) AMPA/NMDA ratios (D) Total connectivity for postsynaptic genotypes (AMPA connections + Silent connections)

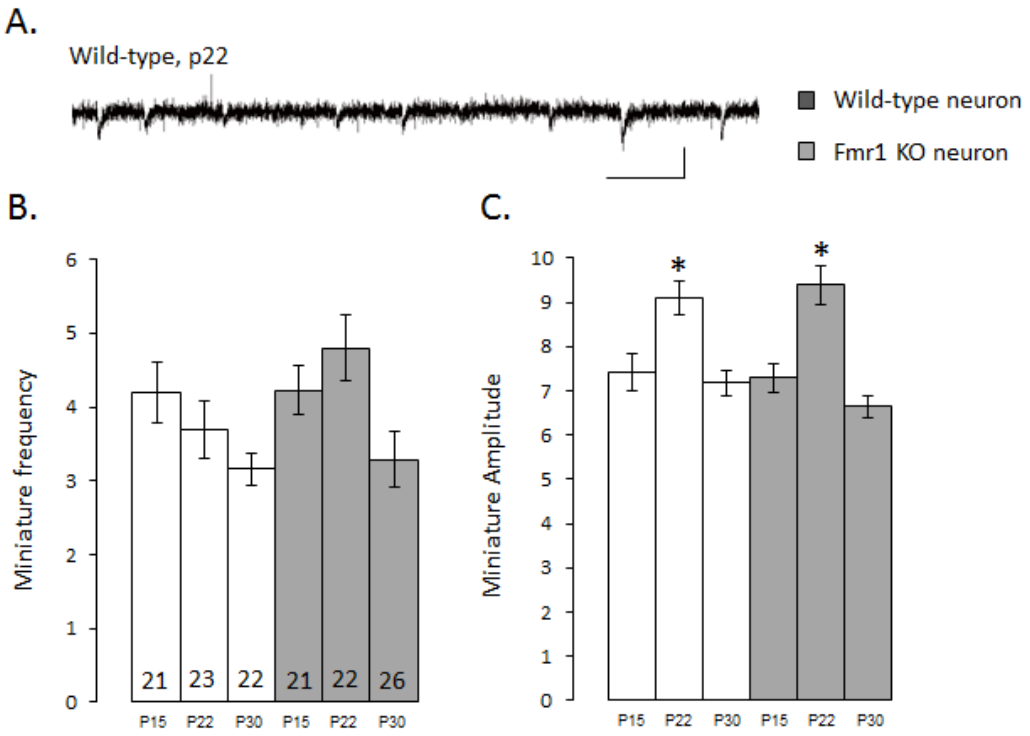

Fig 19. Developmental changes in spontaneous miniature activity A) Example trace of miniature events from a wild-type neuron. Scale bars: vertical = 14 pA; horizontal =143 ms. (B) Miniature frequency with age and (C) Miniature amplitude (pA) with age for wild-type and Fmr1 KO neurons. Miniature amplitudes increased at P22 in both wild-type and Fmr1 KO neurons compared to P15 ($p<0.01$).

A.

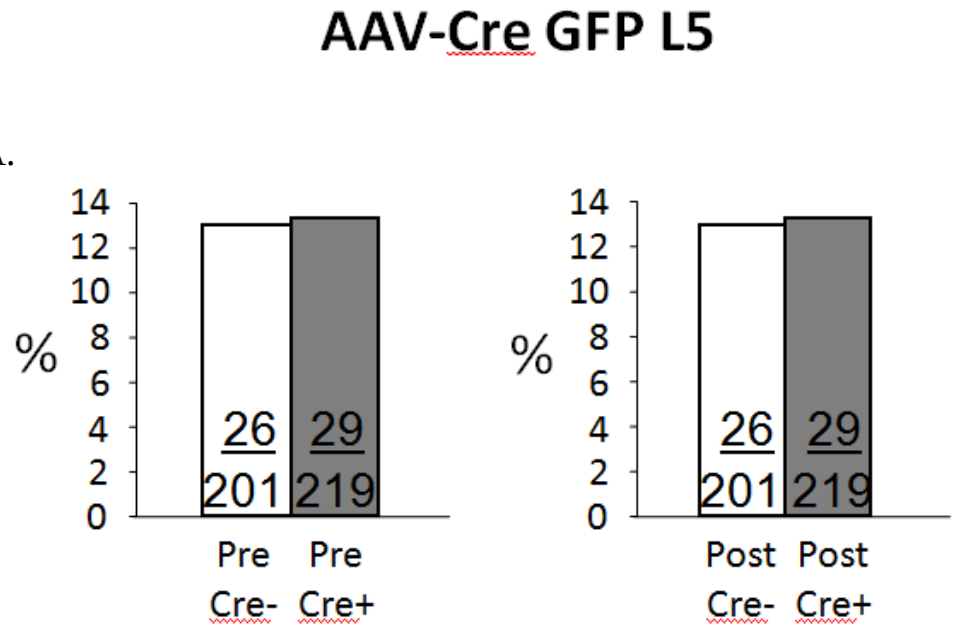

Fig 20. Postnatal deletion of FMRP after p12 does not occlude circuit pruning. A) Connectivity grouped for presynaptic (left) and postsynaptic (right) FMRP genotype in floxed-Fmr1 male mice. Immunostaining for the AAV-Cre GFP-mediated knockdown of FMRP was performed in Fig 14.

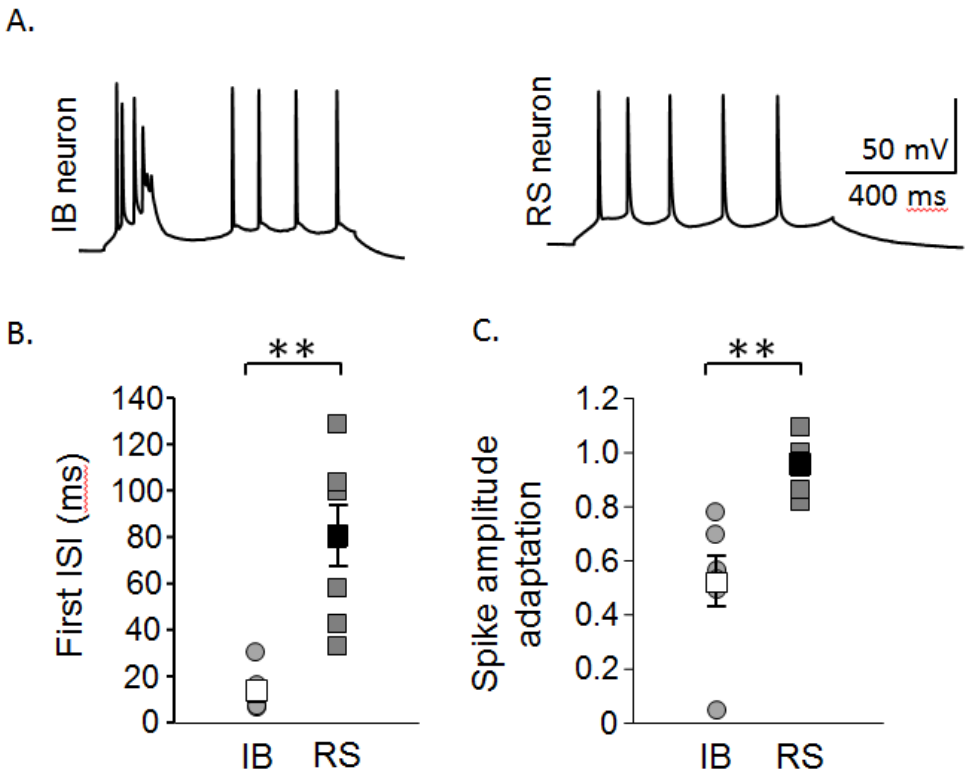

Fig 21. Burst-spiking type vs Regular-spiking type pyramidal neurons (A) Example firing traces of an Intra-burst type (IB, left) and regular-spiking type (RS, right) pyramidal neurons from L5A. We excluded IB, or burst-spiking type, neurons from the overall analysis based on the short first ISI and stronger spike height adaptation characteristics in burst-spiking type neurons defined in previous studies(Jacob et al., 2011). We encountered only 7 bursting neurons out of all recordings. (B) Time of first interspike interval in IB vs RS neurons. RS neurons came from the same experiments as IB neurons. (C) Spike amplitude

adaptation was determined by dividing the minimum spike amplitude during a current step by the first spike amplitude. Same neurons as in B.

WT animal	Rinput (MΩ)	Thresh Cur Step (pA)	Resting Pot (mV)	STP 2/1 (PPR)	CV	Rise Time (ms)	Decay (ms)	Resp Latency (ms)
2 weeks	277 (42)	-	-62.8 (44)	0.59 (20)	0.45 (20)	3.8 (20)	17.1 (20)	
3 weeks	211 (79)	42.2 (43)	-63.2 (79)	0.65 (24)	0.50 (24)	2.8 (24)	14.8 (24)	
4 weeks	190 (41)	88.5 (62)	-68.7 (62)	0.77 (19)	0.36 (19)	3.6 (19)	17.0 (19)	1.94 (19)

KO animal	Rinput	Thresh Cur Step	Resting Pot	STP 2/1 (PPR)	CV	Rise Time	Decay	Resp Latency
2 weeks	454**(51)		-62.5 (54)	0.47 (13)	0.37 (13)	3.3 (13)	15.8 (13)	
3 weeks	218 (73)	56.6 (45)	-66.6**(95)	0.55 (21)	0.42 (21)	2.9 (21)	13.9 (21)	
4 weeks	249**(53)	69.8**(58)	-69.2 (58)	0.61 (34)	0.37 (34)	3.6 (34)	16.5 (34)	2.05 (34)

Excitability (AP number), WT animal

Steps (pA)	30	40	50	60	70	80	90	100	110	120	130	140	150
2 weeks			1.3					4.1					6.0
3 weeks	1.0			2.7									
4 weeks	0			0.5*			1.0						

Excitability (AP number), KO animal

Steps (pA)	30	40	50	60	70	80	90	100	110	120	130	140	150
2 weeks			2.2***					5.3***					7.2***
3 weeks	0.6*			2.1*									
4 weeks	0.2			1.0*			2.2***						

WT mosaic	Rinput	Threshold	Resting Pot	STP 2/1 (PPR)	STP (1/avg 3,4)	CV	Rise Time	Decay	Resp Latency	AP Width HH (0.5 Hz)	AP Width HH (>5 Hz)
2 weeks	347(37)	36.6 (34)	-63.9 (37)	0.64 (32)		0.43 (32)	1.6 (32)	11.2 (32)			
3 weeks	223(25)	50.7 (22)	-64.6 (26)	0.77 (27)	1.97 (26)	0.46 (27)	2.6 (27)	13.6 (27)		1.72 (15)	1.98 (15)
4 weeks	233(81)	57.4 (75)	-67.7 (80)	0.77 (13)		0.62 (13)	1.8 (13)	13.9 (13)	2.17 (13)		

KO mosaic	Rinput	Threshold	Resting Pot	STP 2/1 (PPR)	STP (1/avg 3,4)	CV	Rise Time	Decay	Resp Latency	AP Width HH (0.5 Hz)	AP Width HH (>5 Hz)
2 weeks	336(55)	35.2 (49)	-63.2 (56)	0.56 (27)		0.47 (27)	1.6 (27)	11.0 (27)			
3 weeks	224(22)	54.5 (22)	-64.9 (25)	0.69 (39)	2.00 (25)	0.46 (39)	2.0 (39)	11.7 (39)		1.73 (15)	1.84 (15)
4 weeks	229(76)	57.8 (69)	-67.3 (75)	0.84 (27)		0.57 (27)	2.1 (27)	14.5 (27)	2.70 (27)		

Excitability (AP number), WT mosaic

Steps (pA)	30	40	50	60	70	80	90	100	110	120	130	140	150
2 weeks	0.9			1.9									
3 weeks	0.5			1.8									
4 weeks	0.2			1.6									

Excitability (AP number), KO mosaic

Steps (pA)	30	40	50	60	70	80	90	100	110	120	130	140	150
2 weeks	1.1			2.2									
3 weeks	0.5			1.6									
4 weeks	0.3			1.8									

Table 1. Synaptic and membrane properties L5 pyramidal neurons

(A) Fmr1 KO animals displayed increased Input Resistances, decreased threshold to firing, and increased firing at p15 and p30. No differences in synaptic properties were seen. I speculate that at p22, I did not see increased excitability in Fmr1 KO animals due to resting potentials being significantly hyperpolarized in Fmr1 KO neurons at p22 compared to wild-type littermates (B) Fmr1 KO neurons in Fmr1 mosaic mice do not display any differences in synaptic and membrane properties compared to Fmr1 wild-type neurons at any age.

CHAPTER FIVE: DISCUSSION

Excitation of fast-spiking inhibitory interneurons

In studying a vital synaptic input that terminates onto aspiny dendrites, I identify a role for presynaptic *Fmr1* in basal transmission. I identify that loss of presynaptic, and not postsynaptic *Fmr1* reduces the excitation of layer 4 FS inhibitory neurons. This deficit is predominantly due to a reduction in multivesicular release, akin to reduced release probability (P_{Syn}). These mechanistic deficits are present in both the Fmr1 KO and mosaic model of Fragile X suggesting an impairment at this synapse in Fragile X patients with complete as well as mosaic expression of Fmr1. In testing the excitation of neighboring excitatory neurons, I find that this particular projection is not altered by the loss of presynaptic or postsynaptic Fmr1 suggesting a target-cell specific role for presynaptic Fmr1.

Regulation of synaptic function by Presynaptic Fmr1

Previous work in hippocampal slice culture has identified a cell-autonomous role for presynaptic FMRP using the GFP/Fmr1 mosaic mouse, and identified that unitary connection probability was reduced with presynaptic, and not postsynaptic Fmr1 deletion (Hanson and Madison, 2007). The study did not

identify any effect on synaptic strength at existing connections. Complimentary to this theme of reduced excitatory drive with presynaptic loss of Fmr1, my findings too suggest a decrease in excitatory drive, even though the underlying mechanism is a reduction in release probability and not connection probability. These differences may be attributable to differences in brain region, cultured development versus intact in vivo development or projection-specific differences.

Mechanistically, I identified no effect on short-term plasticity, assessed by measuring paired-pulse ratio even though my multivesicular release experiments clearly showed a deficit in release probability. While short-term plasticity is often related to changes in release probability (Regehr and Stevens, 2001), at synapses that are release-independent, the relationship is absent (Brody and Yue, 2000; Dobrunz et al., 1997; Kraushaar and Jonas, 2000; Luthi et al., 2001). Indeed, a component of release-independent short-term plasticity was identified at the excitatory inputs onto fast-spiking interneurons in my studies. Specifically, I saw that regardless of the prior occurrence of a synaptic response to an action potential, synaptic response 50ms after always had decreased release probability (Fig. 15; 73±0.04% versus 44±0.07%, probability of EPSC, first versus second action potential, $p<0.05$, $n=10$). Additionally, wash-in of CdCl did not alter short-term plasticity (Fig 11). It is possible that besides the proof of release-independence, lack of a difference in short-term plasticity is due to alterations in

vesicle number, recycling, residual Ca^{2+} caused by the loss of presynaptic Fmr1. Indeed, previous studies have shown changes in terminal structures and proteins and short-term plasticity (Deng et al., 2011; Klemmer et al., 2011).

Does the loss of presynaptic Fmr1 have structural effects at the synapse? In observing the connection probability between spiny-stellate excitatory neurons and fast-spiking interneurons, I observed a small decrease (calculated from all pairs in the study), but our mimic and rescue experiments suggest that connectivity has a minimal role in the excitatory strength deficit onto FS interneurons (Figs 11, 12). This is not surprising as it has been previously shown that synapse number within layer 4 barrel cortex at this age in the Fmr1 KO mouse is unaltered (Till et al., 2012). Additionally, no difference was identified in the miniature EPSC frequency of layer 4 excitatory neurons (Gibson et al., 2008). Unpublished data from the work in (Bureau et al., 2008) saw no differences in total axonal length in layer 4 barrel cortex of the Fmr1 KO mouse and no differences in axonal length density as a function of horizontal or vertical distance from excitatory neuron somas (4.8±0.3 versus 4.2±0.5 mm, n=14,11; WT,KO). These findings suggest that within these circuits, loss of presynaptic Fmr1 does not disrupt structural development of excitatory projections onto FS interneurons, but rather disrupts the functional transmission at these inputs.

Mechanisms of regulation

FMRP has been shown to associate with 800 mRNA targets. Many of these targets are in presynaptic terminals, and are critical to the optimal function of vesicular machinery and synaptic release (Darnell et al., 2011). It remains unknown what effect loss of presynaptic FMRP has on the translation and function of these proteins and alterations of which specific proteins disrupts multivesicular release at excitatory projections onto FS interneurons. Given that FMRP has been localized in presynaptic terminals (Till et al., 2012), it is possible that it functions in an ongoing manner to regulate these presynaptic proteins to maintain optimal multivesicular release. Indeed, my finding for reduced transmission induced by acute loss of FMRP using AAV-Cre mediated postnatal knockdown suggests this is likely.

Mosaic versus constitutive Fmr1 mouse models

Much of the neocortical circuit phenotypes in Fragile X have come to recognize a role for FMRP globally, but little evidence has clarified whether FMRP functions in a cell-autonomous manner, presynaptic or postsynaptic.

In my measure of the excitation of fast-spiking interneurons in both Fmr1 KO and Fmr1 mosaic mice, I identify that reduced excitation of FS interneurons caused by the loss of global FMRP in the Fmr1 KO mouse is due to the loss of FMRP in presynaptic neurons. This begins to recognize which circuit phenotypes may be due to cell-autonomous and non-cell autonomous mechanisms, thus providing a better understanding of the molecular mechanisms that may be causing circuit disruptions in Fragile X.

Some differences between in the exciatatory projection onto FS interneurons were seen between the Fmr1 KO mouse and Fmr1 mosaic mouse. The deficit in unitary strength in the mosaic animal was more pronounced and more detectable compared to the Fmr1 KO – 40% versus 25% (Gibson et al., 2008) which may be due to differences in mouse strains used or differences in the ratio of Fmr1 WT and Fmr1 KO neurons in a circuit. Additionally, studying the excitatory inputs onto FS interneurons in the Fmr1 KO mouse did not reveal a significant reduction in the CV, although there was a trend(For CV, 0.37±0.03, 0.44±0.04; p=0.13. For failures, 0.04±0.02 vs. 0.08±0.02; p=0.16. n=26,31; WT,KO) (Gibson et al., 2008), while in the mosaic mouse, CV was robustly elevated with the loss of Fmr1. Because the unitary amplitudes in the mosaic were roughly double the size compared to the Fmr1 KO and Fmr1 wild-type animals, CV measurements may have avoided noise contamination in the mosaics.

Besides providing cell-autonomous proof of function for FMRP, studies performed in the mosaic mouse model may also provide an understanding on how circuits that have 50% FMRP-expressing neurons contribute to the less severe behavioral outcomes suggested in mosaic Fmr1 human patients (Hagerman et al., 2009). Because my findings suggest a common effect between the models, it can be suggested that the lack of severe impairments in mosaic patients may be due to compensatory rescues of non-cell-autonomous phenotypes.

In conclusion, my work shows a common deficit in two models of Fragile X, and suggests that the a deficit in the excitation of FS interneurons may contribute to the behavioral impairments in Fragile X due to the specific loss of presynaptic and not postsynaptic Fmr1.

Loss of postsynaptic Fmr1 disrupts circuit pruning

My second project has functionally proven developmental pruning in a local neocortical circuit and the effect of postsynaptic loss of *Fmr1*on this important process. The work identifies the functional circuits that developmentally establish with the loss of *Fmr1* that provides a clearer view of information flow within the canonical circuit. Complimentary to previous notions that synaptic development during early postnatal periods is characterized by redundant synaptogenesis followed by subsequent elimination, my work shows that postsynaptic expression of FMRP in pyramidal neurons of layer 5A manifests this developmental pruning by cell-to-cell (circuit) pruning, and not strength (weight) pruning. Indeed, loss of postsynaptic, and not presynaptic *Fmr1* results in lack of developmental circuit pruning suggesting that FMRP, cell-autonomously, in the postsynaptic compartment, regulates circuit pruning.

This functional evidence for pruning of interconnections within the pyramidal neurons of layer 5A for the first time compliments the structural work that previously identified pruning of spine density of layer 5 pyramidal neurons at these similar ages (Galvez and Greenough, 2005). Mechanistically, the dependence on postsynaptic FMRP for developmental pruning also compliments previous work that has shown that transfection of postsynaptic FMRP in CA1

pyramidal neurons reduces synapse number (Pfeiffer and Huber, 2007). My work more directly recognizes FMRP's regulation of cell-to-cell pruning in an intact in vivo circuit.

Delayed maturation may be a recurring theme in many circuits of Fragile X. In my developmental study of pyramidal interconnectivities, I identified that local connectivity early in development (~p15) onto Fmr1 KO neurons were predominantly silent synapses, such that they expressed NMDA receptors but not AMPA receptors. At the same age, *Fmr1* wild-type neurons were predominantly mature – expressing both AMPA and NMDA receptors. This finding was similar to the delayed unsilencing of thalamic synapses onto layer 4 spiny-stellate neurons (Harlow et al., 2010). Delayed maturity of Fmr1 KO neurons may render local excitatory networks to prolonged, if not permanent, hyperconnectivity if pruning is specific to a developmental period (Tessier and Broadie, 2008; Wang and Zhang, 2008).

CHAPTER SIX: FUTURE DIRECTIONS

While I recognize that loss of only a single gene, FMR1, and its protein product, FMRP, causes Fragile X Syndrome, the pathology of the disease is idiopathic. Involved in the molecular and cellular mechanisms of learning and memory, the activity-dependent development and refinement of brain circuitry, and its association with several hundred mRNAs involved in cellular biology and synaptic function, lead to a complicated eventual synaptic etiology caused by the loss of FMRP. This characteristic of FMRP function demands that developmental, functional studies outline the underlying effects on circuit structure and plasticity induced by sensory experiences.

Excitation of fast-spiking inhibitory interneurons

While the significance of FMRP has been attributed to the postsynaptic compartment of the synapse – mostly due to the numerous structural evidence for aberrant spine characteristics in Fragile X – little evidence for the role of presynaptic FMRP has been suggested. For the development of interventional therapies, it will be necessary to identify whether treatments that target postsynaptic physiological anomalies will be effective, or even counter-functional, for synaptic dysfunctions that are determined by presynaptic FMRP.

In my first project, I have identified the significance for presynaptic FMRP at the excitatory aspiny synapses onto fast-spiking interneurons. This finding is yet more evidence to the previously identified role for presynaptic FMRP in mediating connectivity (Hanson and Madison, 2007), and suggests that synaptic etiology of Fragile X may not be purely be due to the functional loss of postsynaptic FMRP. While I identify that the mechanism of this deficit – a reduction in multivesicular release - it remains unclear which molecular mechanisms dependent on FMRP are disrupted to determine the phenotype. Numerous target mRNAs of FMRP have been recently identified (Darnell et al., 2011) (See Fig. 1) and based on the synaptic mechanisms that I identified, some of the involved target mRNAs could be targeted.

In the presynaptic compartment, a temporal and spatial coherence of vesicular trafficking, commonly known as synaptic vesicle (SV) cycle, mediates synaptic release. The regulation of this process is complex and involves many proteins. Bassoon and Piccolo, large cytoskeletal-like proteins, which exist in an interactive complex, are expressed very early in terminals of developing nascent synapses (Friedman et al., 2000; Zhai et al., 2001) which suggests their involvement in establishing vesicular machinery for synaptic function. Ultrastructural analysis of presynaptic compartments has shown that Bassoon and

Piccolo span the entire presynaptic terminal active zone compartments, from the plasma membrane where synaptic vesicles fuse, to the open presynaptic space above (Brandstatter et al., 1999; Dick et al., 2001; Zhang et al., 2000) (see Fig 1).

Recent work has shown that Bassoon strongly interacts with FMRP (Darnell et al., 2011), suggesting that FMRP may translationally regulate Bassoon in the formation of a functional synapse. Work in Bassoon deficient mice show decreased evoked synaptic responses in hippocampal slice cultures, with no alterations in vesicular release probability, and an increased fraction of silent synapses (Altrock et al., 2003). At p14, hippocampal mossy fiber synapses show reduced evoked responses, with increased failure rate and no change in paired-pulse facilitation (Lanore et al., 2010). At retinal ribbon synapses of the inner hair cells (IHCs), which function in a multivesicular release manner, knockdown of Bassoon reduces the size of presynaptic calcium currents (attributed to an insufficient recruitment of voltage-gated calcium channels (VGCCs), reducing the readily releasable pool of vesicles. At the cerebellar mossy-fiber-granule cell synapses, bassoon deficiency doesn't disrupt evoked or miniature synaptic responses, displays enhanced depression and slower vesicle-reloading after high frequency stimulation with no change in quantal size (Hallermann et al., 2010).

While mechanistically, the role of Bassoon seems variable between conventional and non-conventional synapses, the reduced evoked responses in the Bassoon-deficient mice does mimic the deficit I identified at excitatory inputs onto FS interneurons in Fragile X mice. Interestingly, another mRNA target of FMRP in the presynaptic compartment are voltage-gated calcium channels (VGCCs), which are suggested to exist in close proximity to bassoon at the plasma membrane such that releaseable vesicles are in close proximity to VGCCs to mediate calcium-channel dependent vesicle fusion and release. If the link between VGCCs and Bassoon is disrupted with the loss of presynaptic FMRP, then influx of action potential-induced calcium through VGCCs may not be in close proximity to releaseable vesicles and thus these fused vesicles remains unreleased. This would functionally mimic the phenotype I see. Given that I see the ability of high external calcium to rescue the release of vesicles in presynaptic KO neurons, this possibility is likely. Enhanced calcium driving force, induced by elevating the external calcium concentration, may extend the presence of calcium to more distant sites along the presynaptic membrane and mediate release of vesicles not in close proximity to VGCCs. Future experiments should look into the expression, function and localization of Bassoon and VGCCs at this synapse in presynaptic FMRP KO neurons.

Loss of FMRP has shown significant disruptions in plasticity as mentioned earlier. Excitatory synapses onto fast-spiking interneurons can undergo Hebbian plasticity (Lamsa et al., 2005). It would be interesting to understand whether loss of presynaptic FMRP disrupts this form of plasticity at the synapse, and what mechanisms are involved given the presynaptic nature of the transmission deficit. Given that I do see a mild deficit in excitatory connectivity onto FS interneurons, it is possible that a deficiency in Hebbian plasticity at this synapse is the cause of this. If plasticity is altered at this synapse it would be worth investigating how this can be corrected to rescue the connectivity deficits and circuit inhibition in response to excitatory activity during sensory experience.

Another interesting finding from my study of the excitatory deficit onto fast-spiking interneurons caused by the loss of presynaptic FMRP comes from the fact that this is a target-cell specific deficit. Excitation onto neighboring excitatory neurons failed to show any functional deficit, even though the very same neurons show a robust deficit in excitation onto FS interneurons. This is particularly surprising given that excitation onto neighboring excitatory neurons also mediates multivesicular release (Huang et al., 2010). It remains an interesting question as to whether the deficit in multivesicular release persists even at excitatory-excitatory synapses but has no functional deficit because of postsynaptic saturation. If this is the case, then what impact does reduced multivesicular release at these synapses

have? Does reduced quantal content affect the activity of perisynaptic receptors such as mGluR receptors?

Loss of postsynaptic Fmr1 disrupts circuit pruning

Spine overabundance, a hallmark phenotype of Fragile X Syndrome, suggests that loss of *Fmr1* disrupts synaptic pruning and in effect alters neocortical circuitry, but the functional network architectures that develop as a result of disrupted pruning has remained largely unexplored. Using multi-patch recordings between layer 5A pyramidal neurons, I show that loss of complete or postsynaptic *Fmr1* disrupts developmental pruning of recurrent pyramidal networks. I also show a delayed maturity of synapses highlights the lack of developmental pruning with the loss of *Fmr1*.

It is interesting that postsynaptic FMRP, cell-autonomously determines the timely abundance of redundant connectivity and the subsequent elimination of redundant connectivity. This narrows down the viewpoint to identifying postsynaptic mechanisms of FMRP that mediate these developmental changes in connectivity between excitatory neuronal networks. In my study I identify that loss of FMRP delays the abundance of redundant connectivity, and this is not a

structural deficit because NMDA-mediated connectivity is comparable to wild-type levels. Thus, FMRP may be critical for the timely maturation of synapses. Interestingly, even though NMDA connectivity is intact with the loss of *Fmr1*, and NMDA-activity is what drives synapse elimination (Zhang et al., 2013), the fact that *Fmr1* KO neurons still do not undergo elimination during my probed developmental period suggests that postsynaptic signaling mechanisms dependent on NMDA function may be altered in *Fmr1* KO neurons that prevent synapse elimination. Alternatively, it is also possible that at these projections, AMPA connectivity is necessary for NMDA-activity (assuming little NMDA function in the presence of external magnesium and little intrinsic depolarizations in vivo). In such a scenario, lack of NMDA-activity in immature *Fmr1* KO neurons would fail to induce the signaling mechanisms necessary for synapse elimination. Given that AMPA connectivity in the *Fmr1* KO neurons is comparable to the pre-pruning level of AMPA connectivity in the *Fmr1* wild-type neurons at 4 weeks age, future studies at older ages should assess whether *Fmr1* KO neurons undergo circuit pruning and synapse elimination after having acquired AMPA-connectivity. In the drosophila fly model of Fragile X, delayed axonal pruning is evident (Tessier and Broadie, 2008). Interestingly, unlike the wild-type, the delayed pruning in the dFXR is not activity-dependent. This suggests that if neocortical circuit pruning in the *Fmr1* KO neurons does occur in the delayed manner, it may not be experience-dependent and therefore may not achieve fine-

scale circuitry (Yoshimura et al., 2005). Given that previous studies do recognize elimination to be developmental-period and activity dependent (Tessier and Broadie, 2008; Wang and Zhang, 2008), it is quite possible that delayed pruning *Fmr1* KO neurons does not occur. Using the AAV-Cre infusion into p1 pups, I have also attempted to temporally restrict knockdown of *Fmr1* after p12 in floxed- *Fmr1* mice. Deletion of *Fmr1* after p12 failed to disrupt connectivity at p22 when compared to non-infected wild-type neurons (Fig 18). This suggests that circuit pruning in *Fmr1* deleted neurons may still occur because *Fmr1* in those neurons was present during the critical period when NMDA-functionality and NMDA-mediated elimination is determined. Future studies that can target deletion of *Fmr1* specifically during the critical period should be performed to validate the temporal requirement for *Fmr1* toward timely abundance of redundant connectivity and the subsequent elimination of redundant connectivity. The use of in-utero electroporation could accomplish this (Borrell et al., 2005).

Recent work has shown that the development of early silent synapses can be unsilenced, in-turn enforced to maturity, by treating acute slices in 0 Mg^{+2} (Anastasiades and Butt, 2012). In the *Fmr1* KO mouse, a recent study identified a lack of L-type calcium channel expression and an elevated threshold for spike-timing dependent LTP in the prefrontal cortex (Meredith et al., 2007).

Remarkably, environmental enrichment of *Fmr1* KO mice rescued the elevated threshold for spike-timing dependent LTP, suggesting that increased activity onto *Fmr1* KO neurons may underlie therapeutic rescue of circuit function. If elevating neural activity, through environmental enrichment or relief of NMDA receptor blockade through pharmacological treatment, can rescue the timely maturity of *Fmr1* KO synapses, then subsequent circuit pruning may too be rescued. Indeed, environmental enrichment has rescued some behavioral and structural phenotypes of Fragile X mice (Restivo et al., 2005).

In my analysis of circuit pruning of wild-type animals it is seen that the source of circuit pruning is predominantly of non-recurrent, or unidirectional synapses as connection probabilities of bidirectional recurrent synapses remain the same throughout the entire period that undergoes a 50% circuit pruning (Fig. 22). This suggests that layer 5 circuits may mature into predominantly recurrent connections. Recent work has shown that when 2 neurons in layer 5 are bidirectionally connected, they share a 4-fold higher probability of receiving common inputs from layer 2/3 (Kampa et al., 2006). Thus, circuit pruning in layer 5 may leave specific fine-scale circuitry that represents unique sensory features. While I show that loss of postsynaptic *Fmr1* disrupts circuit pruning during this period, if delayed circuit pruning does occur in *Fmr1* KO neurons, it would be worth determining whether delayed circuit pruning in the *Fmr1* KO neurons is

due to elimination of non-recurrent, unidirectional synapses and whether *Fmr1* KO circuits mature into predominantly recurrent connections. It is likely, that if *Fmr1* KO neurons undergo delayed circuit pruning, lack of a predominant recurrent connectivity would spread excitation from layer 2/3 and potentially overlap sensory feature representations (see Fig. 24). When connectivity in the *Fmr1* KO at p30 peaks to the wild-type connectivity at p15 however, there is a trend for higher recurrent connectivity in the *Fmr1* KO (Fig. 24; WT p15, 6/179 vs KO p30, 14/212) so it is difficult to assert what the eventual recurrent/non-recurrent balance would be after delayed pruning in the *Fmr1* KO mouse. Future studies will have to assess these very interesting questions.

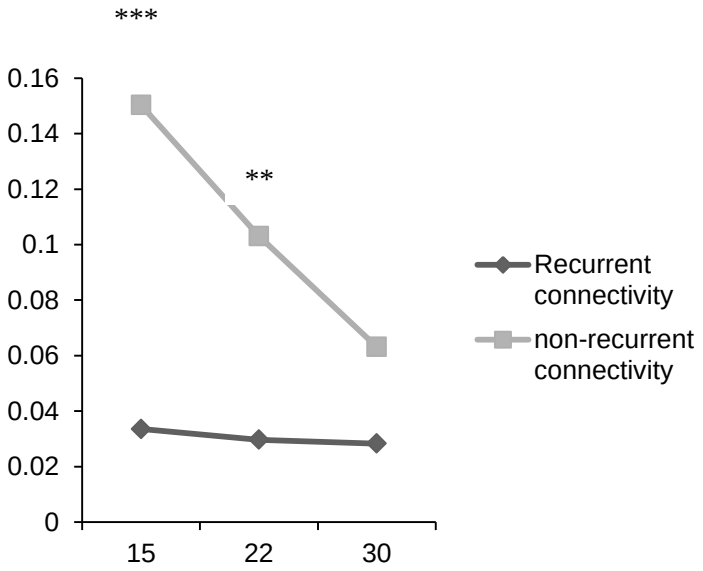

Fig 22. Circuit pruning is of non-recurrent and not recurrent synapses in layer 5 pyramidal circuits of Fmr1 wild-type animals. A) Recurrent and non-recurrent connectivity versus age in wild-type animals (reccurent connectivities, p15 = 6/179, p22 = 6/202, p30 = 8/212; non-recurrent connectivities, p15 = 26/179, p22 = 20/202, p30 = 11/212).

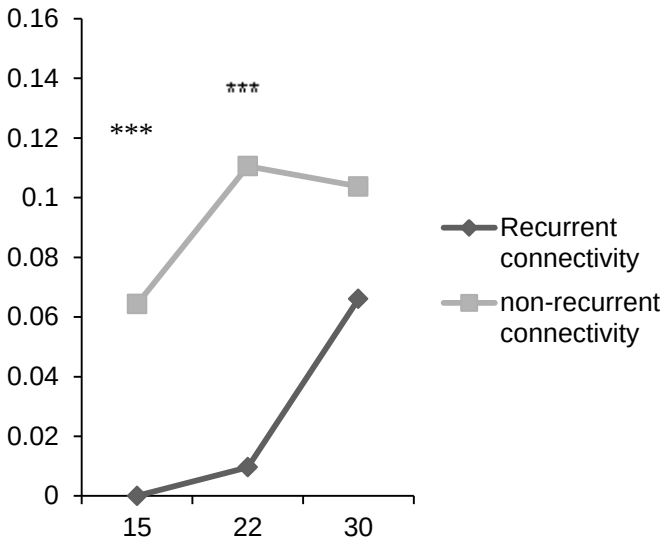

Fig 23. Circuit pruning is of non-recurrent and not recurrent synapses in layer 5 pyramidal circuits of Fmr1 KO animals. A) Recurrent and non-recurrent connectivity versus age in Fmr1 KO animals. (reccurent connectivities, p15 = 0/202, p22 = 2/208, p30 = 14/212; non-recurrent connectivities, p15 = 13/202, p22 = 23/208, p30 = 22/212).

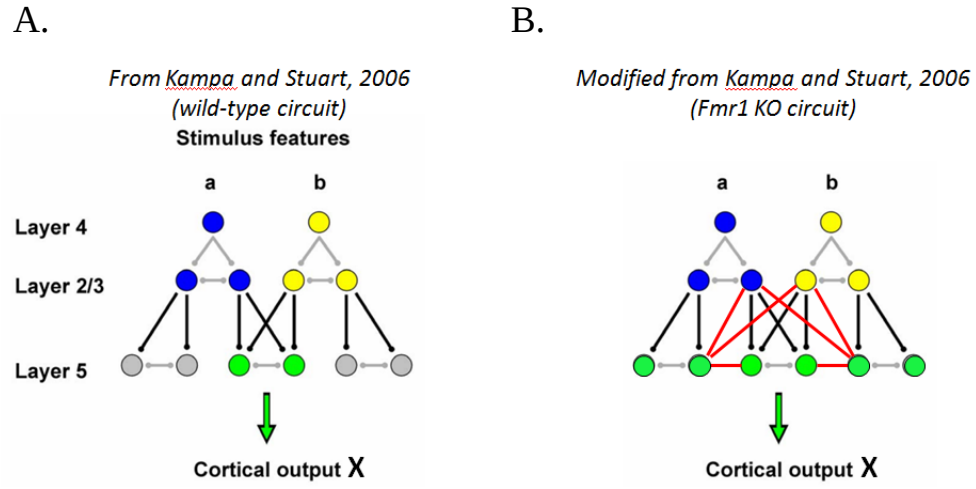

Fig 24. Hypothesized barrel circuitry in Fmr1 KO animals. A) Fine-scale microcircuit development in somatosensory cortex from Kampa et al., 2006. When neurons are bidirectionally connected in layer 5 they have a 4-fold higher probability of receiving common inputs from layer 2/3. When neurons are bidirectionally *not* connected in layer 2/3 they have a 3-fold higher probability of outputting to the same neurons in layer 5. B) Proposed circuit connectivity in Fmr1 KO animals due to hyperconnectivity (from the lack of pruning), or a smaller recurrent/non-recurrent ratio due to delayed pruning.

CHAPTER 7: APPENDIX: UNPUBLISHED DATA

Multiple-probability fluctuation analysis at excitatory synapses onto FS interneurons. *This work was not published as its interpretation was deemed controversial given that control experiments indicated my kynurenate concentration (to relieve saturation) was too low to accurately determine quantal parameters.*

MPFA was employed to estimate N_V, P_V, and q at a unitary connection (Silver, 2003) (See Methods). This method relies on measuring the mean and the variance of the uEPSC at different release probabilities (P_V) and then fitting these data to the parabolic equation, $Variance_A = q*A-(A^2/ N_V)$, where A is the average uEPSC amplitude.

I varied P_V by applying a short train of presynaptic action potentials and varying external Ca^{2+} concentration (Fig. 6A, see Methods). In these experiments, the average uEPSC amplitude in 2 mm Ca^{2+} trended to being smaller with presynaptic *Fmr1* deletion (78 ± 24 vs. 32 ± 6 pA; p=0.05; n=15,15; WT,KO). Based on fitting the parabolic function, I found that P_V was decreased by 38% with presynaptic *Fmr1* deletion (0.66 ± 0.04 vs. 0.41 ± 0.05; $p<0.01$) while N_V and q were unaltered (Fig. 6B-D). Moreover, when I add other experiments that did not qualify for the complete mean-variance analysis, I observed that more presynaptic KO connections displayed a strictly linear relationship between mean and variance in 2 mM Ca^{2+} (11/33 [33%] vs. 25/42

[60%]; $p<0.05$, Chi-Square test; WT,KO). Such a relationship indicates low release probability (Huang et al., 2010; Lu and Trussell, 2000), and therefore, this is also consistent with lower P_V with presynaptic *Fmr1* deletion. The derived amplitude of q is what I expected based on the amplitude measured in the Cd^{2+} experiments (see Fig. 4E) and the attenuation due to kynurenate in the bath (~50% attenuation). In summary, these data suggest that the decrease in glutamate release at single synapses (P_{Syn}) primarily originates from a decrease in the release probability of a single vesicle at a single release site (P_V) and not a decrease in release site number (N_V). This also represents further confirmation of a specific impairment in release probability.

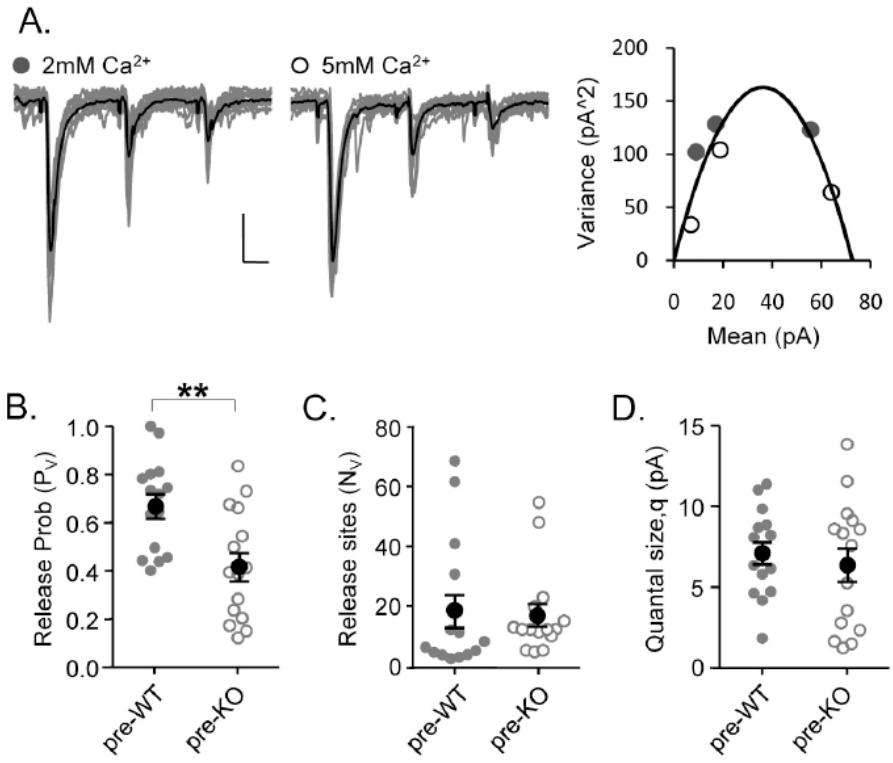

Fig. 25 MPFA of excitatory synapses onto FS interneurons

(A) An example of a single experiment employing the MPFA technique. I evoked trains of stimuli at 2 different Ca2+ concentrations to achieve different PV states (black=average, gray=individual trace). Then the variance is plotted against the mean for every PV state and a parabolic function is fitted to the data (right). Scale bars: 20 pA, 10 ms. (B-D) From a function fitted for every experiment, values for PV, NV, and q were derived and plotted. * $p < 0.05$.

While the MPFA data above suggests that Pv is reduced without a change in N, evidence suggests that if multivesicular release saturates postsynaptic

receptor occupancy N is also altered (Silver, 2003). The distinctive alterations in Pr and N can be achieved if saturation is prevented when performing MPFA. While I added 250µM Kynurenate to relieve saturation – a concentration that averagely blocks basal transmission in 2mM external Calcium by ~30% – it may have not have prevented saturation when I washed-in the necessary elevated external calcium to shape linear mean-variance responses of low Pr synapses into parabolic high Pr synapses (a necessity to interpret quantal parameters besides quantal size; See Methods). Indeed, the parabolic, and not linear, outcome of the variance/EPSCmax below is proof of the presence of saturation in my studies.

Another oversight in performing these experiments was the assumption that long stimulus-train induced depression reflects decreases in release probability. At multivesicular release synapses short-term depression is due to vesicle depletion and not due to changes in release probability (Foster and Reghr, 2004). Thus, only by measuring single-evoked responses in different external calcium concentrations to vary release probability can an actual variance-mean analysis that is based on probability fluctuation be carried out.

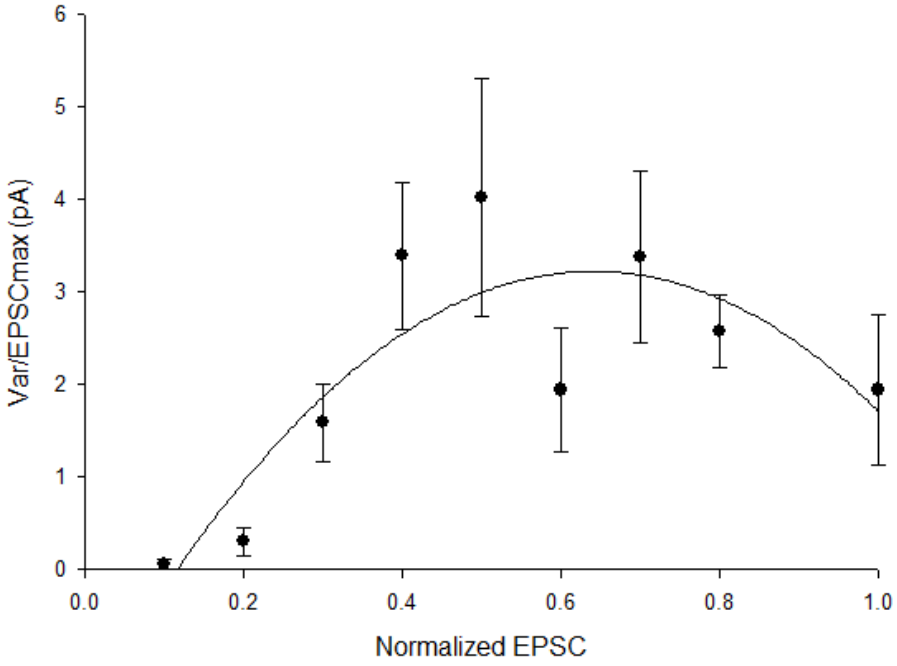
Var/EPSCmax (pA)
Normalized EPSC
0
1
2
3
4
5
6
0.0
0.2
0.4
0.6
0.8
1.0

BIBLIOGRAPHY

Agmon, A., and Connors, B.W. (1991). Thalamocortical responses of mouse somatosensory (barrel) cortex in vitro. Neuroscience *41*, 365-379.

Akins, M.R., Berk-Rauch, H.E., and Fallon, J.R. (2009). Presynaptic translation: stepping out of the postsynaptic shadow. Frontiers in neural circuits *3*, 17.

Allen, C.B., Celikel, T., and Feldman, D.E. (2003). Long-term depression induced by sensory deprivation during cortical map plasticity in vivo. Nature neuroscience *6*, 291-299.

Altrock, W.D., tom Dieck, S., Sokolov, M., Meyer, A.C., Sigler, A., Brakebusch, C., Fassler, R., Richter, K., Boeckers, T.M., Potschka, H., *et al.* (2003). Functional inactivation of a fraction of excitatory synapses in mice deficient for the active zone protein bassoon. Neuron *37*, 787-800.

Anastasiades, P.G., and Butt, S.J. (2012). A role for silent synapses in the development of the pathway from layer 2/3 to 5 pyramidal cells in the neocortex. The Journal of neuroscience : the official journal of the Society for Neuroscience *32*, 13085-13099.

Antar, L.N., Li, C., Zhang, H., Carroll, R.C., and Bassell, G.J. (2006a). Local functions for FMRP in axon growth cone motility and activity-dependent regulation of filopodia and spine synapses. Molecular and cellular neurosciences *32*, 37-48.

Antar, L.N., Li, C., Zhang, H., Carroll, R.C., and Bassell, G.J. (2006b). Local functions for FMRP in axon growth cone motility and activity-dependent regulation of filopodia and spine synapses. Molecular and cellular neurosciences.

Arnth-Jensen, N., Jabaudon, D., and Scanziani, M. (2002). Cooperation between independent hippocampal synapses is controlled by glutamate uptake. Nature neuroscience *5*, 325-331.

Atallah, B.V., Bruns, W., Carandini, M., and Scanziani, M. (2012). Parvalbumin-expressing interneurons linearly transform cortical responses to visual stimuli. Neuron *73*, 159-170.

Bagnall, M.W., Hull, C., Bushong, E.A., Ellisman, M.H., and Scanziani, M. (2011). Multiple clusters of release sites formed by individual thalamic afferents onto cortical interneurons ensure reliable transmission. Neuron *71*, 180-194.

Bakker, D.B. (1994). Fmr1 knockout mice: a model to study fragile X mental retardation. The Dutch-Belgian Fragile X Consortium. Cell *78*, 23-33.

Balmer, T.S., Carels, V.M., Frisch, J.L., and Nick, T.A. (2009). Modulation of perineuronal nets and parvalbumin with developmental song learning. The Journal of neuroscience : the official journal of the Society for Neuroscience *29*, 12878-12885.

Bartley, A.F., Huang, Z.J., Huber, K.M., and Gibson, J.R. (2008). Differential activity-dependent, homeostatic plasticity of two neocortical inhibitory circuits. Journal of neurophysiology *100*, 1983-1994.

Bassell, G.J., and Warren, S.T. (2008). Fragile X syndrome: loss of local mRNA regulation alters synaptic development and function. Neuron *60*, 201-214.

Belmonte, M.K., and Bourgeron, T. (2006). Fragile X syndrome and autism at the intersection of genetic and neural networks. Nature neuroscience *9*, 1221-1225.

Berry-Kravis, E. (2002). Epilepsy in fragile X syndrome. Developmental medicine and child neurology *44*, 724-728.

Bolduc, F.V., Bell, K., Cox, H., Broadie, K.S., and Tully, T. (2008). Excess protein synthesis in Drosophila fragile X mutants impairs long-term memory. Nature neuroscience *11*, 1143-1145.

Borrell, V., Yoshimura, Y., and Callaway, E.M. (2005). Targeted gene delivery to telencephalic inhibitory neurons by directional in utero electroporation. Journal of neuroscience methods *143*, 151-158.

Bourgeois, J.-P., Goldman-Rakic, P.S., and Rakic, P. (2000). Formation, elimination , and stabilization of synapses in the primate cerbral cortex. In The New Cognitive Neurosciences, M.S. Gazzaniga, ed. (Cambridge, Mass: MIT Press), pp. 45-53.

Brandstatter, J.H., Fletcher, E.L., Garner, C.C., Gundelfinger, E.D., and Wassle, H. (1999). Differential expression of the presynaptic cytomatrix protein bassoon among ribbon synapses in the mammalian retina. The European journal of neuroscience *11*, 3683-3693.

Brody, D.L., and Yue, D.T. (2000). Release-independent short-term synaptic depression in cultured hippocampal neurons. The Journal of neuroscience : the official journal of the Society for Neuroscience *20*, 2480-2494.

Brown, M.R., Kronengold, J., Gazula, V.R., Chen, Y., Strumbos, J.G., Sigworth, F.J., Navaratnam, D., and Kaczmarek, L.K. (2010). Fragile X mental retardation protein controls gating of the sodium-activated potassium channel Slack. Nature neuroscience *13*, 819-821.

Bureau, I., Shepherd, G.M., and Svoboda, K. (2008). Circuit and plasticity defects in the developing somatosensory cortex of FMR1 knock-out mice. The Journal of neuroscience : the official journal of the Society for Neuroscience *28*, 5178-5188.

Castro-Alamancos, M.A., and Connors, B.W. (1997). Distinct forms of short-term plasticity at excitatory synapses of hippocampus and neocortex. Proceedings of the National Academy of Sciences of the United States of America *94*, 4161-4166.

Caudy, A.A., Myers, M., Hannon, G.J., and Hammond, S.M. (2002). Fragile X-related protein and VIG associate with the RNA interference machinery. Genes & development *16*, 2491-2496.

Cauli, B., Audinat, E., Lambolez, B., Angulo, M.C., Ropert, N., Tsuzuki, K., Hestrin, S., and Rossier, J. (1997). Molecular and physiological diversity of cortical nonpyramidal cells. The Journal of neuroscience : the official journal of the Society for Neuroscience *17*, 3894-3906.

CDC (2004). Economic costs associated with mental retardation, cerebral palsy, hearing loss, and vision impairment--United States, 2003. MMWR Morb Mortal Wkly Rep *53*, 57-59.

Centonze, D., Rossi, S., Mercaldo, V., Napoli, I., Ciotti, M.T., De Chiara, V., Musella, A., Prosperetti, C., Calabresi, P., Bernardi, G., *et al.* (2008). Abnormal striatal GABA transmission in the mouse model for the fragile X syndrome. Biological psychiatry *63*, 963-973.

Chalifoux, J.R., and Carter, A.G. (2010). GABAB receptors modulate NMDA receptor calcium signals in dendritic spines. Neuron *66*, 101-113.

Chang, M.C., Park, J.M., Pelkey, K.A., Grabenstatter, H.L., Xu, D., Linden, D.J., Sutula, T.P., McBain, C.J., and Worley, P.F. (2010). Narp regulates homeostatic scaling of excitatory synapses on parvalbumin-expressing interneurons. Nature neuroscience *13*, 1090-1097.

Cheever, A., and Ceman, S. (2009a). Phosphorylation of FMRP inhibits association with Dicer. Rna *15*, 362-366.

Cheever, A., and Ceman, S. (2009b). Translation regulation of mRNAs by the fragile X family of proteins through the microRNA pathway. RNA biology *6*, 175-178.

Chklovskii, D.B., Mel, B.W., and Svoboda, K. (2004). Cortical rewiring and information storage. Nature *431*, 782-788.

Christie, J.M., and Jahr, C.E. (2006). Multivesicular release at Schaffer collateral-CA1 hippocampal synapses. The Journal of neuroscience : the official journal of the Society for Neuroscience *26*, 210-216.

Christie, S.B., Akins, M.R., Schwob, J.E., and Fallon, J.R. (2009). The FXG: a presynaptic fragile X granule expressed in a subset of developing brain circuits. The

Journal of neuroscience : the official journal of the Society for Neuroscience *29*, 1514-1524.

Coffee, R.L., Jr., Tessier, C.R., Woodruff, E.A., 3rd, and Broadie, K. (2010). Fragile X mental retardation protein has a unique, evolutionarily conserved neuronal function not shared with FXR1P or FXR2P. Disease models & mechanisms *3*, 471-485.

Comery, T.A., Harris, J.B., Willems, P.J., Oostra, B.A., Irwin, S.A., Weiler, I.J., and Greenough, W.T. (1997). Abnormal dendritic spines in fragile X knockout mice: Maturation and pruning deficits. Proceedings of the National Academy of Sciences *94*, 5401-5404.

Connors, B.W., and Gutnick, M.J. (1990). Intrinsic firing patterns of diverse neocortical neurons. Trends in neurosciences *13*, 99-104.

Crepel, F., Mariani, J., and Delhaye-Bouchaud, N. (1976). Evidence for a multiple innervation of Purkinje cells by climbing fibers in the immature rat cerebellum. Journal of neurobiology *7*, 567-578.

Cruz-Martin, A., Crespo, M., and Portera-Cailliau, C. (2010). Delayed stabilization of dendritic spines in fragile X mice. The Journal of neuroscience : the official journal of the Society for Neuroscience *30*, 7793-7803.

Curia, G., Papouin, T., Seguela, P., and Avoli, M. (2008). Downregulation of Tonic GABAergic Inhibition in a Mouse Model of Fragile X Syndrome. Cerebral cortex.

D'Hulst, C., and Kooy, R.F. (2007). The GABAA receptor: a novel target for treatment of fragile X? Trends in neurosciences *30*, 425-431.

Darnell, J.C., Van Driesche, S.J., Zhang, C., Hung, K.Y., Mele, A., Fraser, C.E., Stone, E.F., Chen, C., Fak, J.J., Chi, S.W., *et al.* (2011). FMRP stalls ribosomal translocation on mRNAs linked to synaptic function and autism. Cell *146*, 247-261.

Dick, O., Hack, I., Altrock, W.D., Garner, C.C., Gundelfinger, E.D., and Brandstatter, J.H. (2001). Localization of the presynaptic cytomatrix protein Piccolo at ribbon and conventional synapses in the rat retina: comparison with Bassoon. The Journal of comparative neurology *439*, 224-234.

DiGregorio, D.A., Nusser, Z., and Silver, R.A. (2002). Spillover of glutamate onto synaptic AMPA receptors enhances fast transmission at a cerebellar synapse. Neuron *35*, 521-533.

Dobrunz, L.E., Huang, E.P., and Stevens, C.F. (1997). Very short-term plasticity in hippocampal synapses. Proceedings of the National Academy of Sciences of the United States of America *94*, 14843-14847.

Dolen, G., Osterweil, E., Rao, B.S., Smith, G.B., Auerbach, B.D., Chattarji, S., and Bear, M.F. (2007). Correction of fragile X syndrome in mice. Neuron *56*, 955-962.

Edbauer, D., Neilson, J.R., Foster, K.A., Wang, C.F., Seeburg, D.P., Batterton, M.N., Tada, T., Dolan, B.M., Sharp, P.A., and Sheng, M. (2010). Regulation of synaptic structure and function by FMRP-associated microRNAs miR-125b and miR-132. Neuron *65*, 373-384.

Feldmeyer, D., and Radnikow, G. (2009). Developmental alterations in the functional properties of excitatory neocortical synapses. The Journal of physiology *587*, 1889-1896.

Feng, Y., Gutekunst, C.A., Eberhart, D.E., Yi, H., Warren, S.T., and Hersch, S.M. (1997). Fragile X mental retardation protein: nucleocytoplasmic shuttling and association with somatodendritic ribosomes. The Journal of neuroscience : the official journal of the Society for Neuroscience *17*, 1539-1547.

Foster, K.A., Kreitzer, A.C., and Regehr, W.G. (2002). Interaction of postsynaptic receptor saturation with presynaptic mechanisms produces a reliable synapse. Neuron *36*, 1115-1126.

Frick, A., Feldmeyer, D., and Sakmann, B. (2007). Postnatal development of synaptic transmission in local networks of L5A pyramidal neurons in rat somatosensory cortex. The Journal of physiology *585*, 103-116.

Friedman, H.V., Bresler, T., Garner, C.C., and Ziv, N.E. (2000). Assembly of new individual excitatory synapses: time course and temporal order of synaptic molecule recruitment. Neuron *27*, 57-69.

Fuchs, E.C., Zivkovic, A.R., Cunningham, M.O., Middleton, S., Lebeau, F.E., Bannerman, D.M., Rozov, A., Whittington, M.A., Traub, R.D., Rawlins, J.N., *et al.* (2007). Recruitment of parvalbumin-positive interneurons determines hippocampal function and associated behavior. Neuron *53*, 591-604.

Gabel, L.A., Won, S., Kawai, H., McKinney, M., Tartakoff, A.M., and Fallon, J.R. (2004). Visual experience regulates transient expression and dendritic localization of fragile X mental retardation protein. The Journal of neuroscience : the official journal of the Society for Neuroscience *24*, 10579-10583.

Galarreta, M., and Hestrin, S. (1998). Frequency-dependent synaptic depression and the balance of excitation and inhibition in the neocortex. Nature neuroscience *1*, 587-594.

Galvez, R., Gopal, A.R., and Greenough, W.T. (2003). Somatosensory cortical barrel dendritic abnormalities in a mouse model of the fragile X mental retardation syndrome. Brain research *971*, 83-89.

Galvez, R., and Greenough, W.T. (2005). Sequence of abnormal dendritic spine development in primary somatosensory cortex of a mouse model of the fragile X mental retardation syndrome. American journal of medical genetics Part A *135*, 155-160.

Gatto, C.L., and Broadie, K. (2008). Temporal requirements of the fragile X mental retardation protein in the regulation of synaptic structure. Development *135*, 2637-2648.

Gatto, C.L., and Broadie, K. (2009). The fragile X mental retardation protein in circadian rhythmicity and memory consolidation. Molecular neurobiology *39*, 107-129.

Gdalyahu, A., Tring, E., Polack, P.O., Gruver, R., Golshani, P., Fanselow, M.S., Silva, A.J., and Trachtenberg, J.T. (2012). Associative fear learning enhances sparse network coding in primary sensory cortex. Neuron *75*, 121-132.

Gibson, J.R., Bartley, A.F., Hays, S.A., and Huber, K.M. (2008). Imbalance of neocortical excitation and inhibition and altered UP states reflect network hyperexcitability in the mouse model of fragile X syndrome. Journal of neurophysiology *100*, 2615-2626.

Gibson, J.R., Beierlein, M., and Connors, B.W. (1999). Two networks of electrically coupled inhibitory neurons in neocortex. Nature *402*, 75-79.

Gibson, J.R., Huber, K.M., and Sudhof, T.C. (2009). Neuroligin-2 deletion selectively decreases inhibitory synaptic transmission originating from fast-spiking but not from somatostatin-positive interneurons. The Journal of neuroscience : the official journal of the Society for Neuroscience *29*, 13883-13897.

Gil, Z., Connors, B.W., and Amitai, Y. (1999). Efficacy of thalamocortical and intracortical synaptic connections: quanta, innervation, and reliability. Neuron *23*, 385-397.

Grossman, A.W., Aldridge, G.M., Weiler, I.J., and Greenough, W.T. (2006). Local protein synthesis and spine morphogenesis: Fragile X syndrome and beyond. The Journal of neuroscience : the official journal of the Society for Neuroscience *26*, 7151-7155.

Guzowski, J.F., Lyford, G.L., Stevenson, G.D., Houston, F.P., McGaugh, J.L., Worley, P.F., and Barnes, C.A. (2000). Inhibition of activity-dependent arc protein expression in the rat hippocampus impairs the maintenance of long-term potentiation and the consolidation of long-term memory. The Journal of neuroscience : the official journal of the Society for Neuroscience *20*, 3993-4001.

Hadjantonakis, A.K., Cox, L.L., Tam, P.P., and Nagy, A. (2001). An X-linked GFP transgene reveals unexpected paternal X-chromosome activity in trophoblastic giant cells of the mouse placenta. Genesis *29*, 133-140.

Hagerman, R.J., Berry-Kravis, E., Kaufmann, W.E., Ono, M.Y., Tartaglia, N., Lachiewicz, A., Kronk, R., Delahunty, C., Hessl, D., Visootsak, J., *et al.* (2009). Advances in the treatment of fragile X syndrome. Pediatrics *123*, 378-390.

Hallermann, S., Fejtova, A., Schmidt, H., Weyhersmuller, A., Silver, R.A., Gundelfinger, E.D., and Eilers, J. (2010). Bassoon speeds vesicle reloading at a central excitatory synapse. Neuron *68*, 710-723.

Hanson, J.E., and Madison, D.V. (2007). Presynaptic FMR1 genotype influences the degree of synaptic connectivity in a mosaic mouse model of fragile X syndrome. The Journal of neuroscience : the official journal of the Society for Neuroscience *27*, 4014-4018.

Harlow, E.G., Till, S.M., Russell, T.A., Wijetunge, L.S., Kind, P., and Contractor, A. (2010). Critical period plasticity is disrupted in the barrel cortex of FMR1 knockout mice. Neuron *65*, 385-398.

Hayashi, Y., Shi, S.H., Esteban, J.A., Piccini, A., Poncer, J.C., and Malinow, R. (2000). Driving AMPA receptors into synapses by LTP and CaMKII: requirement for GluR1 and PDZ domain interaction. Science *287*, 2262-2267.

Hensch, T.K. (2005). Critical period plasticity in local cortical circuits. Nat Rev Neurosci *6*, 877-888.

Hinton, V.J., Brown, W.T., Wisniewski, K., and Rudelli, R.D. (1991). Analysis of neocortex in three males with the fragile X syndrome. American journal of medical genetics *41*, 289-294.

Huang, C.H., Bao, J., and Sakaba, T. (2010). Multivesicular release differentiates the reliability of synaptic transmission between the visual cortex and the somatosensory cortex. The Journal of neuroscience : the official journal of the Society for Neuroscience *30*, 11994-12004.

Hubel, D.H., Wiesel, T.N., and LeVay, S. (1977). Plasticity of ocular dominance columns in monkey striate cortex. Philosophical transactions of the Royal Society of London Series B, Biological sciences *278*, 377-409.

Huber, K.M., and Bear, M.F. (1998). Activation of group I metabotropic glutamate receptors induces long-term depression of synaptic transmision in area CA1 of rat hippocampus. Soc Neurosci Abs *22*.

Huber, K.M., Gallagher, S.M., Warren, S.T., and Bear, M.F. (2002). Altered synaptic plasticity in a mouse model of fragile X mental retardation. Proceedings of the National Academy of Sciences of the United States of America *99*, 7746-7750.

Huber, K.M., Kayser, M.S., and Bear, M.F. (2000). Role for rapid dendritic protein synthesis in hippocampal mGluR-dependent LTD. Science *288*, 1254-1257.

Irwin, S.A., Patel, B., Idupulapati, M., Harris, J.B., Crisostomo, R.A., Larsen, B.P., Kooy, F., Willems, P.J., Cras, P., Kozlowski, P.B., *et al.* (2001). Abnormal dendritic spine characteristics in the temporal and visual cortices of patients with fragile-X syndrome: a quantitative examination. American journal of medical genetics *98*, 161-167.

Isaacson, J.S., Solis, J.M., and Nicoll, R.A. (1993). Local and diffuse synaptic actions of GABA in the hippocampus. Neuron *10*, 165-175.

Jacob, V., Petreanu, L., Wright, N., Svoboda, K., and Fox, K. (2011). Regular spiking and intrinsic bursting pyramidal cells show orthogonal forms of experience-dependent plasticity in layer V of barrel cortex. Neuron *73*, 391-404.

Jacobs, S., Nathwani, M., and Doering, L.C. (2010). Fragile X astrocytes induce developmental delays in dendrite maturation and synaptic protein expression. BMC neuroscience *11*, 132.

Jimenez-Diaz, L., Geranton, S.M., Passmore, G.M., Leith, J.L., Fisher, A.S., Berliocchi, L., Sivasubramaniam, A.K., Sheasby, A., Lumb, B.M., and Hunt, S.P. (2008). Local translation in primary afferent fibers regulates nociception. PloS one *3*, e1961.

Johnston, D., and Wu, S. (1995). Foundations of Cellular Neurophysiology (Cambridge, MA: The MIT Press).

Kamenetz, F., Tomita, T., Hsieh, H., Seabrook, G., Borchelt, D., Iwatsubo, T., Sisodia, S., and Malinow, R. (2003). APP processing and synaptic function. Neuron *37*, 925-937.

Kampa, B.M., Letzkus, J.J., and Stuart, G.J. (2006). Cortical feed-forward networks for binding different streams of sensory information. Nature neuroscience *9*, 1472-1473.

Kasai, H., Fukuda, M., Watanabe, S., Hayashi-Takagi, A., and Noguchi, J. (2010). Structural dynamics of dendritic spines in memory and cognition. Trends in neurosciences *33*, 121-129.

Koekkoek, S.K., Yamaguchi, K., Milojkovic, B.A., Dortland, B.R., Ruigrok, T.J., Maex, R., De Graaf, W., Smit, A.E., VanderWerf, F., Bakker, C.E., *et al.* (2005). Deletion of FMR1 in Purkinje cells enhances parallel fiber LTD, enlarges spines, and attenuates cerebellar eyelid conditioning in Fragile X syndrome. Neuron *47*, 339-352.

Kogan, M.D., Strickland, B.B., Blumberg, S.J., Singh, G.K., Perrin, J.M., and van Dyck, P.C. (2008). A national profile of the health care experiences and family impact of autism spectrum disorder among children in the United States, 2005-2006. Pediatrics *122*, e1149-1158.

Kraushaar, U., and Jonas, P. (2000). Efficacy and stability of quantal GABA release at a hippocampal interneuron-principal neuron synapse. The Journal of neuroscience : the official journal of the Society for Neuroscience *20*, 5594-5607.

Lamsa, K., Heeroma, J.H., and Kullmann, D.M. (2005). Hebbian LTP in feed-forward inhibitory interneurons and the temporal fidelity of input discrimination. Nature neuroscience *8*, 916-924.

Lanore, F., Blanchet, C., Fejtova, A., Pinheiro, P., Richter, K., Balschun, D., Gundelfinger, E., and Mulle, C. (2010). Impaired development of hippocampal mossy fibre synapses in mouse mutants for the presynaptic scaffold protein Bassoon. The Journal of physiology *588*, 2133-2145.

Lee, H.Y., Ge, W.P., Huang, W., He, Y., Wang, G.X., Rowson-Baldwin, A., Smith, S.J., Jan, Y.N., and Jan, L.Y. (2011). Bidirectional regulation of dendritic voltage-gated potassium channels by the fragile X mental retardation protein. Neuron *72*, 630-642.

Lendvai, B., Stern, E.A., Chen, B., and Svoboda, K. (2000). Experience-dependent plasticity of dendritic spines in the developing rat barrel cortex in vivo. Nature *404*, 876-881.

Li, C., Bassell, G.J., and Sasaki, Y. (2009). Fragile X Mental Retardation Protein is Involved in Protein Synthesis-Dependent Collapse of Growth Cones Induced by Semaphorin-3A. Frontiers in neural circuits *3*, 11.

Liao, D., Zhang, X., O'Brien, R., Ehlers, M.D., and Huganir, R.L. (1999). Regulation of morphological postsynaptic silent synapses in developing hippocampal neurons. Nature neuroscience *2*, 37-43.

Lichtman, J.W. (1977). The reorganization of synaptic connexions in the rat submandibular ganglion during post-natal development. The Journal of physiology *273*, 155-177.

Lichtman, J.W., and Colman, H. (2000). Synapse elimination and indelible memory. Neuron *25*, 269-278.

Lohof, A.M., Delhaye-Bouchaud, N., and Mariani, J. (1996). Synapse elimination in the central nervous system: functional significance and cellular mechanisms. Reviews in the neurosciences *7*, 85-101.

Lovett-Barron, M., Turi, G.F., Kaifosh, P., Lee, P.H., Bolze, F., Sun, X.H., Nicoud, J.F., Zemelman, B.V., Sternson, S.M., and Losonczy, A. (2012). Regulation of neuronal input transformations by tunable dendritic inhibition. Nature neuroscience *15*, 423-430, S421-423.

Lu, T., and Trussell, L.O. (2000). Inhibitory transmission mediated by asynchronous transmitter release. Neuron *26*, 683-694.

Lu, W., Shi, Y., Jackson, A.C., Bjorgan, K., During, M.J., Sprengel, R., Seeburg, P.H., and Nicoll, R.A. (2009). Subunit composition of synaptic AMPA receptors revealed by a single-cell genetic approach. Neuron *62*, 254-268.

Luthi, A., Di Paolo, G., Cremona, O., Daniell, L., De Camilli, P., and McCormick, D.A. (2001). Synaptojanin 1 contributes to maintaining the stability of GABAergic transmission in primary cultures of cortical neurons. The Journal of neuroscience : the official journal of the Society for Neuroscience *21*, 9101-9111.

Matsuzaki, M., Ellis-Davies, G.C., Nemoto, T., Miyashita, Y., Iino, M., and Kasai, H. (2001). Dendritic spine geometry is critical for AMPA receptor expression in hippocampal CA1 pyramidal neurons. Nature neuroscience *4*, 1086-1092.

McKinney, B.C., Grossman, A.W., Elisseou, N.M., and Greenough, W.T. (2005). Dendritic spine abnormalities in the occipital cortex of C57BL/6 Fmr1 knockout mice. American journal of medical genetics Part B, Neuropsychiatric genetics : the official publication of the International Society of Psychiatric Genetics *136*, 98-102.

Meredith, R.M., Dawitz, J., and Kramvis, I. (2012). Sensitive time-windows for susceptibility in neurodevelopmental disorders. Trends in neurosciences *35*, 335-344.

Meredith, R.M., Holmgren, C.D., Weidum, M., Burnashev, N., and Mansvelder, H.D. (2007). Increased threshold for spike-timing-dependent plasticity is caused by unreliable calcium signaling in mice lacking fragile X gene FMR1. Neuron *54*, 627-638.

Morishita, W., Marie, H., and Malenka, R.C. (2005). Distinct triggering and expression mechanisms underlie LTD of AMPA and NMDA synaptic responses. Nature neuroscience *8*, 1043-1050.

Narayanan, U., Nalavadi, V., Nakamoto, M., Pallas, D.C., Ceman, S., Bassell, G.J., and Warren, S.T. (2007). FMRP phosphorylation reveals an immediate-early signaling pathway triggered by group I mGluR and mediated by PP2A. The Journal of neuroscience : the official journal of the Society for Neuroscience *27*, 14349-14357.

Niere, F., Wilkerson, J.R., and Huber, K.M. (2012). Evidence for a fragile X mental retardation protein-mediated translational switch in metabotropic glutamate receptor-triggered Arc translation and long-term depression. The Journal of neuroscience : the official journal of the Society for Neuroscience *32*, 5924-5936.

Nimchinsky, E.A., Oberlander, A.M., and Svoboda, K. (2001). Abnormal development of dendritic spines in FMR1 knock-out mice. The Journal of neuroscience : the official journal of the Society for Neuroscience *21*, 5139-5146.

Nolin, S.L., Glicksman, A., Houck, G.E., Jr., Brown, W.T., and Dobkin, C.S. (1994). Mosaicism in fragile X affected males. American journal of medical genetics *51*, 509-512.

Nosyreva, E.D., and Huber, K.M. (2005). Developmental switch in synaptic mechanisms of hippocampal metabotropic glutamate receptor-dependent long-term depression. The Journal of neuroscience : the official journal of the Society for Neuroscience *25*, 2992-3001.

Oertner, T.G., Sabatini, B.L., Nimchinsky, E.A., and Svoboda, K. (2002). Facilitation at single synapses probed with optical quantal analysis. Nature neuroscience *5*, 657-664.

Olmos-Serrano, J.L., Paluszkiewicz, S.M., Martin, B.S., Kaufmann, W.E., Corbin, J.G., and Huntsman, M.M. (2010). Defective GABAergic neurotransmission and pharmacological rescue of neuronal hyperexcitability in the amygdala in a mouse model of fragile X syndrome. The Journal of neuroscience : the official journal of the Society for Neuroscience *30*, 9929-9938.

Paluszkiewicz, S.M., Olmos-Serrano, J.L., Corbin, J.G., and Huntsman, M.M. (2011). Impaired inhibitory control of cortical synchronization in fragile X syndrome. Journal of neurophysiology *106*, 2264-2272.

Peebles, C.L., Yoo, J., Thwin, M.T., Palop, J.J., Noebels, J.L., and Finkbeiner, S. (2010). Arc regulates spine morphology and maintains network stability in vivo. Proceedings of the National Academy of Sciences of the United States of America *107*, 18173-18178.

Pfeiffer, B.E., and Huber, K.M. (2007). Fragile X mental retardation protein induces synapse loss through acute postsynaptic translational regulation. The Journal of neuroscience : the official journal of the Society for Neuroscience *27*, 3120-3130.

Pfeiffer, B.E., and Huber, K.M. (2009). The state of synapses in fragile X syndrome. The Neuroscientist : a review journal bringing neurobiology, neurology and psychiatry *15*, 549-567.

Pfeiffer, B.E., Zang, T., Wilkerson, J.R., Taniguchi, M., Maksimova, M.A., Smith, L.N., Cowan, C.W., and Huber, K.M. (2010). Fragile X Mental Retardation Protein Is Required for Synapse Elimination by the Activity-Dependent Transcription Factor MEF2. Neuron *66*, 191-197.

Pieretti, M., Zhang, F.P., Fu, Y.H., Warren, S.T., Oostra, B.A., Caskey, C.T., and Nelson, D.L. (1991). Absence of expression of the FMR-1 gene in fragile X syndrome. Cell *66*, 817-822.

Portera-Cailliau, C. (2012). Which comes first in fragile X syndrome, dendritic spine dysgenesis or defects in circuit plasticity? The Neuroscientist : a review journal bringing neurobiology, neurology and psychiatry *18*, 28-44.

Price, T.J., Flores, C.M., Cervero, F., and Hargreaves, K.M. (2006). The RNA binding and transport proteins staufen and fragile X mental retardation protein are expressed by rat primary afferent neurons and localize to peripheral and central axons. Neuroscience *141*, 2107-2116.

Price, T.J., Rashid, M.H., Millecamps, M., Sanoja, R., Entrena, J.M., and Cervero, F. (2007). Decreased nociceptive sensitization in mice lacking the fragile X mental retardation protein: role of mGluR1/5 and mTOR. The Journal of neuroscience : the official journal of the Society for Neuroscience *27*, 13958-13967.

Regehr, W.G., and Stevens, C.F. (2001). Physiology of Synaptic Transmission and Short-Term Plasticity. In Synapses, W.M. Cowan, T.C. Sudhof, and C.F. Stevens, eds. (Baltimore: The Johns Hopkins University Press), pp. 135-175.

Restivo, L., Ferrari, F., Passino, E., Sgobio, C., Bock, J., Oostra, B.A., Bagni, C., and Ammassari-Teule, M. (2005). Enriched environment promotes behavioral and morphological recovery in a mouse model for the fragile X syndrome. Proceedings of the National Academy of Sciences of the United States of America *102*, 11557-11562.

Rosenmund, C., Clements, J.D., and Westbrook, G.L. (1993). Nonuniform probability of glutamate release at a hippocampal synapse. Science *262*, 754-757.

Rozov, A., Jerecic, J., Sakmann, B., and Burnashev, N. (2001). AMPA receptor channels with long-lasting desensitization in bipolar interneurons contribute to synaptic depression in a novel feedback circuit in layer 2/3 of rat neocortex. The Journal of neuroscience : the official journal of the Society for Neuroscience *21*, 8062-8071.

Rudelli, R.D., Brown, W.T., Wisniewski, K., Jenkins, E.C., Laure-Kamionowska, M., Connell, F., and Wisniewski, H.M. (1985). Adult fragile X syndrome. Clinico-neuropathologic findings. Acta Neuropathol (Berl) *67*, 289-295.

Rudolph, S., Overstreet-Wadiche, L., and Wadiche, J.I. (2011). Desynchronization of multivesicular release enhances Purkinje cell output. Neuron *70*, 991-1004.

Sanders, J., Cowansage, K., Baumgartel, K., and Mayford, M. (2012). Elimination of dendritic spines with long-term memory is specific to active circuits. The Journal of neuroscience : the official journal of the Society for Neuroscience *32*, 12570-12578.

Selby, L., Zhang, C., and Sun, Q.Q. (2007). Major defects in neocortical GABAergic inhibitory circuits in mice lacking the fragile X mental retardation protein. Neurosci Lett *412*, 227-232.

Shepherd, G.M., Pologruto, T.A., and Svoboda, K. (2003). Circuit analysis of experience-dependent plasticity in the developing rat barrel cortex. Neuron *38*, 277-289.

Shepherd, J.D., Rumbaugh, G., Wu, J., Chowdhury, S., Plath, N., Kuhl, D., Huganir, R.L., and Worley, P.F. (2006). Arc/Arg3.1 mediates homeostatic synaptic scaling of AMPA receptors. Neuron *52*, 475-484.

Shinoda, Y., Kamikubo, Y., Egashira, Y., Tominaga-Yoshino, K., and Ogura, A. (2005). Repetition of mGluR-dependent LTD causes slowly developing persistent reduction in synaptic strength accompanied by synapse elimination. Brain research *1042*, 99-107.

Silver, R.A. (2003). Estimation of nonuniform quantal parameters with multiple-probability fluctuation analysis: theory, application and limitations. Journal of neuroscience methods *130*, 127-141.

Sittler, A., Devys, D., Weber, C., and Mandel, J.L. (1996). Alternative splicing of exon 14 determines nuclear or cytoplasmic localisation of fmr1 protein isoforms. Human molecular genetics *5*, 95-102.

Soden, M.E., and Chen, L. (2010). Fragile X protein FMRP is required for homeostatic plasticity and regulation of synaptic strength by retinoic acid. The Journal of neuroscience : the official journal of the Society for Neuroscience *30*, 16910-16921.

Sohal, V.S., Zhang, F., Yizhar, O., and Deisseroth, K. (2009). Parvalbumin neurons and gamma rhythms enhance cortical circuit performance. Nature *459*, 698-702.

Sun, Y.G., and Beierlein, M. (2011). Receptor saturation controls short-term synaptic plasticity at corticothalamic synapses. Journal of neurophysiology *105*, 2319-2329.

Tessier, C.R., and Broadie, K. (2008). Drosophila fragile X mental retardation protein developmentally regulates activity-dependent axon pruning. Development *135*, 1547-1557.

Testa-Silva, G., Loebel, A., Giugliano, M., de Kock, C.P., Mansvelder, H.D., and Meredith, R.M. (2011). Hyperconnectivity and Slow Synapses during Early Development of Medial Prefrontal Cortex in a Mouse Model for Mental Retardation and Autism. Cerebral cortex.

Till, S.M., Wijetunge, L.S., Seidel, V.G., Harlow, E., Wright, A.K., Bagni, C., Contractor, A., Gillingwater, T.H., and Kind, P.C. (2012). Altered maturation of the primary somatosensory cortex in a mouse model of fragile X syndrome. Human molecular genetics.

Todd, P.K., and Mack, K.J. (2000). Sensory stimulation increases cortical expression of the fragile X mental retardation protein in vivo. Brain research Molecular brain research *80*, 17-25.

Todd, P.K., Mack, K.J., and Malter, J.S. (2003). The fragile X mental retardation protein is required for type-I metabotropic glutamate receptor-dependent translation of PSD-95.

Proceedings of the National Academy of Sciences of the United States of America *100*, 14374-14378.

van Versendaal, D., Rajendran, R., Saiepour, M.H., Klooster, J., Smit-Rigter, L., Sommeijer, J.P., De Zeeuw, C.I., Hofer, S.B., Heimel, J.A., and Levelt, C.N. (2012). Elimination of inhibitory synapses is a major component of adult ocular dominance plasticity. Neuron *74*, 374-383.

Wadiche, J.I., and Jahr, C.E. (2001). Multivesicular release at climbing fiber-Purkinje cell synapses. Neuron *32*, 301-313.

Wan, L., Dockendorff, T.C., Jongens, T.A., and Dreyfuss, G. (2000). Characterization of dFMR1, a Drosophila melanogaster homolog of the fragile X mental retardation protein. Molecular and cellular biology *20*, 8536-8547.

Wang, H., and Zhang, Z.W. (2008). A critical window for experience-dependent plasticity at whisker sensory relay synapse in the thalamus. The Journal of neuroscience : the official journal of the Society for Neuroscience *28*, 13621-13628.

Watanabe, J., Rozov, A., and Wollmuth, L.P. (2005). Target-specific regulation of synaptic amplitudes in the neocortex. The Journal of neuroscience : the official journal of the Society for Neuroscience *25*, 1024-1033.

Weiler, I.J., Irwin, S.A., Klintsova, A.Y., Spencer, C.M., Brazelton, A.D., Miyashiro, K., Comery, T.A., Patel, B., Eberwine, J., and Greenough, W.T. (1997). Fragile X mental retardation protein is translated near synapses in response to neurotransmitter activation. Proceedings of the National Academy of Sciences of the United States of America *94*, 5395-5400.

Wilson, B.M., and Cox, C.L. (2007). Absence of metabotropic glutamate receptor-mediated plasticity in the neocortex of fragile X mice. Proceedings of the National Academy of Sciences of the United States of America *104*, 2454-2459.

Yang, B., Desai, R., and Kaczmarek, L.K. (2007). Slack and Slick K(Na) channels regulate the accuracy of timing of auditory neurons. The Journal of neuroscience : the official journal of the Society for Neuroscience *27*, 2617-2627.

Yasuda, M., Johnson-Venkatesh, E.M., Zhang, H., Parent, J.M., Sutton, M.A., and Umemori, H. (2011). Multiple forms of activity-dependent competition refine hippocampal circuits in vivo. Neuron *70*, 1128-1142.

Yoshimura, Y., Dantzker, J.L., and Callaway, E.M. (2005). Excitatory cortical neurons form fine-scale functional networks. Nature *433*, 868-873.

Zhai, R.G., Vardinon-Friedman, H., Cases-Langhoff, C., Becker, B., Gundelfinger, E.D., Ziv, N.E., and Garner, C.C. (2001). Assembling the presynaptic active zone: a characterization of an active one precursor vesicle. Neuron *29*, 131-143.

Zhang, L., Volknandt, W., Gundelfinger, E.D., and Zimmermann, H. (2000). A comparison of synaptic protein localization in hippocampal mossy fiber terminals and neurosecretory endings of the neurohypophysis using the cryo-immunogold technique. Journal of neurocytology *29*, 19-30.

Zhang, Y.Q., Bailey, A.M., Matthies, H.J., Renden, R.B., Smith, M.A., Speese, S.D., Rubin, G.M., and Broadie, K. (2001). Drosophila fragile X-related gene regulates the MAP1B homolog Futsch to control synaptic structure and function. Cell *107*, 591-603.

Zhang, Z.W., Peterson, M., and Liu, H. (2013). Essential role of postsynaptic NMDA receptors in developmental refinement of excitatory synapses. Proceedings of the National Academy of Sciences of the United States of America *110*, 1095-1100.

Zuo, Y., Yang, G., Kwon, E., and Gan, W.B. (2005). Long-term sensory deprivation prevents dendritic spine loss in primary somatosensory cortex. Nature *436*, 261-265.